Part III

Deep Learning Research

This part of the book describes the more ambitious and advanced approaches to deep learning, currently pursued by the research community.

In the previous parts of the book, we have shown how to solve supervised learning problems—how to learn to map one vector to another, given enough examples of the mapping.

Not all problems we might want to solve fall into this category. We may wish to generate new examples, or determine how likely some point is, or handle missing values and take advantage of a large set of unlabeled examples or examples from related tasks. A shortcoming of the current state of the art for industrial applications is that our learning algorithms require large amounts of supervised data to achieve good accuracy. In this part of the book, we discuss some of the speculative approaches to reducing the amount of labeled data necessary for existing models to work well and be applicable across a broader range of tasks. Accomplishing these goals usually requires some form of unsupervised or semi-supervised learning.

Many deep learning algorithms have been designed to tackle unsupervised learning problems, but none have truly solved the problem in the same way that deep learning has largely solved the supervised learning problem for a wide variety of tasks. In this part of the book, we describe the existing approaches to unsupervised learning and some of the popular thought about how we can make progress in this field.

A central cause of the difficulties with unsupervised learning is the high dimensionality of the random variables being modeled. This brings two distinct challenges: a statistical challenge and a computational challenge. The *statistical challenge* regards generalization: the number of configurations we may want to distinguish can grow exponentially with the number of dimensions of interest, and this quickly becomes much larger than the number of examples one can possibly have (or use with bounded computational resources). The *computational challenge* associated with high-dimensional distributions arises because many algorithms for learning or using a trained model (especially those based on estimating an explicit probability function) involve intractable computations that grow exponentially with the number of dimensions.

With probabilistic models, this computational challenge arises from the need to perform intractable inference or simply from the need to normalize the distribution.

- *Intractable inference*: inference is discussed mostly in chapter 19. It regards the question of guessing the probable values of some variables a, given other variables b, with respect to a model that captures the joint distribution over

a, b and c. In order to even compute such conditional probabilities one needs to sum over the values of the variables c, as well as compute a normalization constant which sums over the values of a and c.

- *Intractable normalization constants (the partition function)*: the partition function is discussed mostly in chapter 18. Normalizing constants of probability functions come up in inference (above) as well as in learning. Many probabilistic models involve such a normalizing constant. Unfortunately, learning such a model often requires computing the gradient of the logarithm of the partition function with respect to the model parameters. That computation is generally as intractable as computing the partition function itself. Monte Carlo Markov chain (MCMC) methods (chapter 17) are often used to deal with the partition function (computing it or its gradient). Unfortunately, MCMC methods suffer when the modes of the model distribution are numerous and well-separated, especially in high-dimensional spaces (section 17.5).

One way to confront these intractable computations is to approximate them, and many approaches have been proposed as discussed in this third part of the book. Another interesting way, also discussed here, would be to avoid these intractable computations altogether by design, and methods that do not require such computations are thus very appealing. Several generative models have been proposed in recent years, with that motivation. A wide variety of contemporary approaches to generative modeling are discussed in chapter 20.

Part III is the most important for a researcher—someone who wants to understand the breadth of perspectives that have been brought to the field of deep learning, and push the field forward towards true artificial intelligence.

Chapter 13

Linear Factor Models

Many of the research frontiers in deep learning involve building a probabilistic model of the input, $p_{\text{model}}(\boldsymbol{x})$. Such a model can, in principle, use probabilistic inference to predict any of the variables in its environment given any of the other variables. Many of these models also have latent variables $\boldsymbol{h}$, with $p_{\text{model}}(\boldsymbol{x}) = \mathbb{E}_{\boldsymbol{h}} p_{\text{model}}(\boldsymbol{x} \mid \boldsymbol{h})$. These latent variables provide another means of representing the data. Distributed representations based on latent variables can obtain all of the advantages of representation learning that we have seen with deep feedforward and recurrent networks.

In this chapter, we describe some of the simplest probabilistic models with latent variables: linear factor models. These models are sometimes used as building blocks of mixture models (Hinton *et al.*, 1995a; Ghahramani and Hinton, 1996; Roweis *et al.*, 2002) or larger, deep probabilistic models (Tang *et al.*, 2012). They also show many of the basic approaches necessary to build generative models that the more advanced deep models will extend further.

A linear factor model is defined by the use of a stochastic, linear decoder function that generates $\boldsymbol{x}$ by adding noise to a linear transformation of $\boldsymbol{h}$.

These models are interesting because they allow us to discover explanatory factors that have a simple joint distribution. The simplicity of using a linear decoder made these models some of the first latent variable models to be extensively studied.

A linear factor model describes the data generation process as follows. First, we sample the explanatory factors $\boldsymbol{h}$ from a distribution

$$\mathbf{h} \sim p(\boldsymbol{h}), \tag{13.1}$$

where $p(\boldsymbol{h})$ is a factorial distribution, with $p(\boldsymbol{h}) = \prod_i p(h_i)$, so that it is easy to

sample from. Next we sample the real-valued observable variables given the factors:

$$\boldsymbol{x} = \boldsymbol{W}\boldsymbol{h} + \boldsymbol{b} + \text{noise} \tag{13.2}$$

where the noise is typically Gaussian and diagonal (independent across dimensions). This is illustrated in figure 13.1.

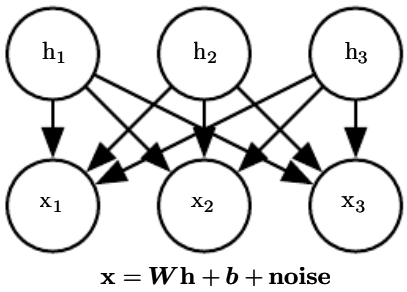

Figure 13.1: The directed graphical model describing the linear factor model family, in which we assume that an observed data vector $\boldsymbol{x}$ is obtained by a linear combination of independent latent factors $\boldsymbol{h}$, plus some noise. Different models, such as probabilistic PCA, factor analysis or ICA, make different choices about the form of the noise and of the prior $p(\boldsymbol{h})$.

13.1 Probabilistic PCA and Factor Analysis

Probabilistic PCA (principal components analysis), factor analysis and other linear factor models are special cases of the above equations (13.1 and 13.2) and only differ in the choices made for the noise distribution and the model's prior over latent variables $\boldsymbol{h}$ before observing $\boldsymbol{x}$.

In **factor analysis** (Bartholomew, 1987; Basilevsky, 1994), the latent variable prior is just the unit variance Gaussian

$$\mathbf{h} \sim \mathcal{N}(\boldsymbol{h}; \mathbf{0}, \boldsymbol{I}) \tag{13.3}$$

while the observed variables x_i are assumed to be **conditionally independent**, given $\boldsymbol{h}$. Specifically, the noise is assumed to be drawn from a diagonal covariance Gaussian distribution, with covariance matrix $\boldsymbol{\psi} = \text{diag}(\boldsymbol{\sigma}^2)$, with $\boldsymbol{\sigma}^2 = [\sigma_1^2, \sigma_2^2, \ldots, \sigma_n^2]^\top$ a vector of per-variable variances.

The role of the latent variables is thus to *capture the dependencies* between the different observed variables x_i. Indeed, it can easily be shown that $\boldsymbol{x}$ is just a multivariate normal random variable, with

$$\mathbf{x} \sim \mathcal{N}(\boldsymbol{x}; \boldsymbol{b}, \boldsymbol{W}\boldsymbol{W}^\top + \boldsymbol{\psi}). \tag{13.4}$$

In order to cast PCA in a probabilistic framework, we can make a slight modification to the factor analysis model, making the conditional variances σ_i^2 equal to each other. In that case the covariance of $\boldsymbol{x}$ is just $\boldsymbol{W}\boldsymbol{W}^\top + \sigma^2\boldsymbol{I}$, where σ^2 is now a scalar. This yields the conditional distribution

$$\mathbf{x} \sim \mathcal{N}(\boldsymbol{x}; \boldsymbol{b}, \boldsymbol{W}\boldsymbol{W}^\top + \sigma^2\boldsymbol{I}) \tag{13.5}$$

or equivalently

$$\mathbf{x} = \boldsymbol{W}\mathbf{h} + \boldsymbol{b} + \sigma\mathbf{z} \tag{13.6}$$

where $\mathbf{z} \sim \mathcal{N}(\boldsymbol{z}; \mathbf{0}, \boldsymbol{I})$ is Gaussian noise. Tipping and Bishop (1999) then show an iterative EM algorithm for estimating the parameters $\boldsymbol{W}$ and σ^2.

This **probabilistic PCA** model takes advantage of the observation that most variations in the data can be captured by the latent variables $\boldsymbol{h}$, up to some small residual **reconstruction error** σ^2. As shown by Tipping and Bishop (1999), probabilistic PCA becomes PCA as $\sigma \to 0$. In that case, the conditional expected value of $\boldsymbol{h}$ given $\boldsymbol{x}$ becomes an orthogonal projection of $\boldsymbol{x} - \boldsymbol{b}$ onto the space spanned by the d columns of $\boldsymbol{W}$, like in PCA.

As $\sigma \to 0$, the density model defined by probabilistic PCA becomes very sharp around these d dimensions spanned by the columns of $\boldsymbol{W}$. This can make the model assign very low likelihood to the data if the data does not actually cluster near a hyperplane.

13.2 Independent Component Analysis (ICA)

Independent component analysis (ICA) is among the oldest representation learning algorithms (Herault and Ans, 1984; Jutten and Herault, 1991; Comon, 1994; Hyvärinen, 1999; Hyvärinen *et al.*, 2001a; Hinton *et al.*, 2001; Teh *et al.*, 2003). It is an approach to modeling linear factors that seeks to separate an observed signal into many underlying signals that are scaled and added together to form the observed data. These signals are intended to be fully independent, rather than merely decorrelated from each other.[1]

Many different specific methodologies are referred to as ICA. The variant that is most similar to the other generative models we have described here is a variant (Pham *et al.*, 1992) that trains a fully parametric generative model. The prior distribution over the underlying factors, $p(\boldsymbol{h})$, must be fixed ahead of time by the user. The model then deterministically generates $\boldsymbol{x} = \boldsymbol{W}\boldsymbol{h}$. We can perform a

[1] See section 3.8 for a discussion of the difference between uncorrelated variables and independent variables.

nonlinear change of variables (using equation 3.47) to determine $p(\boldsymbol{x})$. Learning the model then proceeds as usual, using maximum likelihood.

The motivation for this approach is that by choosing $p(\boldsymbol{h})$ to be independent, we can recover underlying factors that are as close as possible to independent. This is commonly used, not to capture high-level abstract causal factors, but to recover low-level signals that have been mixed together. In this setting, each training example is one moment in time, each x_i is one sensor's observation of the mixed signals, and each h_i is one estimate of one of the original signals. For example, we might have n people speaking simultaneously. If we have n different microphones placed in different locations, ICA can detect the changes in the volume between each speaker as heard by each microphone, and separate the signals so that each h_i contains only one person speaking clearly. This is commonly used in neuroscience for electroencephalography, a technology for recording electrical signals originating in the brain. Many electrode sensors placed on the subject's head are used to measure many electrical signals coming from the body. The experimenter is typically only interested in signals from the brain, but signals from the subject's heart and eyes are strong enough to confound measurements taken at the subject's scalp. The signals arrive at the electrodes mixed together, so ICA is necessary to separate the electrical signature of the heart from the signals originating in the brain, and to separate signals in different brain regions from each other.

As mentioned before, many variants of ICA are possible. Some add some noise in the generation of $\boldsymbol{x}$ rather than using a deterministic decoder. Most do not use the maximum likelihood criterion, but instead aim to make the elements of $\boldsymbol{h} = \boldsymbol{W}^{-1}\boldsymbol{x}$ independent from each other. Many criteria that accomplish this goal are possible. Equation 3.47 requires taking the determinant of $\boldsymbol{W}$, which can be an expensive and numerically unstable operation. Some variants of ICA avoid this problematic operation by constraining $\boldsymbol{W}$ to be orthogonal.

All variants of ICA require that $p(\boldsymbol{h})$ be non-Gaussian. This is because if $p(\boldsymbol{h})$ is an independent prior with Gaussian components, then $\boldsymbol{W}$ is not identifiable. We can obtain the same distribution over $p(\boldsymbol{x})$ for many values of $\boldsymbol{W}$. This is very different from other linear factor models like probabilistic PCA and factor analysis, that often require $p(\boldsymbol{h})$ to be Gaussian in order to make many operations on the model have closed form solutions. In the maximum likelihood approach where the user explicitly specifies the distribution, a typical choice is to use $p(h_i) = \frac{d}{dh_i}\sigma(h_i)$. Typical choices of these non-Gaussian distributions have larger peaks near 0 than does the Gaussian distribution, so we can also see most implementations of ICA as learning sparse features.

Many variants of ICA are not generative models in the sense that we use the phrase. In this book, a generative model either represents $p(\boldsymbol{x})$ or can draw samples from it. Many variants of ICA only know how to transform between $\boldsymbol{x}$ and $\boldsymbol{h}$, but do not have any way of representing $p(\boldsymbol{h})$, and thus do not impose a distribution over $p(\boldsymbol{x})$. For example, many ICA variants aim to increase the sample kurtosis of $\boldsymbol{h} = \boldsymbol{W}^{-1}\boldsymbol{x}$, because high kurtosis indicates that $p(\boldsymbol{h})$ is non-Gaussian, but this is accomplished without explicitly representing $p(\boldsymbol{h})$. This is because ICA is more often used as an analysis tool for separating signals, rather than for generating data or estimating its density.

Just as PCA can be generalized to the nonlinear autoencoders described in chapter 14, ICA can be generalized to a nonlinear generative model, in which we use a nonlinear function f to generate the observed data. See Hyvärinen and Pajunen (1999) for the initial work on nonlinear ICA and its successful use with ensemble learning by Roberts and Everson (2001) and Lappalainen *et al.* (2000). Another nonlinear extension of ICA is the approach of **nonlinear independent components estimation**, or NICE (Dinh *et al.*, 2014), which stacks a series of invertible transformations (encoder stages) that have the property that the determinant of the Jacobian of each transformation can be computed efficiently. This makes it possible to compute the likelihood exactly and, like ICA, attempts to transform the data into a space where it has a factorized marginal distribution, but is more likely to succeed thanks to the nonlinear encoder. Because the encoder is associated with a decoder that is its perfect inverse, it is straightforward to generate samples from the model (by first sampling from $p(\boldsymbol{h})$ and then applying the decoder).

Another generalization of ICA is to learn groups of features, with statistical dependence allowed within a group but discouraged between groups (Hyvärinen and Hoyer, 1999; Hyvärinen *et al.*, 2001b). When the groups of related units are chosen to be non-overlapping, this is called **independent subspace analysis**. It is also possible to assign spatial coordinates to each hidden unit and form overlapping groups of spatially neighboring units. This encourages nearby units to learn similar features. When applied to natural images, this **topographic ICA** approach learns Gabor filters, such that neighboring features have similar orientation, location or frequency. Many different phase offsets of similar Gabor functions occur within each region, so that pooling over small regions yields translation invariance.

13.3 Slow Feature Analysis

Slow feature analysis (SFA) is a linear factor model that uses information from

time signals to learn invariant features (Wiskott and Sejnowski, 2002).

Slow feature analysis is motivated by a general principle called the slowness principle. The idea is that the important characteristics of scenes change very slowly compared to the individual measurements that make up a description of a scene. For example, in computer vision, individual pixel values can change very rapidly. If a zebra moves from left to right across the image, an individual pixel will rapidly change from black to white and back again as the zebra's stripes pass over the pixel. By comparison, the feature indicating whether a zebra is in the image will not change at all, and the feature describing the zebra's position will change slowly. We therefore may wish to regularize our model to learn features that change slowly over time.

The slowness principle predates slow feature analysis and has been applied to a wide variety of models (Hinton, 1989; Földiák, 1989; Mobahi *et al.*, 2009; Bergstra and Bengio, 2009). In general, we can apply the slowness principle to any differentiable model trained with gradient descent. The slowness principle may be introduced by adding a term to the cost function of the form

$$\lambda \sum_t L(f(\boldsymbol{x}^{(t+1)}), f(\boldsymbol{x}^{(t)})) \tag{13.7}$$

where λ is a hyperparameter determining the strength of the slowness regularization term, t is the index into a time sequence of examples, f is the feature extractor to be regularized, and L is a loss function measuring the distance between $f(\boldsymbol{x}^{(t)})$ and $f(\boldsymbol{x}^{(t+1)})$. A common choice for L is the mean squared difference.

Slow feature analysis is a particularly efficient application of the slowness principle. It is efficient because it is applied to a linear feature extractor, and can thus be trained in closed form. Like some variants of ICA, SFA is not quite a generative model per se, in the sense that it defines a linear map between input space and feature space but does not define a prior over feature space and thus does not impose a distribution $p(\boldsymbol{x})$ on input space.

The SFA algorithm (Wiskott and Sejnowski, 2002) consists of defining $f(\boldsymbol{x}; \boldsymbol{\theta})$ to be a linear transformation, and solving the optimization problem

$$\min_{\boldsymbol{\theta}} \mathbb{E}_t (f(\boldsymbol{x}^{(t+1)})_i - f(\boldsymbol{x}^{(t)})_i)^2 \tag{13.8}$$

subject to the constraints

$$\mathbb{E}_t f(\boldsymbol{x}^{(t)})_i = 0 \tag{13.9}$$

and

$$\mathbb{E}_t [f(\boldsymbol{x}^{(t)})_i^2] = 1. \tag{13.10}$$

The constraint that the learned feature have zero mean is necessary to make the problem have a unique solution; otherwise we could add a constant to all feature values and obtain a different solution with equal value of the slowness objective. The constraint that the features have unit variance is necessary to prevent the pathological solution where all features collapse to 0. Like PCA, the SFA features are ordered, with the first feature being the slowest. To learn multiple features, we must also add the constraint

$$\forall i < j, \mathbb{E}_t[f(\boldsymbol{x}^{(t)})_i f(\boldsymbol{x}^{(t)})_j] = 0. \tag{13.11}$$

This specifies that the learned features must be linearly decorrelated from each other. Without this constraint, all of the learned features would simply capture the one slowest signal. One could imagine using other mechanisms, such as minimizing reconstruction error, to force the features to diversify, but this decorrelation mechanism admits a simple solution due to the linearity of SFA features. The SFA problem may be solved in closed form by a linear algebra package.

SFA is typically used to learn nonlinear features by applying a nonlinear basis expansion to $\boldsymbol{x}$ before running SFA. For example, it is common to replace $\boldsymbol{x}$ by the quadratic basis expansion, a vector containing elements $x_i x_j$ for all i and j. Linear SFA modules may then be composed to learn deep nonlinear slow feature extractors by repeatedly learning a linear SFA feature extractor, applying a nonlinear basis expansion to its output, and then learning another linear SFA feature extractor on top of that expansion.

When trained on small spatial patches of videos of natural scenes, SFA with quadratic basis expansions learns features that share many characteristics with those of complex cells in V1 cortex (Berkes and Wiskott, 2005). When trained on videos of random motion within 3-D computer rendered environments, deep SFA learns features that share many characteristics with the features represented by neurons in rat brains that are used for navigation (Franzius *et al.*, 2007). SFA thus seems to be a reasonably biologically plausible model.

A major advantage of SFA is that it is possibly to theoretically predict which features SFA will learn, even in the deep, nonlinear setting. To make such theoretical predictions, one must know about the dynamics of the environment in terms of configuration space (e.g., in the case of random motion in the 3-D rendered environment, the theoretical analysis proceeds from knowledge of the probability distribution over position and velocity of the camera). Given the knowledge of how the underlying factors actually change, it is possible to analytically solve for the optimal functions expressing these factors. In practice, experiments with deep SFA applied to simulated data seem to recover the theoretically predicted functions.

This is in comparison to other learning algorithms where the cost function depends highly on specific pixel values, making it much more difficult to determine what features the model will learn.

Deep SFA has also been used to learn features for object recognition and pose estimation (Franzius *et al.*, 2008). So far, the slowness principle has not become the basis for any state of the art applications. It is unclear what factor has limited its performance. We speculate that perhaps the slowness prior is too strong, and that, rather than imposing a prior that features should be approximately constant, it would be better to impose a prior that features should be easy to predict from one time step to the next. The position of an object is a useful feature regardless of whether the object's velocity is high or low, but the slowness principle encourages the model to ignore the position of objects that have high velocity.

13.4 Sparse Coding

Sparse coding (Olshausen and Field, 1996) is a linear factor model that has been heavily studied as an unsupervised feature learning and feature extraction mechanism. Strictly speaking, the term "sparse coding" refers to the process of inferring the value of $\boldsymbol{h}$ in this model, while "sparse modeling" refers to the process of designing and learning the model, but the term "sparse coding" is often used to refer to both.

Like most other linear factor models, it uses a linear decoder plus noise to obtain reconstructions of $\boldsymbol{x}$, as specified in equation 13.2. More specifically, sparse coding models typically assume that the linear factors have Gaussian noise with isotropic precision β:

$$p(\boldsymbol{x} \mid \boldsymbol{h}) = \mathcal{N}(\boldsymbol{x}; \boldsymbol{W}\boldsymbol{h} + \boldsymbol{b}, \frac{1}{\beta}\boldsymbol{I}). \tag{13.12}$$

The distribution $p(\boldsymbol{h})$ is chosen to be one with sharp peaks near 0 (Olshausen and Field, 1996). Common choices include factorized Laplace, Cauchy or factorized Student-t distributions. For example, the Laplace prior parametrized in terms of the sparsity penalty coefficient λ is given by

$$p(h_i) = \text{Laplace}(h_i; 0, \frac{2}{\lambda}) = \frac{\lambda}{4} e^{-\frac{1}{2}\lambda|h_i|} \tag{13.13}$$

and the Student-t prior by

$$p(h_i) \propto \frac{1}{(1 + \frac{h_i^2}{\nu})^{\frac{\nu+1}{2}}}. \tag{13.14}$$

Training sparse coding with maximum likelihood is intractable. Instead, the training alternates between encoding the data and training the decoder to better reconstruct the data given the encoding. This approach will be justified further as a principled approximation to maximum likelihood later, in section 19.3.

For models such as PCA, we have seen the use of a parametric encoder function that predicts $\boldsymbol{h}$ and consists only of multiplication by a weight matrix. The encoder that we use with sparse coding is not a parametric encoder. Instead, the encoder is an optimization algorithm, that solves an optimization problem in which we seek the single most likely code value:

$$\boldsymbol{h}^* = f(\boldsymbol{x}) = \arg\max_{\boldsymbol{h}} p(\boldsymbol{h} \mid \boldsymbol{x}). \tag{13.15}$$

When combined with equation 13.13 and equation 13.12, this yields the following optimization problem:

$$\arg\max_{\boldsymbol{h}} p(\boldsymbol{h} \mid \boldsymbol{x}) \tag{13.16}$$

$$= \arg\max_{\boldsymbol{h}} \log p(\boldsymbol{h} \mid \boldsymbol{x}) \tag{13.17}$$

$$= \arg\min_{\boldsymbol{h}} \lambda ||\boldsymbol{h}||_1 + \beta ||\boldsymbol{x} - \boldsymbol{W}\boldsymbol{h}||_2^2, \tag{13.18}$$

where we have dropped terms not depending on $\boldsymbol{h}$ and divided by positive scaling factors to simplify the equation.

Due to the imposition of an L^1 norm on $\boldsymbol{h}$, this procedure will yield a sparse $\boldsymbol{h}^*$ (See section 7.1.2).

To train the model rather than just perform inference, we alternate between minimization with respect to $\boldsymbol{h}$ and minimization with respect to $\boldsymbol{W}$. In this presentation, we treat β as a hyperparameter. Typically it is set to 1 because its role in this optimization problem is shared with λ and there is no need for both hyperparameters. In principle, we could also treat β as a parameter of the model and learn it. Our presentation here has discarded some terms that do not depend on $\boldsymbol{h}$ but do depend on β. To learn β, these terms must be included, or β will collapse to 0.

Not all approaches to sparse coding explicitly build a $p(\boldsymbol{h})$ and a $p(\boldsymbol{x} \mid \boldsymbol{h})$. Often we are just interested in learning a dictionary of features with activation values that will often be zero when extracted using this inference procedure.

If we sample $\boldsymbol{h}$ from a Laplace prior, it is in fact a zero probability event for an element of $\boldsymbol{h}$ to actually be zero. The generative model itself is not especially sparse, only the feature extractor is. Goodfellow *et al.* (2013d) describe approximate

inference in a different model family, the spike and slab sparse coding model, for which samples from the prior usually contain true zeros.

The sparse coding approach combined with the use of the non-parametric encoder can in principle minimize the combination of reconstruction error and log-prior better than any specific parametric encoder. Another advantage is that there is no generalization error to the encoder. A parametric encoder must learn how to map $\boldsymbol{x}$ to $\boldsymbol{h}$ in a way that generalizes. For unusual $\boldsymbol{x}$ that do not resemble the training data, a learned, parametric encoder may fail to find an $\boldsymbol{h}$ that results in accurate reconstruction or a sparse code. For the vast majority of formulations of sparse coding models, where the inference problem is convex, the optimization procedure will always find the optimal code (unless degenerate cases such as replicated weight vectors occur). Obviously, the sparsity and reconstruction costs can still rise on unfamiliar points, but this is due to generalization error in the decoder weights, rather than generalization error in the encoder. The lack of generalization error in sparse coding's optimization-based encoding process may result in better generalization when sparse coding is used as a feature extractor for a classifier than when a parametric function is used to predict the code. Coates and Ng (2011) demonstrated that sparse coding features generalize better for object recognition tasks than the features of a related model based on a parametric encoder, the linear-sigmoid autoencoder. Inspired by their work, Goodfellow *et al.* (2013d) showed that a variant of sparse coding generalizes better than other feature extractors in the regime where extremely few labels are available (twenty or fewer labels per class).

The primary disadvantage of the non-parametric encoder is that it requires greater time to compute $\boldsymbol{h}$ given $\boldsymbol{x}$ because the non-parametric approach requires running an iterative algorithm. The parametric autoencoder approach, developed in chapter 14, uses only a fixed number of layers, often only one. Another disadvantage is that it is not straight-forward to back-propagate through the non-parametric encoder, which makes it difficult to pretrain a sparse coding model with an unsupervised criterion and then fine-tune it using a supervised criterion. Modified versions of sparse coding that permit approximate derivatives do exist but are not widely used (Bagnell and Bradley, 2009).

Sparse coding, like other linear factor models, often produces poor samples, as shown in figure 13.2. This happens even when the model is able to reconstruct the data well and provide useful features for a classifier. The reason is that each individual feature may be learned well, but the factorial prior on the hidden code results in the model including random subsets of all of the features in each generated sample. This motivates the development of deeper models that can impose a non-

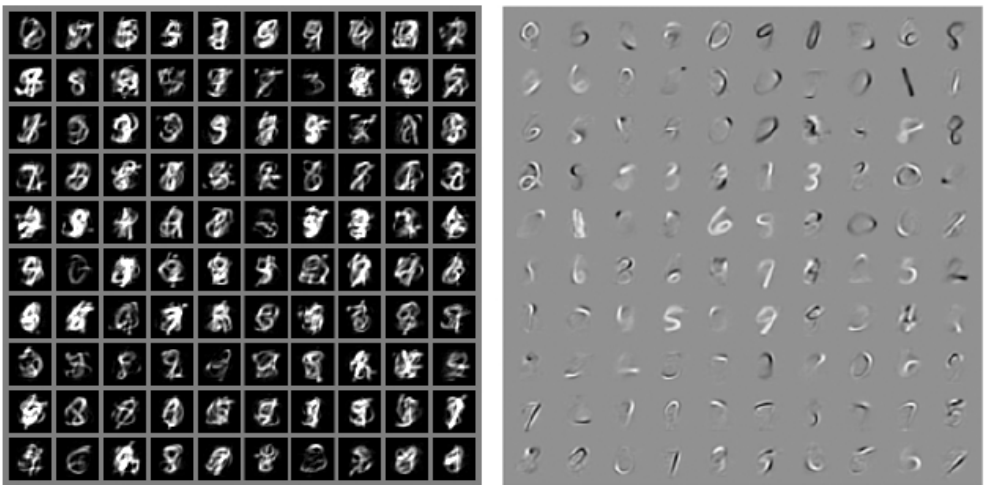

Figure 13.2: Example samples and weights from a spike and slab sparse coding model trained on the MNIST dataset. *(Left)*The samples from the model do not resemble the training examples. At first glance, one might assume the model is poorly fit. *(Right)*The weight vectors of the model have learned to represent penstrokes and sometimes complete digits. The model has thus learned useful features. The problem is that the factorial prior over features results in random subsets of features being combined. Few such subsets are appropriate to form a recognizable MNIST digit. This motivates the development of generative models that have more powerful distributions over their latent codes. Figure reproduced with permission from Goodfellow *et al.* (2013d).

factorial distribution on the deepest code layer, as well as the development of more sophisticated shallow models.

13.5 Manifold Interpretation of PCA

Linear factor models including PCA and factor analysis can be interpreted as learning a manifold (Hinton *et al.*, 1997). We can view probabilistic PCA as defining a thin pancake-shaped region of high probability—a Gaussian distribution that is very narrow along some axes, just as a pancake is very flat along its vertical axis, but is elongated along other axes, just as a pancake is wide along its horizontal axes. This is illustrated in figure 13.3. PCA can be interpreted as aligning this pancake with a linear manifold in a higher-dimensional space. This interpretation applies not just to traditional PCA but also to any linear autoencoder that learns matrices $\boldsymbol{W}$ and $\boldsymbol{V}$ with the goal of making the reconstruction of $\boldsymbol{x}$ lie as close to $\boldsymbol{x}$ as possible,

Let the encoder be

$$\boldsymbol{h} = f(\boldsymbol{x}) = \boldsymbol{W}^\top(\boldsymbol{x} - \boldsymbol{\mu}). \tag{13.19}$$

The encoder computes a low-dimensional representation of h. With the autoencoder view, we have a decoder computing the reconstruction

$$\hat{\boldsymbol{x}} = g(\boldsymbol{h}) = \boldsymbol{b} + \boldsymbol{V}\boldsymbol{h}. \tag{13.20}$$

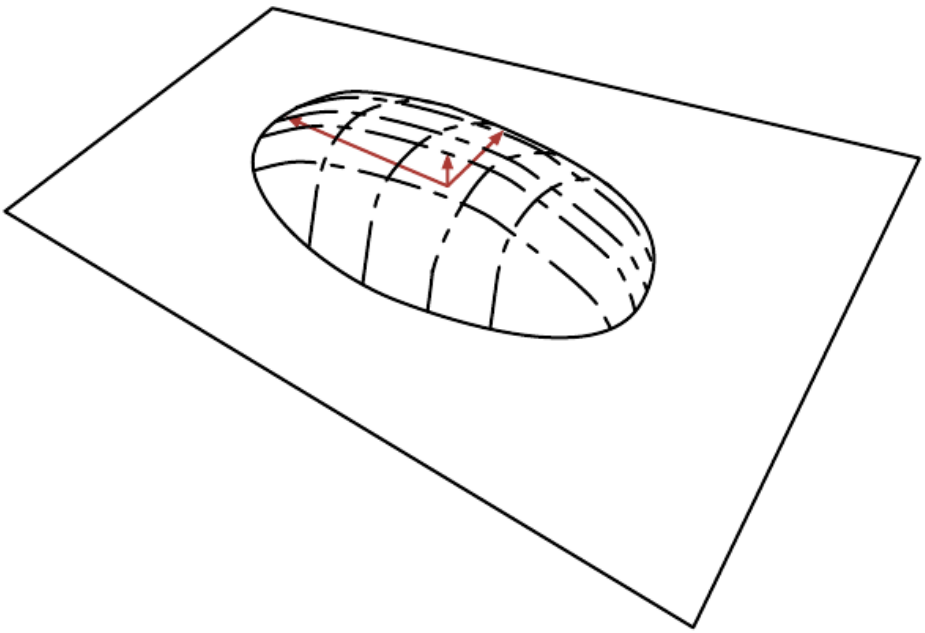

Figure 13.3: Flat Gaussian capturing probability concentration near a low-dimensional manifold. The figure shows the upper half of the "pancake" above the "manifold plane" which goes through its middle. The variance in the direction orthogonal to the manifold is very small (arrow pointing out of plane) and can be considered like "noise," while the other variances are large (arrows in the plane) and correspond to "signal," and a coordinate system for the reduced-dimension data.

The choices of linear encoder and decoder that minimize reconstruction error

$$\mathbb{E}[||\boldsymbol{x} - \hat{\boldsymbol{x}}||^2] \tag{13.21}$$

correspond to $\boldsymbol{V} = \boldsymbol{W}$, $\boldsymbol{\mu} = \boldsymbol{b} = \mathbb{E}[\boldsymbol{x}]$ and the columns of $\boldsymbol{W}$ form an orthonormal basis which spans the same subspace as the principal eigenvectors of the covariance matrix

$$\boldsymbol{C} = \mathbb{E}[(\boldsymbol{x} - \boldsymbol{\mu})(\boldsymbol{x} - \boldsymbol{\mu})^\top]. \tag{13.22}$$

In the case of PCA, the columns of $\boldsymbol{W}$ are these eigenvectors, ordered by the magnitude of the corresponding eigenvalues (which are all real and non-negative).

One can also show that eigenvalue λ_i of $\boldsymbol{C}$ corresponds to the variance of $\boldsymbol{x}$ in the direction of eigenvector $\boldsymbol{v}^{(i)}$. If $\boldsymbol{x} \in \mathbb{R}^D$ and $\boldsymbol{h} \in \mathbb{R}^d$ with $d < D$, then the

optimal reconstruction error (choosing $\boldsymbol{\mu}$, $\boldsymbol{b}$, $\boldsymbol{V}$ and $\boldsymbol{W}$ as above) is

$$\min \mathbb{E}[||\boldsymbol{x} - \hat{\boldsymbol{x}}||^2] = \sum_{i=d+1}^{D} \lambda_i . \tag{13.23}$$

Hence, if the covariance has rank d, the eigenvalues λ_{d+1} to λ_D are 0 and reconstruction error is 0.

Furthermore, one can also show that the above solution can be obtained by maximizing the variances of the elements of $\boldsymbol{h}$, under orthogonal $\boldsymbol{W}$, instead of minimizing reconstruction error.

Linear factor models are some of the simplest generative models and some of the simplest models that learn a representation of data. Much as linear classifiers and linear regression models may be extended to deep feedforward networks, these linear factor models may be extended to autoencoder networks and deep probabilistic models that perform the same tasks but with a much more powerful and flexible model family.

Chapter 14

Autoencoders

An **autoencoder** is a neural network that is trained to attempt to copy its input to its output. Internally, it has a hidden layer $\boldsymbol{h}$ that describes a **code** used to represent the input. The network may be viewed as consisting of two parts: an encoder function $\boldsymbol{h} = f(\boldsymbol{x})$ and a decoder that produces a reconstruction $\boldsymbol{r} = g(\boldsymbol{h})$. This architecture is presented in figure 14.1. If an autoencoder succeeds in simply learning to set $g(f(\boldsymbol{x})) = \boldsymbol{x}$ everywhere, then it is not especially useful. Instead, autoencoders are designed to be unable to learn to copy perfectly. Usually they are restricted in ways that allow them to copy only approximately, and to copy only input that resembles the training data. Because the model is forced to prioritize which aspects of the input should be copied, it often learns useful properties of the data.

Modern autoencoders have generalized the idea of an encoder and a decoder beyond deterministic functions to stochastic mappings $p_{\text{encoder}}(\boldsymbol{h} \mid \boldsymbol{x})$ and $p_{\text{decoder}}(\boldsymbol{x} \mid \boldsymbol{h})$.

The idea of autoencoders has been part of the historical landscape of neural networks for decades (LeCun, 1987; Bourlard and Kamp, 1988; Hinton and Zemel, 1994). Traditionally, autoencoders were used for dimensionality reduction or feature learning. Recently, theoretical connections between autoencoders and latent variable models have brought autoencoders to the forefront of generative modeling, as we will see in chapter 20. Autoencoders may be thought of as being a special case of feedforward networks, and may be trained with all of the same techniques, typically minibatch gradient descent following gradients computed by back-propagation. Unlike general feedforward networks, autoencoders may also be trained using **recirculation** (Hinton and McClelland, 1988), a learning algorithm based on comparing the activations of the network on the original input

to the activations on the reconstructed input. Recirculation is regarded as more biologically plausible than back-propagation, but is rarely used for machine learning applications.

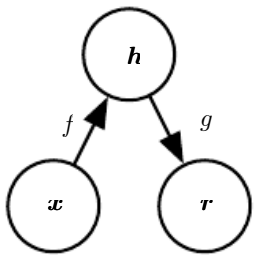

Figure 14.1: The general structure of an autoencoder, mapping an input $\boldsymbol{x}$ to an output (called reconstruction) $\boldsymbol{r}$ through an internal representation or code $\boldsymbol{h}$. The autoencoder has two components: the encoder f (mapping $\boldsymbol{x}$ to $\boldsymbol{h}$) and the decoder g (mapping $\boldsymbol{h}$ to $\boldsymbol{r}$).

14.1 Undercomplete Autoencoders

Copying the input to the output may sound useless, but we are typically not interested in the output of the decoder. Instead, we hope that training the autoencoder to perform the input copying task will result in $\boldsymbol{h}$ taking on useful properties.

One way to obtain useful features from the autoencoder is to constrain $\boldsymbol{h}$ to have smaller dimension than $\boldsymbol{x}$. An autoencoder whose code dimension is less than the input dimension is called **undercomplete**. Learning an undercomplete representation forces the autoencoder to capture the most salient features of the training data.

The learning process is described simply as minimizing a loss function

$$L(\boldsymbol{x}, g(f(\boldsymbol{x}))) \tag{14.1}$$

where L is a loss function penalizing $g(f(\boldsymbol{x}))$ for being dissimilar from $\boldsymbol{x}$, such as the mean squared error.

When the decoder is linear and L is the mean squared error, an undercomplete autoencoder learns to span the same subspace as PCA. In this case, an autoencoder trained to perform the copying task has learned the principal subspace of the training data as a side-effect.

Autoencoders with nonlinear encoder functions f and nonlinear decoder functions g can thus learn a more powerful nonlinear generalization of PCA. Unfortu-

nately, if the encoder and decoder are allowed too much capacity, the autoencoder can learn to perform the copying task without extracting useful information about the distribution of the data. Theoretically, one could imagine that an autoencoder with a one-dimensional code but a very powerful nonlinear encoder could learn to represent each training example $\boldsymbol{x}^{(i)}$ with the code i. The decoder could learn to map these integer indices back to the values of specific training examples. This specific scenario does not occur in practice, but it illustrates clearly that an autoencoder trained to perform the copying task can fail to learn anything useful about the dataset if the capacity of the autoencoder is allowed to become too great.

14.2 Regularized Autoencoders

Undercomplete autoencoders, with code dimension less than the input dimension, can learn the most salient features of the data distribution. We have seen that these autoencoders fail to learn anything useful if the encoder and decoder are given too much capacity.

A similar problem occurs if the hidden code is allowed to have dimension equal to the input, and in the **overcomplete** case in which the hidden code has dimension greater than the input. In these cases, even a linear encoder and linear decoder can learn to copy the input to the output without learning anything useful about the data distribution.

Ideally, one could train any architecture of autoencoder successfully, choosing the code dimension and the capacity of the encoder and decoder based on the complexity of distribution to be modeled. Regularized autoencoders provide the ability to do so. Rather than limiting the model capacity by keeping the encoder and decoder shallow and the code size small, regularized autoencoders use a loss function that encourages the model to have other properties besides the ability to copy its input to its output. These other properties include sparsity of the representation, smallness of the derivative of the representation, and robustness to noise or to missing inputs. A regularized autoencoder can be nonlinear and overcomplete but still learn something useful about the data distribution even if the model capacity is great enough to learn a trivial identity function.

In addition to the methods described here which are most naturally interpreted as regularized autoencoders, nearly any generative model with latent variables and equipped with an inference procedure (for computing latent representations given input) may be viewed as a particular form of autoencoder. Two generative modeling approaches that emphasize this connection with autoencoders are the descendants of the Helmholtz machine (Hinton *et al.*, 1995b), such as the variational

autoencoder (section 20.10.3) and the generative stochastic networks (section 20.12). These models naturally learn high-capacity, overcomplete encodings of the input and do not require regularization for these encodings to be useful. Their encodings are naturally useful because the models were trained to approximately maximize the probability of the training data rather than to copy the input to the output.

14.2.1 Sparse Autoencoders

A sparse autoencoder is simply an autoencoder whose training criterion involves a sparsity penalty $\Omega(\boldsymbol{h})$ on the code layer $\boldsymbol{h}$, in addition to the reconstruction error:

$$L(\boldsymbol{x}, g(f(\boldsymbol{x}))) + \Omega(\boldsymbol{h}) \tag{14.2}$$

where $g(\boldsymbol{h})$ is the decoder output and typically we have $\boldsymbol{h} = f(\boldsymbol{x})$, the encoder output.

Sparse autoencoders are typically used to learn features for another task such as classification. An autoencoder that has been regularized to be sparse must respond to unique statistical features of the dataset it has been trained on, rather than simply acting as an identity function. In this way, training to perform the copying task with a sparsity penalty can yield a model that has learned useful features as a byproduct.

We can think of the penalty $\Omega(\boldsymbol{h})$ simply as a regularizer term added to a feedforward network whose primary task is to copy the input to the output (unsupervised learning objective) and possibly also perform some supervised task (with a supervised learning objective) that depends on these sparse features. Unlike other regularizers such as weight decay, there is not a straightforward Bayesian interpretation to this regularizer. As described in section 5.6.1, training with weight decay and other regularization penalties can be interpreted as a MAP approximation to Bayesian inference, with the added regularizing penalty corresponding to a prior probability distribution over the model parameters. In this view, regularized maximum likelihood corresponds to maximizing $p(\boldsymbol{\theta} \mid \boldsymbol{x})$, which is equivalent to maximizing $\log p(\boldsymbol{x} \mid \boldsymbol{\theta}) + \log p(\boldsymbol{\theta})$. The $\log p(\boldsymbol{x} \mid \boldsymbol{\theta})$ term is the usual data log-likelihood term and the $\log p(\boldsymbol{\theta})$ term, the log-prior over parameters, incorporates the preference over particular values of $\boldsymbol{\theta}$. This view was described in section 5.6. Regularized autoencoders defy such an interpretation because the regularizer depends on the data and is therefore by definition not a prior in the formal sense of the word. We can still think of these regularization terms as implicitly expressing a preference over functions.

Rather than thinking of the sparsity penalty as a regularizer for the copying task, we can think of the entire sparse autoencoder framework as approximating

maximum likelihood training of a generative model that has latent variables. Suppose we have a model with visible variables $\boldsymbol{x}$ and latent variables $\boldsymbol{h}$, with an explicit joint distribution $p_{\text{model}}(\boldsymbol{x}, \boldsymbol{h}) = p_{\text{model}}(\boldsymbol{h}) p_{\text{model}}(\boldsymbol{x} \mid \boldsymbol{h})$. We refer to $p_{\text{model}}(\boldsymbol{h})$ as the model's prior distribution over the latent variables, representing the model's beliefs prior to seeing $\boldsymbol{x}$. This is different from the way we have previously used the word "prior," to refer to the distribution $p(\boldsymbol{\theta})$ encoding our beliefs about the model's parameters before we have seen the training data. The log-likelihood can be decomposed as

$$\log p_{\text{model}}(\boldsymbol{x}) = \log \sum_{\boldsymbol{h}} p_{\text{model}}(\boldsymbol{h}, \boldsymbol{x}). \tag{14.3}$$

We can think of the autoencoder as approximating this sum with a point estimate for just one highly likely value for $\boldsymbol{h}$. This is similar to the sparse coding generative model (section 13.4), but with $\boldsymbol{h}$ being the output of the parametric encoder rather than the result of an optimization that infers the most likely $\boldsymbol{h}$. From this point of view, with this chosen $\boldsymbol{h}$, we are maximizing

$$\log p_{\text{model}}(\boldsymbol{h}, \boldsymbol{x}) = \log p_{\text{model}}(\boldsymbol{h}) + \log p_{\text{model}}(\boldsymbol{x} \mid \boldsymbol{h}). \tag{14.4}$$

The $\log p_{\text{model}}(\boldsymbol{h})$ term can be sparsity-inducing. For example, the Laplace prior,

$$p_{\text{model}}(h_i) = \frac{\lambda}{2} e^{-\lambda |h_i|}, \tag{14.5}$$

corresponds to an absolute value sparsity penalty. Expressing the log-prior as an absolute value penalty, we obtain

$$\Omega(\boldsymbol{h}) = \lambda \sum_i |h_i| \tag{14.6}$$

$$-\log p_{\text{model}}(\boldsymbol{h}) = \sum_i \left(\lambda |h_i| - \log \frac{\lambda}{2} \right) = \Omega(\boldsymbol{h}) + \text{const} \tag{14.7}$$

where the constant term depends only on λ and not $\boldsymbol{h}$. We typically treat λ as a hyperparameter and discard the constant term since it does not affect the parameter learning. Other priors such as the Student-t prior can also induce sparsity. From this point of view of sparsity as resulting from the effect of $p_{\text{model}}(\boldsymbol{h})$ on approximate maximum likelihood learning, the sparsity penalty is not a regularization term at all. It is just a consequence of the model's distribution over its latent variables. This view provides a different motivation for training an autoencoder: it is a way of approximately training a generative model. It also provides a different reason for

why the features learned by the autoencoder are useful: they describe the latent variables that explain the input.

Early work on sparse autoencoders (Ranzato *et al.*, 2007a, 2008) explored various forms of sparsity and proposed a connection between the sparsity penalty and the $\log Z$ term that arises when applying maximum likelihood to an undirected probabilistic model $p(\boldsymbol{x}) = \frac{1}{Z}\tilde{p}(\boldsymbol{x})$. The idea is that minimizing $\log Z$ prevents a probabilistic model from having high probability everywhere, and imposing sparsity on an autoencoder prevents the autoencoder from having low reconstruction error everywhere. In this case, the connection is on the level of an intuitive understanding of a general mechanism rather than a mathematical correspondence. The interpretation of the sparsity penalty as corresponding to $\log p_{\text{model}}(\boldsymbol{h})$ in a directed model $p_{\text{model}}(\boldsymbol{h})p_{\text{model}}(\boldsymbol{x} \mid \boldsymbol{h})$ is more mathematically straightforward.

One way to achieve *actual zeros* in $\boldsymbol{h}$ for sparse (and denoising) autoencoders was introduced in Glorot *et al.* (2011b). The idea is to use rectified linear units to produce the code layer. With a prior that actually pushes the representations to zero (like the absolute value penalty), one can thus indirectly control the average number of zeros in the representation.

14.2.2 Denoising Autoencoders

Rather than adding a penalty Ω to the cost function, we can obtain an autoencoder that learns something useful by changing the reconstruction error term of the cost function.

Traditionally, autoencoders minimize some function

$$L(\boldsymbol{x}, g(f(\boldsymbol{x}))) \tag{14.8}$$

where L is a loss function penalizing $g(f(\boldsymbol{x}))$ for being dissimilar from $\boldsymbol{x}$, such as the L^2 norm of their difference. This encourages $g \circ f$ to learn to be merely an identity function if they have the capacity to do so.

A **denoising autoencoder** or DAE instead minimizes

$$L(\boldsymbol{x}, g(f(\tilde{\boldsymbol{x}}))), \tag{14.9}$$

where $\tilde{\boldsymbol{x}}$ is a copy of $\boldsymbol{x}$ that has been corrupted by some form of noise. Denoising autoencoders must therefore undo this corruption rather than simply copying their input.

Denoising training forces f and g to implicitly learn the structure of $p_{\text{data}}(\boldsymbol{x})$, as shown by Alain and Bengio (2013) and Bengio *et al.* (2013c). Denoising

autoencoders thus provide yet another example of how useful properties can emerge as a byproduct of minimizing reconstruction error. They are also an example of how overcomplete, high-capacity models may be used as autoencoders so long as care is taken to prevent them from learning the identity function. Denoising autoencoders are presented in more detail in section 14.5.

14.2.3 Regularizing by Penalizing Derivatives

Another strategy for regularizing an autoencoder is to use a penalty Ω as in sparse autoencoders,

$$L(\boldsymbol{x}, g(f(\boldsymbol{x}))) + \Omega(\boldsymbol{h}, \boldsymbol{x}), \tag{14.10}$$

but with a different form of Ω:

$$\Omega(\boldsymbol{h}, \boldsymbol{x}) = \lambda \sum_i ||\nabla_{\boldsymbol{x}} h_i||^2. \tag{14.11}$$

This forces the model to learn a function that does not change much when $\boldsymbol{x}$ changes slightly. Because this penalty is applied only at training examples, it forces the autoencoder to learn features that capture information about the training distribution.

An autoencoder regularized in this way is called a **contractive autoencoder** or CAE. This approach has theoretical connections to denoising autoencoders, manifold learning and probabilistic modeling. The CAE is described in more detail in section 14.7.

14.3 Representational Power, Layer Size and Depth

Autoencoders are often trained with only a single layer encoder and a single layer decoder. However, this is not a requirement. In fact, using deep encoders and decoders offers many advantages.

Recall from section 6.4.1 that there are many advantages to depth in a feedforward network. Because autoencoders are feedforward networks, these advantages also apply to autoencoders. Moreover, the encoder is itself a feedforward network as is the decoder, so each of these components of the autoencoder can individually benefit from depth.

One major advantage of non-trivial depth is that the universal approximator theorem guarantees that a feedforward neural network with at least one hidden layer can represent an approximation of any function (within a broad class) to an

arbitrary degree of accuracy, provided that it has enough hidden units. This means that an autoencoder with a single hidden layer is able to represent the identity function along the domain of the data arbitrarily well. However, the mapping from input to code is shallow. This means that we are not able to enforce arbitrary constraints, such as that the code should be sparse. A deep autoencoder, with at least one additional hidden layer inside the encoder itself, can approximate any mapping from input to code arbitrarily well, given enough hidden units.

Depth can exponentially reduce the computational cost of representing some functions. Depth can also exponentially decrease the amount of training data needed to learn some functions. See section 6.4.1 for a review of the advantages of depth in feedforward networks.

Experimentally, deep autoencoders yield much better compression than corresponding shallow or linear autoencoders (Hinton and Salakhutdinov, 2006).

A common strategy for training a deep autoencoder is to greedily pretrain the deep architecture by training a stack of shallow autoencoders, so we often encounter shallow autoencoders, even when the ultimate goal is to train a deep autoencoder.

14.4 Stochastic Encoders and Decoders

Autoencoders are just feedforward networks. The same loss functions and output unit types that can be used for traditional feedforward networks are also used for autoencoders.

As described in section 6.2.2.4, a general strategy for designing the output units and the loss function of a feedforward network is to define an output distribution $p(\boldsymbol{y} \mid \boldsymbol{x})$ and minimize the negative log-likelihood $-\log p(\boldsymbol{y} \mid \boldsymbol{x})$. In that setting, $\boldsymbol{y}$ was a vector of targets, such as class labels.

In the case of an autoencoder, $\boldsymbol{x}$ is now the target as well as the input. However, we can still apply the same machinery as before. Given a hidden code $\boldsymbol{h}$, we may think of the decoder as providing a conditional distribution $p_{\text{decoder}}(\boldsymbol{x} \mid \boldsymbol{h})$. We may then train the autoencoder by minimizing $-\log p_{\text{decoder}}(\boldsymbol{x} \mid \boldsymbol{h})$. The exact form of this loss function will change depending on the form of p_{decoder}. As with traditional feedforward networks, we usually use linear output units to parametrize the mean of a Gaussian distribution if $\boldsymbol{x}$ is real-valued. In that case, the negative log-likelihood yields a mean squared error criterion. Similarly, binary $\boldsymbol{x}$ values correspond to a Bernoulli distribution whose parameters are given by a sigmoid output unit, discrete $\boldsymbol{x}$ values correspond to a softmax distribution, and so on.

Typically, the output variables are treated as being conditionally independent given $\boldsymbol{h}$ so that this probability distribution is inexpensive to evaluate, but some techniques such as mixture density outputs allow tractable modeling of outputs with correlations.

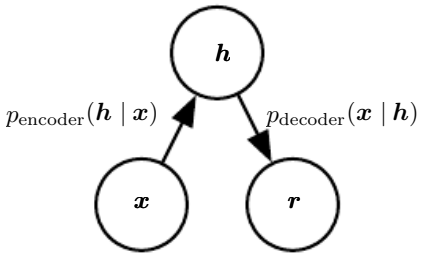

Figure 14.2: The structure of a stochastic autoencoder, in which both the encoder and the decoder are not simple functions but instead involve some noise injection, meaning that their output can be seen as sampled from a distribution, $p_{\text{encoder}}(\boldsymbol{h} \mid \boldsymbol{x})$ for the encoder and $p_{\text{decoder}}(\boldsymbol{x} \mid \boldsymbol{h})$ for the decoder.

To make a more radical departure from the feedforward networks we have seen previously, we can also generalize the notion of an **encoding function** $f(\boldsymbol{x})$ to an **encoding distribution** $p_{\text{encoder}}(\boldsymbol{h} \mid \boldsymbol{x})$, as illustrated in figure 14.2.

Any latent variable model $p_{\text{model}}(\boldsymbol{h}, \boldsymbol{x})$ defines a stochastic encoder

$$p_{\text{encoder}}(\boldsymbol{h} \mid \boldsymbol{x}) = p_{\text{model}}(\boldsymbol{h} \mid \boldsymbol{x}) \tag{14.12}$$

and a stochastic decoder

$$p_{\text{decoder}}(\boldsymbol{x} \mid \boldsymbol{h}) = p_{\text{model}}(\boldsymbol{x} \mid \boldsymbol{h}). \tag{14.13}$$

In general, the encoder and decoder distributions are not necessarily conditional distributions compatible with a unique joint distribution $p_{\text{model}}(\boldsymbol{x}, \boldsymbol{h})$. Alain *et al.* (2015) showed that training the encoder and decoder as a denoising autoencoder will tend to make them compatible asymptotically (with enough capacity and examples).

14.5 Denoising Autoencoders

The **denoising autoencoder** (DAE) is an autoencoder that receives a corrupted data point as input and is trained to predict the original, uncorrupted data point as its output.

The DAE training procedure is illustrated in figure 14.3. We introduce a corruption process $C(\tilde{\mathbf{x}} \mid \mathbf{x})$ which represents a conditional distribution over

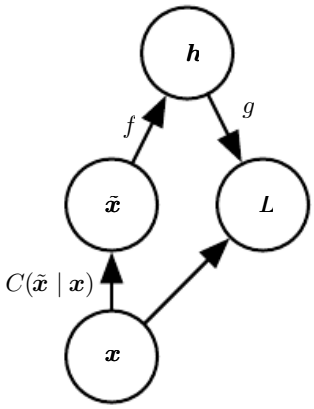

Figure 14.3: The computational graph of the cost function for a denoising autoencoder, which is trained to reconstruct the clean data point $\boldsymbol{x}$ from its corrupted version $\tilde{\boldsymbol{x}}$. This is accomplished by minimizing the loss $L = -\log p_{\text{decoder}}(\boldsymbol{x} \mid \boldsymbol{h} = f(\tilde{\boldsymbol{x}}))$, where $\tilde{\boldsymbol{x}}$ is a corrupted version of the data example $\boldsymbol{x}$, obtained through a given corruption process $C(\tilde{\boldsymbol{x}} \mid \boldsymbol{x})$. Typically the distribution p_{decoder} is a factorial distribution whose mean parameters are emitted by a feedforward network g.

corrupted samples $\tilde{\mathbf{x}}$, given a data sample $\mathbf{x}$. The autoencoder then learns a **reconstruction distribution** $p_{\text{reconstruct}}(\mathbf{x} \mid \tilde{\mathbf{x}})$ estimated from training pairs $(\boldsymbol{x}, \tilde{\boldsymbol{x}})$, as follows:

1. Sample a training example $\boldsymbol{x}$ from the training data.
2. Sample a corrupted version $\tilde{\boldsymbol{x}}$ from $C(\tilde{\mathbf{x}} \mid \mathbf{x} = \boldsymbol{x})$.
3. Use $(\boldsymbol{x}, \tilde{\boldsymbol{x}})$ as a training example for estimating the autoencoder reconstruction distribution $p_{\text{reconstruct}}(\boldsymbol{x} \mid \tilde{\boldsymbol{x}}) = p_{\text{decoder}}(\boldsymbol{x} \mid \boldsymbol{h})$ with $\boldsymbol{h}$ the output of encoder $f(\tilde{\boldsymbol{x}})$ and p_{decoder} typically defined by a decoder $g(\boldsymbol{h})$.

Typically we can simply perform gradient-based approximate minimization (such as minibatch gradient descent) on the negative log-likelihood $-\log p_{\text{decoder}}(\boldsymbol{x} \mid \boldsymbol{h})$. So long as the encoder is deterministic, the denoising autoencoder is a feedforward network and may be trained with exactly the same techniques as any other feedforward network.

We can therefore view the DAE as performing stochastic gradient descent on the following expectation:

$$-\mathbb{E}_{\mathbf{x} \sim \hat{p}_{\text{data}}(\mathbf{x})} \mathbb{E}_{\tilde{\mathbf{x}} \sim C(\tilde{\mathbf{x}} \mid \boldsymbol{x})} \log p_{\text{decoder}}(\boldsymbol{x} \mid \boldsymbol{h} = f(\tilde{\boldsymbol{x}})) \tag{14.14}$$

where $\hat{p}_{\text{data}}(\mathbf{x})$ is the training distribution.

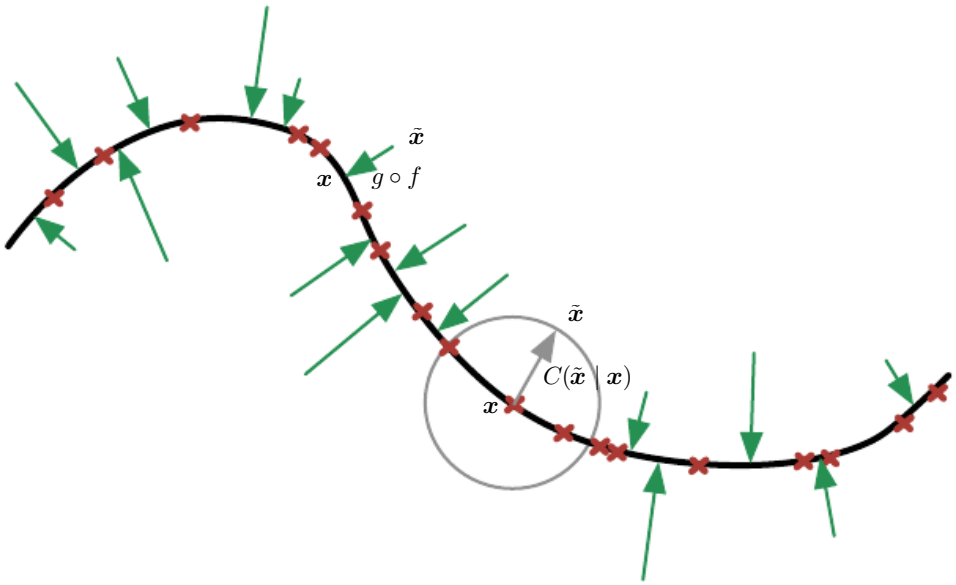

Figure 14.4: A denoising autoencoder is trained to map a corrupted data point $\tilde{\boldsymbol{x}}$ back to the original data point $\boldsymbol{x}$. We illustrate training examples $\boldsymbol{x}$ as red crosses lying near a low-dimensional manifold illustrated with the bold black line. We illustrate the corruption process $C(\tilde{\boldsymbol{x}} \mid \boldsymbol{x})$ with a gray circle of equiprobable corruptions. A gray arrow demonstrates how one training example is transformed into one sample from this corruption process. When the denoising autoencoder is trained to minimize the average of squared errors $||g(f(\tilde{\boldsymbol{x}})) - \boldsymbol{x}||^2$, the reconstruction $g(f(\tilde{\boldsymbol{x}}))$ estimates $\mathbb{E}_{\mathbf{x},\tilde{\mathbf{x}} \sim p_{\text{data}}(\mathbf{x}) C(\tilde{\mathbf{x}} \mid \mathbf{x})}[\mathbf{x} \mid \tilde{\boldsymbol{x}}]$. The vector $g(f(\tilde{\boldsymbol{x}})) - \tilde{\boldsymbol{x}}$ points approximately towards the nearest point on the manifold, since $g(f(\tilde{\boldsymbol{x}}))$ estimates the center of mass of the clean points $\boldsymbol{x}$ which could have given rise to $\tilde{\boldsymbol{x}}$. The autoencoder thus learns a vector field $g(f(\boldsymbol{x})) - \boldsymbol{x}$ indicated by the green arrows. This vector field estimates the score $\nabla_{\boldsymbol{x}} \log p_{\text{data}}(\boldsymbol{x})$ up to a multiplicative factor that is the average root mean square reconstruction error.

14.5.1 Estimating the Score

Score matching (Hyvärinen, 2005) is an alternative to maximum likelihood. It provides a consistent estimator of probability distributions based on encouraging the model to have the same **score** as the data distribution at every training point $\boldsymbol{x}$. In this context, the score is a particular gradient field:

$$\nabla_{\boldsymbol{x}} \log p(\boldsymbol{x}). \tag{14.15}$$

Score matching is discussed further in section 18.4. For the present discussion regarding autoencoders, it is sufficient to understand that learning the gradient field of $\log p_{\text{data}}$ is one way to learn the structure of p_{data} itself.

A very important property of DAEs is that their training criterion (with conditionally Gaussian $p(\boldsymbol{x} \mid \boldsymbol{h})$) makes the autoencoder learn a vector field $(g(f(\boldsymbol{x})) - \boldsymbol{x})$ that estimates the score of the data distribution. This is illustrated in figure 14.4.

Denoising training of a specific kind of autoencoder (sigmoidal hidden units, linear reconstruction units) using Gaussian noise and mean squared error as the reconstruction cost is equivalent (Vincent, 2011) to training a specific kind of undirected probabilistic model called an RBM with Gaussian visible units. This kind of model will be described in detail in section 20.5.1; for the present discussion it suffices to know that it is a model that provides an explicit $p_{\text{model}}(\boldsymbol{x}; \boldsymbol{\theta})$. When the RBM is trained using **denoising score matching** (Kingma and LeCun, 2010), its learning algorithm is equivalent to denoising training in the corresponding autoencoder. With a fixed noise level, regularized score matching is not a consistent estimator; it instead recovers a blurred version of the distribution. However, if the noise level is chosen to approach 0 when the number of examples approaches infinity, then consistency is recovered. Denoising score matching is discussed in more detail in section 18.5.

Other connections between autoencoders and RBMs exist. Score matching applied to RBMs yields a cost function that is identical to reconstruction error combined with a regularization term similar to the contractive penalty of the CAE (Swersky *et al.*, 2011). Bengio and Delalleau (2009) showed that an autoencoder gradient provides an approximation to contrastive divergence training of RBMs.

For continuous-valued $\boldsymbol{x}$, the denoising criterion with Gaussian corruption and reconstruction distribution yields an estimator of the score that is applicable to general encoder and decoder parametrizations (Alain and Bengio, 2013). This means a generic encoder-decoder architecture may be made to estimate the score

by training with the squared error criterion

$$||g(f(\tilde{\boldsymbol{x}})) - \boldsymbol{x}||^2 \tag{14.16}$$

and corruption

$$C(\tilde{\mathbf{x}} = \tilde{\boldsymbol{x}}|\boldsymbol{x}) = \mathcal{N}(\tilde{\boldsymbol{x}}; \mu = \boldsymbol{x}, \Sigma = \sigma^2 I) \tag{14.17}$$

with noise variance σ^2. See figure 14.5 for an illustration of how this works.

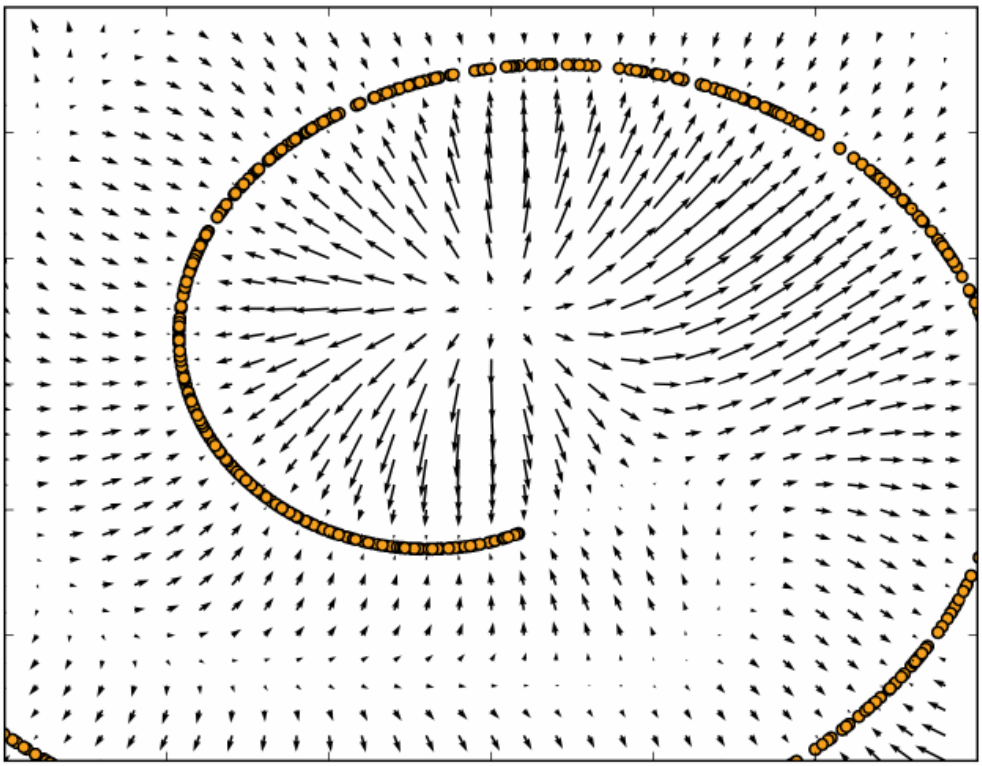

Figure 14.5: Vector field learned by a denoising autoencoder around a 1-D curved manifold near which the data concentrates in a 2-D space. Each arrow is proportional to the reconstruction minus input vector of the autoencoder and points towards higher probability according to the implicitly estimated probability distribution. The vector field has zeros at both maxima of the estimated density function (on the data manifolds) and at minima of that density function. For example, the spiral arm forms a one-dimensional manifold of local maxima that are connected to each other. Local minima appear near the middle of the gap between two arms. When the norm of reconstruction error (shown by the length of the arrows) is large, it means that probability can be significantly increased by moving in the direction of the arrow, and that is mostly the case in places of low probability. The autoencoder maps these low probability points to higher probability reconstructions. Where probability is maximal, the arrows shrink because the reconstruction becomes more accurate. Figure reproduced with permission from Alain and Bengio (2013).

In general, there is no guarantee that the reconstruction $g(f(\boldsymbol{x}))$ minus the input $\boldsymbol{x}$ corresponds to the gradient of any function, let alone to the score. That is

why the early results (Vincent, 2011) are specialized to particular parametrizations where $g(f(\boldsymbol{x})) - \boldsymbol{x}$ may be obtained by taking the derivative of another function. Kamyshanska and Memisevic (2015) generalized the results of Vincent (2011) by identifying a family of shallow autoencoders such that $g(f(\boldsymbol{x})) - \boldsymbol{x}$ corresponds to a score for all members of the family.

So far we have described only how the denoising autoencoder learns to represent a probability distribution. More generally, one may want to use the autoencoder as a generative model and draw samples from this distribution. This will be described later, in section 20.11.

14.5.1.1 Historical Perspective

The idea of using MLPs for denoising dates back to the work of LeCun (1987) and Gallinari *et al.* (1987). Behnke (2001) also used recurrent networks to denoise images. Denoising autoencoders are, in some sense, just MLPs trained to denoise. However, the name "denoising autoencoder" refers to a model that is intended not merely to learn to denoise its input but to learn a good internal representation as a side effect of learning to denoise. This idea came much later (Vincent *et al.*, 2008, 2010). The learned representation may then be used to pretrain a deeper unsupervised network or a supervised network. Like sparse autoencoders, sparse coding, contractive autoencoders and other regularized autoencoders, the motivation for DAEs was to allow the learning of a very high-capacity encoder while preventing the encoder and decoder from learning a useless identity function.

Prior to the introduction of the modern DAE, Inayoshi and Kurita (2005) explored some of the same goals with some of the same methods. Their approach minimizes reconstruction error in addition to a supervised objective while injecting noise in the hidden layer of a supervised MLP, with the objective to improve generalization by introducing the reconstruction error and the injected noise. However, their method was based on a linear encoder and could not learn function families as powerful as can the modern DAE.

14.6 Learning Manifolds with Autoencoders

Like many other machine learning algorithms, autoencoders exploit the idea that data concentrates around a low-dimensional manifold or a small set of such manifolds, as described in section 5.11.3. Some machine learning algorithms exploit this idea only insofar as that they learn a function that behaves correctly on the manifold but may have unusual behavior if given an input that is off the manifold.

Autoencoders take this idea further and aim to learn the structure of the manifold.

To understand how autoencoders do this, we must present some important characteristics of manifolds.

An important characterization of a manifold is the set of its **tangent planes**. At a point $\boldsymbol{x}$ on a d-dimensional manifold, the tangent plane is given by d basis vectors that span the local directions of variation allowed on the manifold. As illustrated in figure 14.6, these local directions specify how one can change $\boldsymbol{x}$ infinitesimally while staying on the manifold.

All autoencoder training procedures involve a compromise between two forces:

1. Learning a representation $\boldsymbol{h}$ of a training example $\boldsymbol{x}$ such that $\boldsymbol{x}$ can be approximately recovered from $\boldsymbol{h}$ through a decoder. The fact that $\boldsymbol{x}$ is drawn from the training data is crucial, because it means the autoencoder need not successfully reconstruct inputs that are not probable under the data generating distribution.

2. Satisfying the constraint or regularization penalty. This can be an architectural constraint that limits the capacity of the autoencoder, or it can be a regularization term added to the reconstruction cost. These techniques generally prefer solutions that are less sensitive to the input.

Clearly, neither force alone would be useful—copying the input to the output is not useful on its own, nor is ignoring the input. Instead, the two forces together are useful because they force the hidden representation to capture information about the structure of the data generating distribution. The important principle is that the autoencoder can afford to represent *only the variations that are needed to reconstruct training examples*. If the data generating distribution concentrates near a low-dimensional manifold, this yields representations that implicitly capture a local coordinate system for this manifold: only the variations tangent to the manifold around $\boldsymbol{x}$ need to correspond to changes in $\boldsymbol{h} = f(\boldsymbol{x})$. Hence the encoder learns a mapping from the input space $\boldsymbol{x}$ to a representation space, a mapping that is only sensitive to changes along the manifold directions, but that is insensitive to changes orthogonal to the manifold.

A one-dimensional example is illustrated in figure 14.7, showing that, by making the reconstruction function insensitive to perturbations of the input around the data points, we cause the autoencoder to recover the manifold structure.

To understand why autoencoders are useful for manifold learning, it is instructive to compare them to other approaches. What is most commonly learned to characterize a manifold is a **representation** of the data points on (or near)

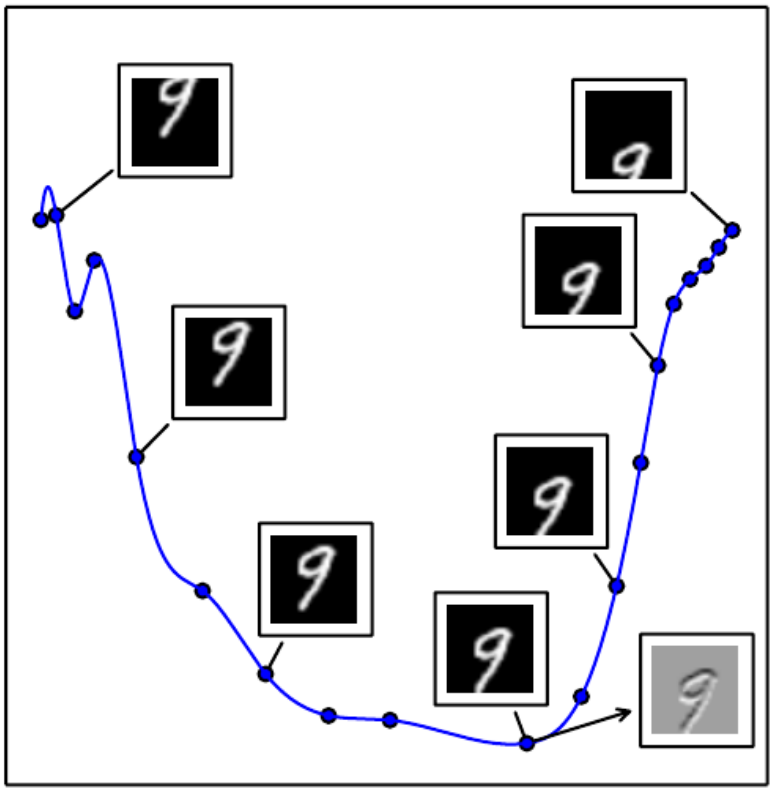

Figure 14.6: An illustration of the concept of a tangent hyperplane. Here we create a one-dimensional manifold in 784-dimensional space. We take an MNIST image with 784 pixels and transform it by translating it vertically. The amount of vertical translation defines a coordinate along a one-dimensional manifold that traces out a curved path through image space. This plot shows a few points along this manifold. For visualization, we have projected the manifold into two dimensional space using PCA. An n-dimensional manifold has an n-dimensional tangent plane at every point. This tangent plane touches the manifold exactly at that point and is oriented parallel to the surface at that point. It defines the space of directions in which it is possible to move while remaining on the manifold. This one-dimensional manifold has a single tangent line. We indicate an example tangent line at one point, with an image showing how this tangent direction appears in image space. Gray pixels indicate pixels that do not change as we move along the tangent line, white pixels indicate pixels that brighten, and black pixels indicate pixels that darken.

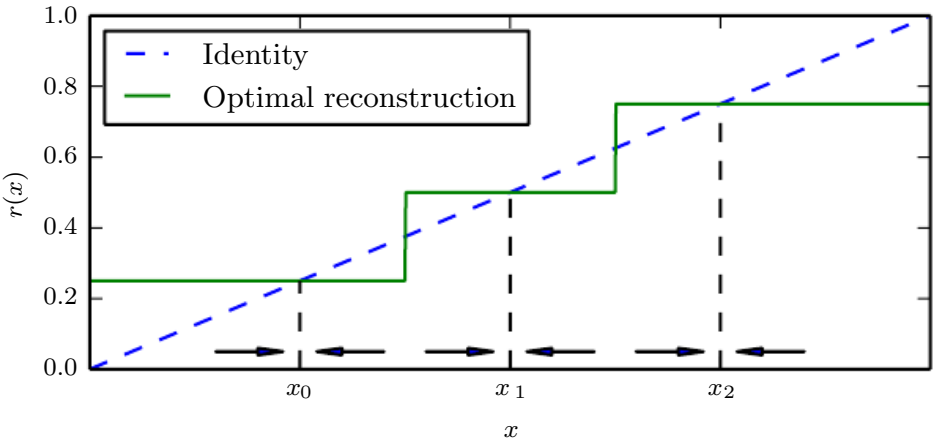

Figure 14.7: If the autoencoder learns a reconstruction function that is invariant to small perturbations near the data points, it captures the manifold structure of the data. Here the manifold structure is a collection of 0-dimensional manifolds. The dashed diagonal line indicates the identity function target for reconstruction. The optimal reconstruction function crosses the identity function wherever there is a data point. The horizontal arrows at the bottom of the plot indicate the $r(\boldsymbol{x}) - \boldsymbol{x}$ reconstruction direction vector at the base of the arrow, in input space, always pointing towards the nearest "manifold" (a single datapoint, in the 1-D case). The denoising autoencoder explicitly tries to make the derivative of the reconstruction function $r(\boldsymbol{x})$ small around the data points. The contractive autoencoder does the same for the encoder. Although the derivative of $r(\boldsymbol{x})$ is asked to be small around the data points, it can be large between the data points. The space between the data points corresponds to the region between the manifolds, where the reconstruction function must have a large derivative in order to map corrupted points back onto the manifold.

the manifold. Such a representation for a particular example is also called its embedding. It is typically given by a low-dimensional vector, with less dimensions than the "ambient" space of which the manifold is a low-dimensional subset. Some algorithms (non-parametric manifold learning algorithms, discussed below) directly learn an embedding for each training example, while others learn a more general mapping, sometimes called an encoder, or representation function, that maps any point in the ambient space (the input space) to its embedding.

Manifold learning has mostly focused on unsupervised learning procedures that attempt to capture these manifolds. Most of the initial machine learning research on learning nonlinear manifolds has focused on **non-parametric** methods based on the **nearest-neighbor graph**. This graph has one node per training example and edges connecting near neighbors to each other. These methods (Schölkopf *et al.*, 1998; Roweis and Saul, 2000; Tenenbaum *et al.*, 2000; Brand, 2003; Belkin

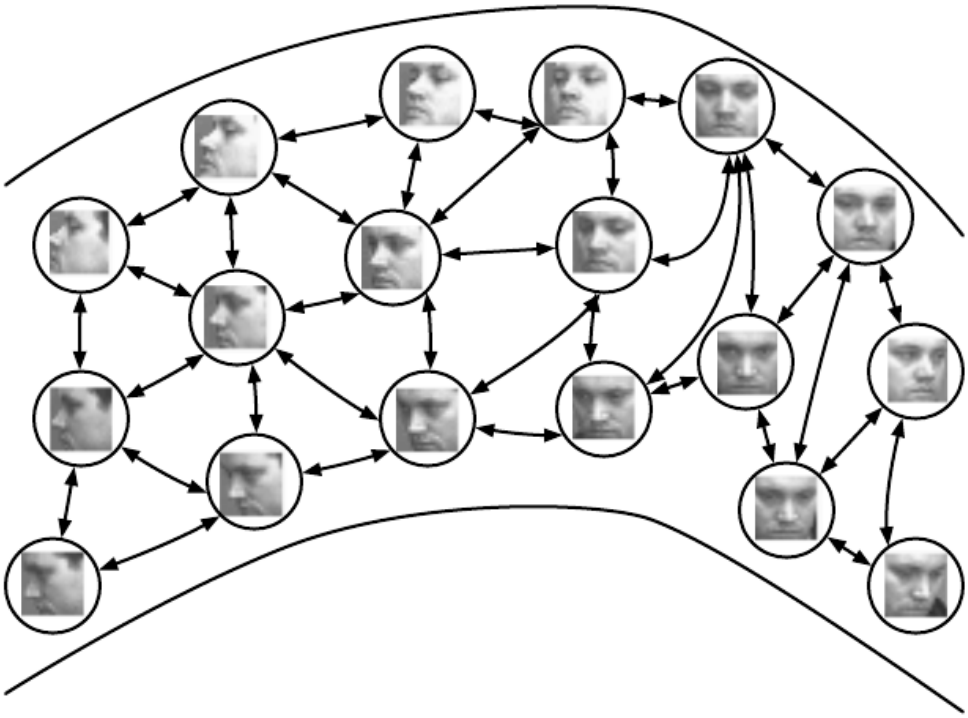

Figure 14.8: Non-parametric manifold learning procedures build a nearest neighbor graph in which nodes represent training examples a directed edges indicate nearest neighbor relationships. Various procedures can thus obtain the tangent plane associated with a neighborhood of the graph as well as a coordinate system that associates each training example with a real-valued vector position, or **embedding**. It is possible to generalize such a representation to new examples by a form of interpolation. So long as the number of examples is large enough to cover the curvature and twists of the manifold, these approaches work well. Images from the QMUL Multiview Face Dataset (Gong *et al.*, 2000).

and Niyogi, 2003; Donoho and Grimes, 2003; Weinberger and Saul, 2004; Hinton and Roweis, 2003; van der Maaten and Hinton, 2008) associate each of nodes with a tangent plane that spans the directions of variations associated with the difference vectors between the example and its neighbors, as illustrated in figure 14.8.

A global coordinate system can then be obtained through an optimization or solving a linear system. Figure 14.9 illustrates how a manifold can be tiled by a large number of locally linear Gaussian-like patches (or "pancakes," because the Gaussians are flat in the tangent directions).

However, there is a fundamental difficulty with such local non-parametric approaches to manifold learning, raised in Bengio and Monperrus (2005): if the manifolds are not very smooth (they have many peaks and troughs and twists), one may need a very large number of training examples to cover each one of

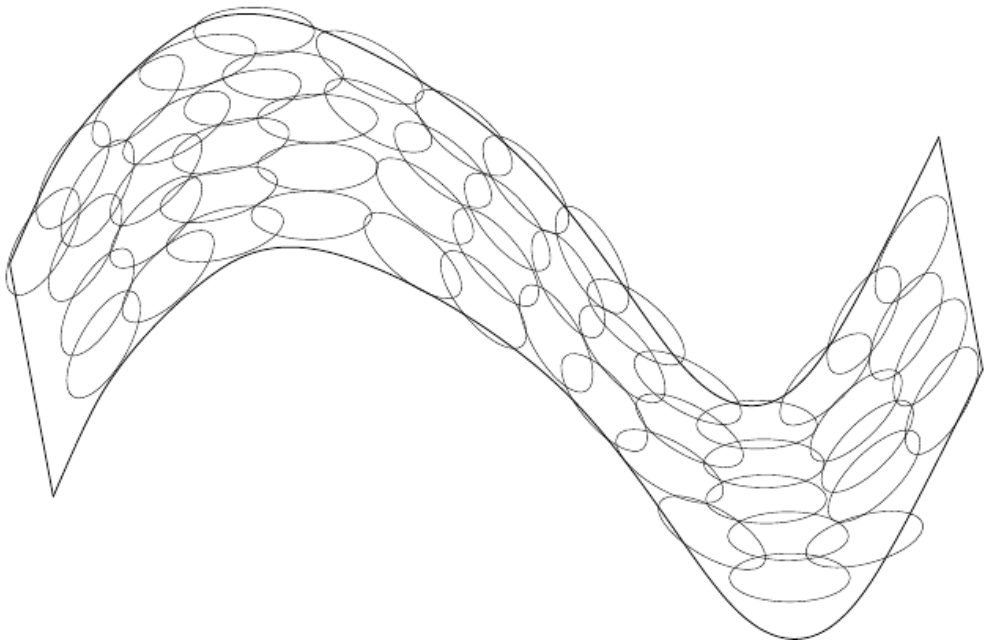

Figure 14.9: If the tangent planes (see figure 14.6) at each location are known, then they can be tiled to form a global coordinate system or a density function. Each local patch can be thought of as a local Euclidean coordinate system or as a locally flat Gaussian, or "pancake," with a very small variance in the directions orthogonal to the pancake and a very large variance in the directions defining the coordinate system on the pancake. A mixture of these Gaussians provides an estimated density function, as in the manifold Parzen window algorithm (Vincent and Bengio, 2003) or its non-local neural-net based variant (Bengio *et al.*, 2006c).

these variations, with no chance to generalize to unseen variations. Indeed, these methods can only generalize the shape of the manifold by interpolating between neighboring examples. Unfortunately, the manifolds involved in AI problems can have very complicated structure that can be difficult to capture from only local interpolation. Consider for example the manifold resulting from translation shown in figure 14.6. If we watch just one coordinate within the input vector, x_i, as the image is translated, we will observe that one coordinate encounters a peak or a trough in its value once for every peak or trough in brightness in the image. In other words, the complexity of the patterns of brightness in an underlying image template drives the complexity of the manifolds that are generated by performing simple image transformations. This motivates the use of distributed representations and deep learning for capturing manifold structure.

14.7 Contractive Autoencoders

The contractive autoencoder (Rifai *et al.*, 2011a,b) introduces an explicit regularizer on the code $\boldsymbol{h} = f(\boldsymbol{x})$, encouraging the derivatives of f to be as small as possible:

$$\Omega(\boldsymbol{h}) = \lambda \left\| \frac{\partial f(\boldsymbol{x})}{\partial \boldsymbol{x}} \right\|_F^2 . \tag{14.18}$$

The penalty $\Omega(\boldsymbol{h})$ is the squared Frobenius norm (sum of squared elements) of the Jacobian matrix of partial derivatives associated with the encoder function.

There is a connection between the denoising autoencoder and the contractive autoencoder: Alain and Bengio (2013) showed that in the limit of small Gaussian input noise, the denoising reconstruction error is equivalent to a contractive penalty on the reconstruction function that maps $\boldsymbol{x}$ to $\boldsymbol{r} = g(f(\boldsymbol{x}))$. In other words, denoising autoencoders make the reconstruction function resist small but finite-sized perturbations of the input, while contractive autoencoders make the feature extraction function resist infinitesimal perturbations of the input. When using the Jacobian-based contractive penalty to pretrain features $f(\boldsymbol{x})$ for use with a classifier, the best classification accuracy usually results from applying the contractive penalty to $f(\boldsymbol{x})$ rather than to $g(f(\boldsymbol{x}))$. A contractive penalty on $f(\boldsymbol{x})$ also has close connections to score matching, as discussed in section 14.5.1.

The name **contractive** arises from the way that the CAE warps space. Specifically, because the CAE is trained to resist perturbations of its input, it is encouraged to map a neighborhood of input points to a smaller neighborhood of output points. We can think of this as contracting the input neighborhood to a smaller output neighborhood.

To clarify, the CAE is contractive only locally—all perturbations of a training point $\boldsymbol{x}$ are mapped near to $f(\boldsymbol{x})$. Globally, two different points $\boldsymbol{x}$ and $\boldsymbol{x}'$ may be mapped to $f(\boldsymbol{x})$ and $f(\boldsymbol{x}')$ points that are farther apart than the original points. It is plausible that f be expanding in-between or far from the data manifolds (see for example what happens in the 1-D toy example of figure 14.7). When the $\Omega(\boldsymbol{h})$ penalty is applied to sigmoidal units, one easy way to shrink the Jacobian is to make the sigmoid units saturate to 0 or 1. This encourages the CAE to encode input points with extreme values of the sigmoid that may be interpreted as a binary code. It also ensures that the CAE will spread its code values throughout most of the hypercube that its sigmoidal hidden units can span.

We can think of the Jacobian matrix $\boldsymbol{J}$ at a point $\boldsymbol{x}$ as approximating the nonlinear encoder $f(\boldsymbol{x})$ as being a linear operator. This allows us to use the word "contractive" more formally. In the theory of linear operators, a linear operator

is said to be contractive if the norm of $\boldsymbol{J}\boldsymbol{x}$ remains less than or equal to 1 for all unit-norm $\boldsymbol{x}$. In other words, $\boldsymbol{J}$ is contractive if it shrinks the unit sphere. We can think of the CAE as penalizing the Frobenius norm of the local linear approximation of $f(\boldsymbol{x})$ at every training point $\boldsymbol{x}$ in order to encourage each of these local linear operator to become a contraction.

As described in section 14.6, regularized autoencoders learn manifolds by balancing two opposing forces. In the case of the CAE, these two forces are reconstruction error and the contractive penalty $\Omega(\boldsymbol{h})$. Reconstruction error alone would encourage the CAE to learn an identity function. The contractive penalty alone would encourage the CAE to learn features that are constant with respect to $\boldsymbol{x}$. The compromise between these two forces yields an autoencoder whose derivatives $\frac{\partial f(\boldsymbol{x})}{\partial \boldsymbol{x}}$ are mostly tiny. Only a small number of hidden units, corresponding to a small number of directions in the input, may have significant derivatives.

The goal of the CAE is to learn the manifold structure of the data. Directions $\boldsymbol{x}$ with large $\boldsymbol{J}\boldsymbol{x}$ rapidly change $\boldsymbol{h}$, so these are likely to be directions which approximate the tangent planes of the manifold. Experiments by Rifai *et al.* (2011a) and Rifai *et al.* (2011b) show that training the CAE results in most singular values of $\boldsymbol{J}$ dropping below 1 in magnitude and therefore becoming contractive. However, some singular values remain above 1, because the reconstruction error penalty encourages the CAE to encode the directions with the most local variance. The directions corresponding to the largest singular values are interpreted as the tangent directions that the contractive autoencoder has learned. Ideally, these tangent directions should correspond to real variations in the data. For example, a CAE applied to images should learn tangent vectors that show how the image changes as objects in the image gradually change pose, as shown in figure 14.6. Visualizations of the experimentally obtained singular vectors do seem to correspond to meaningful transformations of the input image, as shown in figure 14.10.

One practical issue with the CAE regularization criterion is that although it is cheap to compute in the case of a single hidden layer autoencoder, it becomes much more expensive in the case of deeper autoencoders. The strategy followed by Rifai *et al.* (2011a) is to separately train a series of single-layer autoencoders, each trained to reconstruct the previous autoencoder's hidden layer. The composition of these autoencoders then forms a deep autoencoder. Because each layer was separately trained to be locally contractive, the deep autoencoder is contractive as well. The result is not the same as what would be obtained by jointly training the entire architecture with a penalty on the Jacobian of the deep model, but it captures many of the desirable qualitative characteristics.

Another practical issue is that the contraction penalty can obtain useless results

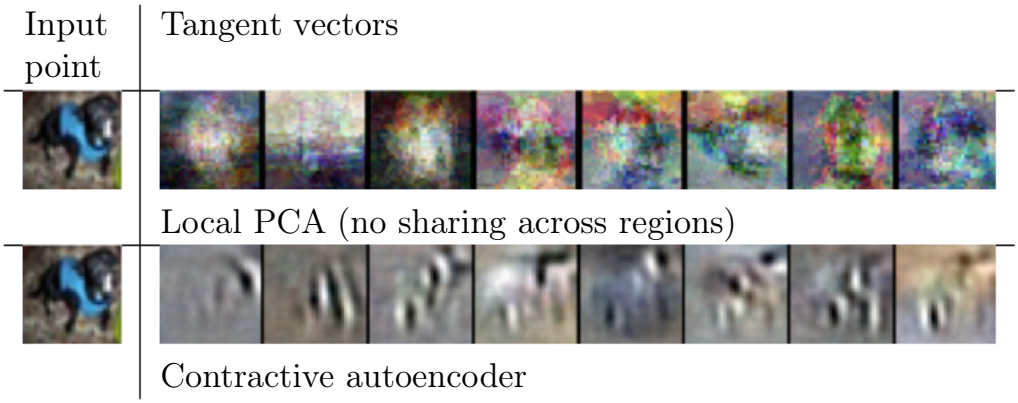

Figure 14.10: Illustration of tangent vectors of the manifold estimated by local PCA and by a contractive autoencoder. The location on the manifold is defined by the input image of a dog drawn from the CIFAR-10 dataset. The tangent vectors are estimated by the leading singular vectors of the Jacobian matrix $\frac{\partial \boldsymbol{h}}{\partial \boldsymbol{x}}$ of the input-to-code mapping. Although both local PCA and the CAE can capture local tangents, the CAE is able to form more accurate estimates from limited training data because it exploits parameter sharing across different locations that share a subset of active hidden units. The CAE tangent directions typically correspond to moving or changing parts of the object (such as the head or legs). Images reproduced with permission from Rifai *et al.* (2011c).

if we do not impose some sort of scale on the decoder. For example, the encoder could consist of multiplying the input by a small constant ϵ and the decoder could consist of dividing the code by ϵ. As ϵ approaches 0, the encoder drives the contractive penalty $\Omega(\boldsymbol{h})$ to approach 0 without having learned anything about the distribution. Meanwhile, the decoder maintains perfect reconstruction. In Rifai *et al.* (2011a), this is prevented by tying the weights of f and g. Both f and g are standard neural network layers consisting of an affine transformation followed by an element-wise nonlinearity, so it is straightforward to set the weight matrix of g to be the transpose of the weight matrix of f.

14.8 Predictive Sparse Decomposition

Predictive sparse decomposition (PSD) is a model that is a hybrid of sparse coding and parametric autoencoders (Kavukcuoglu *et al.*, 2008). A parametric encoder is trained to predict the output of iterative inference. PSD has been applied to unsupervised feature learning for object recognition in images and video (Kavukcuoglu *et al.*, 2009, 2010; Jarrett *et al.*, 2009; Farabet *et al.*, 2011), as well as for audio (Henaff *et al.*, 2011). The model consists of an encoder $f(\boldsymbol{x})$ and a decoder $g(\boldsymbol{h})$ that are both parametric. During training, $\boldsymbol{h}$ is controlled by the

optimization algorithm. Training proceeds by minimizing

$$||\boldsymbol{x} - g(\boldsymbol{h})||^2 + \lambda|\boldsymbol{h}|_1 + \gamma||\boldsymbol{h} - f(\boldsymbol{x})||^2. \tag{14.19}$$

Like in sparse coding, the training algorithm alternates between minimization with respect to $\boldsymbol{h}$ and minimization with respect to the model parameters. Minimization with respect to $\boldsymbol{h}$ is fast because $f(\boldsymbol{x})$ provides a good initial value of $\boldsymbol{h}$ and the cost function constrains $\boldsymbol{h}$ to remain near $f(\boldsymbol{x})$ anyway. Simple gradient descent can obtain reasonable values of $\boldsymbol{h}$ in as few as ten steps.

The training procedure used by PSD is different from first training a sparse coding model and then training $f(\boldsymbol{x})$ to predict the values of the sparse coding features. The PSD training procedure regularizes the decoder to use parameters for which $f(\boldsymbol{x})$ can infer good code values.

Predictive sparse coding is an example of **learned approximate inference**. In section 19.5, this topic is developed further. The tools presented in chapter 19 make it clear that PSD can be interpreted as training a directed sparse coding probabilistic model by maximizing a lower bound on the log-likelihood of the model.

In practical applications of PSD, the iterative optimization is only used during training. The parametric encoder f is used to compute the learned features when the model is deployed. Evaluating f is computationally inexpensive compared to inferring $\boldsymbol{h}$ via gradient descent. Because f is a differentiable parametric function, PSD models may be stacked and used to initialize a deep network to be trained with another criterion.

14.9 Applications of Autoencoders

Autoencoders have been successfully applied to dimensionality reduction and information retrieval tasks. Dimensionality reduction was one of the first applications of representation learning and deep learning. It was one of the early motivations for studying autoencoders. For example, Hinton and Salakhutdinov (2006) trained a stack of RBMs and then used their weights to initialize a deep autoencoder with gradually smaller hidden layers, culminating in a bottleneck of 30 units. The resulting code yielded less reconstruction error than PCA into 30 dimensions and the learned representation was qualitatively easier to interpret and relate to the underlying categories, with these categories manifesting as well-separated clusters.

Lower-dimensional representations can improve performance on many tasks, such as classification. Models of smaller spaces consume less memory and runtime.

Many forms of dimensionality reduction place semantically related examples near each other, as observed by Salakhutdinov and Hinton (2007b) and Torralba *et al.* (2008). The hints provided by the mapping to the lower-dimensional space aid generalization.

One task that benefits even more than usual from dimensionality reduction is **information retrieval**, the task of finding entries in a database that resemble a query entry. This task derives the usual benefits from dimensionality reduction that other tasks do, but also derives the additional benefit that search can become extremely efficient in certain kinds of low dimensional spaces. Specifically, if we train the dimensionality reduction algorithm to produce a code that is low-dimensional and *binary*, then we can store all database entries in a hash table mapping binary code vectors to entries. This hash table allows us to perform information retrieval by returning all database entries that have the same binary code as the query. We can also search over slightly less similar entries very efficiently, just by flipping individual bits from the encoding of the query. This approach to information retrieval via dimensionality reduction and binarization is called **semantic hashing** (Salakhutdinov and Hinton, 2007b, 2009b), and has been applied to both textual input (Salakhutdinov and Hinton, 2007b, 2009b) and images (Torralba *et al.*, 2008; Weiss *et al.*, 2008; Krizhevsky and Hinton, 2011).

To produce binary codes for semantic hashing, one typically uses an encoding function with sigmoids on the final layer. The sigmoid units must be trained to be saturated to nearly 0 or nearly 1 for all input values. One trick that can accomplish this is simply to inject additive noise just before the sigmoid nonlinearity during training. The magnitude of the noise should increase over time. To fight that noise and preserve as much information as possible, the network must increase the magnitude of the inputs to the sigmoid function, until saturation occurs.

The idea of learning a hashing function has been further explored in several directions, including the idea of training the representations so as to optimize a loss more directly linked to the task of finding nearby examples in the hash table (Norouzi and Fleet, 2011).

Chapter 15

Representation Learning

In this chapter, we first discuss what it means to learn representations and how the notion of representation can be useful to design deep architectures. We discuss how learning algorithms share statistical strength across different tasks, including using information from unsupervised tasks to perform supervised tasks. Shared representations are useful to handle multiple modalities or domains, or to transfer learned knowledge to tasks for which few or no examples are given but a task representation exists. Finally, we step back and argue about the reasons for the success of representation learning, starting with the theoretical advantages of distributed representations (Hinton *et al.*, 1986) and deep representations and ending with the more general idea of underlying assumptions about the data generating process, in particular about underlying causes of the observed data.

Many information processing tasks can be very easy or very difficult depending on how the information is represented. This is a general principle applicable to daily life, computer science in general, and to machine learning. For example, it is straightforward for a person to divide 210 by 6 using long division. The task becomes considerably less straightforward if it is instead posed using the Roman numeral representation of the numbers. Most modern people asked to divide CCX by VI would begin by converting the numbers to the Arabic numeral representation, permitting long division procedures that make use of the place value system. More concretely, we can quantify the asymptotic runtime of various operations using appropriate or inappropriate representations. For example, inserting a number into the correct position in a sorted list of numbers is an $O(n)$ operation if the list is represented as a linked list, but only $O(\log n)$ if the list is represented as a red-black tree.

In the context of machine learning, what makes one representation better than

another? Generally speaking, a good representation is one that makes a subsequent learning task easier. The choice of representation will usually depend on the choice of the subsequent learning task.

We can think of feedforward networks trained by supervised learning as performing a kind of representation learning. Specifically, the last layer of the network is typically a linear classifier, such as a softmax regression classifier. The rest of the network learns to provide a representation to this classifier. Training with a supervised criterion naturally leads to the representation at every hidden layer (but more so near the top hidden layer) taking on properties that make the classification task easier. For example, classes that were not linearly separable in the input features may become linearly separable in the last hidden layer. In principle, the last layer could be another kind of model, such as a nearest neighbor classifier (Salakhutdinov and Hinton, 2007a). The features in the penultimate layer should learn different properties depending on the type of the last layer.

Supervised training of feedforward networks does not involve explicitly imposing any condition on the learned intermediate features. Other kinds of representation learning algorithms are often explicitly designed to shape the representation in some particular way. For example, suppose we want to learn a representation that makes density estimation easier. Distributions with more independences are easier to model, so we could design an objective function that encourages the elements of the representation vector $\boldsymbol{h}$ to be independent. Just like supervised networks, unsupervised deep learning algorithms have a main training objective but also learn a representation as a side effect. Regardless of how a representation was obtained, it can be used for another task. Alternatively, multiple tasks (some supervised, some unsupervised) can be learned together with some shared internal representation.

Most representation learning problems face a tradeoff between preserving as much information about the input as possible and attaining nice properties (such as independence).

Representation learning is particularly interesting because it provides one way to perform unsupervised and semi-supervised learning. We often have very large amounts of unlabeled training data and relatively little labeled training data. Training with supervised learning techniques on the labeled subset often results in severe overfitting. Semi-supervised learning offers the chance to resolve this overfitting problem by also learning from the unlabeled data. Specifically, we can learn good representations for the unlabeled data, and then use these representations to solve the supervised learning task.

Humans and animals are able to learn from very few labeled examples. We do

not yet know how this is possible. Many factors could explain improved human performance—for example, the brain may use very large ensembles of classifiers or Bayesian inference techniques. One popular hypothesis is that the brain is able to leverage unsupervised or semi-supervised learning. There are many ways to leverage unlabeled data. In this chapter, we focus on the hypothesis that the unlabeled data can be used to learn a good representation.

15.1 Greedy Layer-Wise Unsupervised Pretraining

Unsupervised learning played a key historical role in the revival of deep neural networks, enabling researchers for the first time to train a deep supervised network without requiring architectural specializations like convolution or recurrence. We call this procedure **unsupervised pretraining**, or more precisely, **greedy layer-wise unsupervised pretraining**. This procedure is a canonical example of how a representation learned for one task (unsupervised learning, trying to capture the shape of the input distribution) can sometimes be useful for another task (supervised learning with the same input domain).

Greedy layer-wise unsupervised pretraining relies on a single-layer representation learning algorithm such as an RBM, a single-layer autoencoder, a sparse coding model, or another model that learns latent representations. Each layer is pretrained using unsupervised learning, taking the output of the previous layer and producing as output a new representation of the data, whose distribution (or its relation to other variables such as categories to predict) is hopefully simpler. See algorithm 15.1 for a formal description.

Greedy layer-wise training procedures based on unsupervised criteria have long been used to sidestep the difficulty of jointly training the layers of a deep neural net for a supervised task. This approach dates back at least as far as the Neocognitron (Fukushima, 1975). The deep learning renaissance of 2006 began with the discovery that this greedy learning procedure could be used to find a good initialization for a joint learning procedure over all the layers, and that this approach could be used to successfully train even fully connected architectures (Hinton *et al.*, 2006; Hinton and Salakhutdinov, 2006; Hinton, 2006; Bengio *et al.*, 2007; Ranzato *et al.*, 2007a). Prior to this discovery, only convolutional deep networks or networks whose depth resulted from recurrence were regarded as feasible to train. Today, we now know that greedy layer-wise pretraining is not required to train fully connected deep architectures, but the unsupervised pretraining approach was the first method to succeed.

Greedy layer-wise pretraining is called **greedy** because it is a **greedy algo-**

rithm, meaning that it optimizes each piece of the solution independently, one piece at a time, rather than jointly optimizing all pieces. It is called **layer-wise** because these independent pieces are the layers of the network. Specifically, greedy layer-wise pretraining proceeds one layer at a time, training the k-th layer while keeping the previous ones fixed. In particular, the lower layers (which are trained first) are not adapted after the upper layers are introduced. It is called **unsupervised** because each layer is trained with an unsupervised representation learning algorithm. However it is also called **pretraining**, because it is supposed to be only a first step before a joint training algorithm is applied to **fine-tune** all the layers together. In the context of a supervised learning task, it can be viewed as a regularizer (in some experiments, pretraining decreases test error without decreasing training error) and a form of parameter initialization.

It is common to use the word "pretraining" to refer not only to the pretraining stage itself but to the entire two phase protocol that combines the pretraining phase and a supervised learning phase. The supervised learning phase may involve training a simple classifier on top of the features learned in the pretraining phase, or it may involve supervised fine-tuning of the entire network learned in the pretraining phase. No matter what kind of unsupervised learning algorithm or what model type is employed, in the vast majority of cases, the overall training scheme is nearly the same. While the choice of unsupervised learning algorithm will obviously impact the details, most applications of unsupervised pretraining follow this basic protocol.

Greedy layer-wise unsupervised pretraining can also be used as initialization for other unsupervised learning algorithms, such as deep autoencoders (Hinton and Salakhutdinov, 2006) and probabilistic models with many layers of latent variables. Such models include deep belief networks (Hinton *et al.*, 2006) and deep Boltzmann machines (Salakhutdinov and Hinton, 2009a). These deep generative models will be described in chapter 20.

As discussed in section 8.7.4, it is also possible to have greedy layer-wise *supervised* pretraining. This builds on the premise that training a shallow network is easier than training a deep one, which seems to have been validated in several contexts (Erhan *et al.*, 2010).

15.1.1 When and Why Does Unsupervised Pretraining Work?

On many tasks, greedy layer-wise unsupervised pretraining can yield substantial improvements in test error for classification tasks. This observation was responsible for the renewed interested in deep neural networks starting in 2006 (Hinton *et al.*,

Algorithm 15.1 *Greedy layer-wise unsupervised pretraining protocol.*
Given the following: Unsupervised feature learning algorithm $\mathcal{L}$, which takes a training set of examples and returns an encoder or feature function f. The raw input data is $\boldsymbol{X}$, with one row per example and $f^{(1)}(\boldsymbol{X})$ is the output of the first stage encoder on $\boldsymbol{X}$. In the case where fine-tuning is performed, we use a learner $\mathcal{T}$ which takes an initial function f, input examples $\boldsymbol{X}$ (and in the supervised fine-tuning case, associated targets $\boldsymbol{Y}$), and returns a tuned function. The number of stages is m.

$f \leftarrow$ Identity function
$\tilde{\boldsymbol{X}} = \boldsymbol{X}$
for $k = 1, \ldots, m$ **do**
  $f^{(k)} = \mathcal{L}(\tilde{\boldsymbol{X}})$
  $f \leftarrow f^{(k)} \circ f$
  $\tilde{\boldsymbol{X}} \leftarrow f^{(k)}(\tilde{\boldsymbol{X}})$
end for
if *fine-tuning* ***then***
  $f \leftarrow \mathcal{T}(f, \boldsymbol{X}, \boldsymbol{Y})$
end if
Return f

2006; Bengio *et al.*, 2007; Ranzato *et al.*, 2007a). On many other tasks, however, unsupervised pretraining either does not confer a benefit or even causes noticeable harm. Ma *et al.* (2015) studied the effect of pretraining on machine learning models for chemical activity prediction and found that, on average, pretraining was slightly harmful, but for many tasks was significantly helpful. Because unsupervised pretraining is sometimes helpful but often harmful it is important to understand when and why it works in order to determine whether it is applicable to a particular task.

At the outset, it is important to clarify that most of this discussion is restricted to greedy unsupervised pretraining in particular. There are other, completely different paradigms for performing semi-supervised learning with neural networks, such as virtual adversarial training described in section 7.13. It is also possible to train an autoencoder or generative model at the same time as the supervised model. Examples of this single-stage approach include the discriminative RBM (Larochelle and Bengio, 2008) and the ladder network (Rasmus *et al.*, 2015), in which the total objective is an explicit sum of the two terms (one using the labels and one only using the input).

Unsupervised pretraining combines two different ideas. First, it makes use of

the idea that the choice of initial parameters for a deep neural network can have a significant regularizing effect on the model (and, to a lesser extent, that it can improve optimization). Second, it makes use of the more general idea that learning about the input distribution can help to learn about the mapping from inputs to outputs.

Both of these ideas involve many complicated interactions between several parts of the machine learning algorithm that are not entirely understood.

The first idea, that the choice of initial parameters for a deep neural network can have a strong regularizing effect on its performance, is the least well understood. At the time that pretraining became popular, it was understood as initializing the model in a location that would cause it to approach one local minimum rather than another. Today, local minima are no longer considered to be a serious problem for neural network optimization. We now know that our standard neural network training procedures usually do not arrive at a critical point of any kind. It remains possible that pretraining initializes the model in a location that would otherwise be inaccessible—for example, a region that is surrounded by areas where the cost function varies so much from one example to another that minibatches give only a very noisy estimate of the gradient, or a region surrounded by areas where the Hessian matrix is so poorly conditioned that gradient descent methods must use very small steps. However, our ability to characterize exactly what aspects of the pretrained parameters are retained during the supervised training stage is limited. This is one reason that modern approaches typically use simultaneous unsupervised learning and supervised learning rather than two sequential stages. One may also avoid struggling with these complicated ideas about how optimization in the supervised learning stage preserves information from the unsupervised learning stage by simply freezing the parameters for the feature extractors and using supervised learning only to add a classifier on top of the learned features.

The other idea, that a learning algorithm can use information learned in the unsupervised phase to perform better in the supervised learning stage, is better understood. The basic idea is that some features that are useful for the unsupervised task may also be useful for the supervised learning task. For example, if we train a generative model of images of cars and motorcycles, it will need to know about wheels, and about how many wheels should be in an image. If we are fortunate, the representation of the wheels will take on a form that is easy for the supervised learner to access. This is not yet understood at a mathematical, theoretical level, so it is not always possible to predict which tasks will benefit from unsupervised learning in this way. Many aspects of this approach are highly dependent on the specific models used. For example, if we wish to add a linear classifier on

top of pretrained features, the features must make the underlying classes linearly separable. These properties often occur naturally but do not always do so. This is another reason that simultaneous supervised and unsupervised learning can be preferable—the constraints imposed by the output layer are naturally included from the start.

From the point of view of unsupervised pretraining as learning a representation, we can expect unsupervised pretraining to be more effective when the initial representation is poor. One key example of this is the use of word embeddings. Words represented by one-hot vectors are not very informative because every two distinct one-hot vectors are the same distance from each other (squared L^2 distance of 2). Learned word embeddings naturally encode similarity between words by their distance from each other. Because of this, unsupervised pretraining is especially useful when processing words. It is less useful when processing images, perhaps because images already lie in a rich vector space where distances provide a low quality similarity metric.

From the point of view of unsupervised pretraining as a regularizer, we can expect unsupervised pretraining to be most helpful when the number of labeled examples is very small. Because the source of information added by unsupervised pretraining is the unlabeled data, we may also expect unsupervised pretraining to perform best when the number of unlabeled examples is very large. The advantage of semi-supervised learning via unsupervised pretraining with many unlabeled examples and few labeled examples was made particularly clear in 2011 with unsupervised pretraining winning two international transfer learning competitions (Mesnil *et al.*, 2011; Goodfellow *et al.*, 2011), in settings where the number of labeled examples in the target task was small (from a handful to dozens of examples per class). These effects were also documented in carefully controlled experiments by Paine *et al.* (2014).

Other factors are likely to be involved. For example, unsupervised pretraining is likely to be most useful when the function to be learned is extremely complicated. Unsupervised learning differs from regularizers like weight decay because it does not bias the learner toward discovering a simple function but rather toward discovering feature functions that are useful for the unsupervised learning task. If the true underlying functions are complicated and shaped by regularities of the input distribution, unsupervised learning can be a more appropriate regularizer.

These caveats aside, we now analyze some success cases where unsupervised pretraining is known to cause an improvement, and explain what is known about why this improvement occurs. Unsupervised pretraining has usually been used to improve classifiers, and is usually most interesting from the point of view of

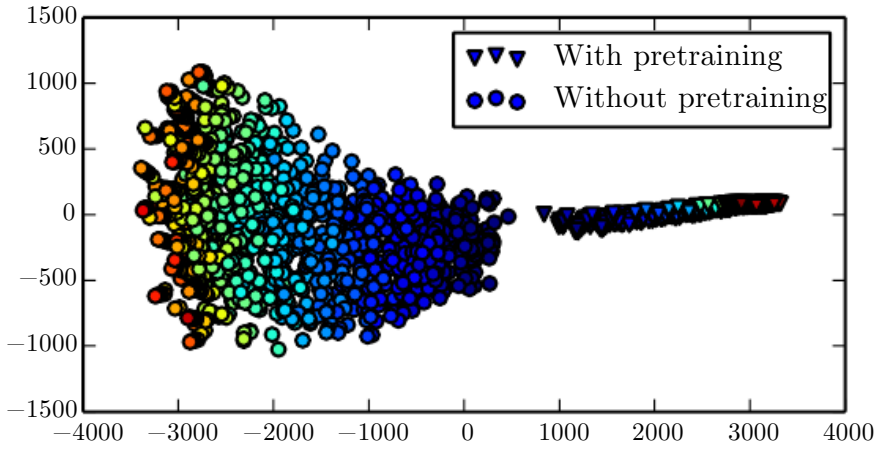

Figure 15.1: Visualization via nonlinear projection of the learning trajectories of different neural networks in *function space* (not parameter space, to avoid the issue of many-to-one mappings from parameter vectors to functions), with different random initializations and with or without unsupervised pretraining. Each point corresponds to a different neural network, at a particular time during its training process. This figure is adapted with permission from Erhan *et al.* (2010). A coordinate in function space is an infinite-dimensional vector associating every input $\boldsymbol{x}$ with an output $\boldsymbol{y}$. Erhan *et al.* (2010) made a linear projection to high-dimensional space by concatenating the $\boldsymbol{y}$ for many specific $\boldsymbol{x}$ points. They then made a further nonlinear projection to 2-D by Isomap (Tenenbaum *et al.*, 2000). Color indicates time. All networks are initialized near the center of the plot (corresponding to the region of functions that produce approximately uniform distributions over the class y for most inputs). Over time, learning moves the function outward, to points that make strong predictions. Training consistently terminates in one region when using pretraining and in another, non-overlapping region when not using pretraining. Isomap tries to preserve global relative distances (and hence volumes) so the small region corresponding to pretrained models may indicate that the pretraining-based estimator has reduced variance.

reducing test set error. However, unsupervised pretraining can help tasks other than classification, and can act to improve optimization rather than being merely a regularizer. For example, it can improve both train and test reconstruction error for deep autoencoders (Hinton and Salakhutdinov, 2006).

Erhan *et al.* (2010) performed many experiments to explain several successes of unsupervised pretraining. Both improvements to training error and improvements to test error may be explained in terms of unsupervised pretraining taking the parameters into a region that would otherwise be inaccessible. Neural network training is non-deterministic, and converges to a different function every time it is run. Training may halt at a point where the gradient becomes small, a point where early stopping ends training to prevent overfitting, or at a point where the gradient is large but it is difficult to find a downhill step due to problems such as stochasticity or poor conditioning of the Hessian. Neural networks that receive unsupervised pretraining consistently halt in the same region of function space, while neural networks without pretraining consistently halt in another region. See figure 15.1 for a visualization of this phenomenon. The region where pretrained networks arrive is smaller, suggesting that pretraining reduces the variance of the estimation process, which can in turn reduce the risk of severe over-fitting. In other words, unsupervised pretraining initializes neural network parameters into a region that they do not escape, and the results following this initialization are more consistent and less likely to be very bad than without this initialization.

Erhan *et al.* (2010) also provide some answers as to *when* pretraining works best—the mean and variance of the test error were most reduced by pretraining for deeper networks. Keep in mind that these experiments were performed before the invention and popularization of modern techniques for training very deep networks (rectified linear units, dropout and batch normalization) so less is known about the effect of unsupervised pretraining in conjunction with contemporary approaches.

An important question is how unsupervised pretraining can act as a regularizer. One hypothesis is that pretraining encourages the learning algorithm to discover features that relate to the underlying causes that generate the observed data. This is an important idea motivating many other algorithms besides unsupervised pretraining, and is described further in section 15.3.

Compared to other forms of unsupervised learning, unsupervised pretraining has the disadvantage that it operates with two separate training phases. Many regularization strategies have the advantage of allowing the user to control the strength of the regularization by adjusting the value of a single hyperparameter. Unsupervised pretraining does not offer a clear way to adjust the the strength of the regularization arising from the unsupervised stage. Instead, there are

very many hyperparameters, whose effect may be measured after the fact but is often difficult to predict ahead of time. When we perform unsupervised and supervised learning simultaneously, instead of using the pretraining strategy, there is a single hyperparameter, usually a coefficient attached to the unsupervised cost, that determines how strongly the unsupervised objective will regularize the supervised model. One can always predictably obtain less regularization by decreasing this coefficient. In the case of unsupervised pretraining, there is not a way of flexibly adapting the strength of the regularization—either the supervised model is initialized to pretrained parameters, or it is not.

Another disadvantage of having two separate training phases is that each phase has its own hyperparameters. The performance of the second phase usually cannot be predicted during the first phase, so there is a long delay between proposing hyperparameters for the first phase and being able to update them using feedback from the second phase. The most principled approach is to use validation set error in the supervised phase in order to select the hyperparameters of the pretraining phase, as discussed in Larochelle *et al.* (2009). In practice, some hyperparameters, like the number of pretraining iterations, are more conveniently set during the pretraining phase, using early stopping on the unsupervised objective, which is not ideal but computationally much cheaper than using the supervised objective.

Today, unsupervised pretraining has been largely abandoned, except in the field of natural language processing, where the natural representation of words as one-hot vectors conveys no similarity information and where very large unlabeled sets are available. In that case, the advantage of pretraining is that one can pretrain once on a huge unlabeled set (for example with a corpus containing billions of words), learn a good representation (typically of words, but also of sentences), and then use this representation or fine-tune it for a supervised task for which the training set contains substantially fewer examples. This approach was pioneered by by Collobert and Weston (2008b), Turian *et al.* (2010), and Collobert *et al.* (2011a) and remains in common use today.

Deep learning techniques based on supervised learning, regularized with dropout or batch normalization, are able to achieve human-level performance on very many tasks, but only with extremely large labeled datasets. These same techniques outperform unsupervised pretraining on medium-sized datasets such as CIFAR-10 and MNIST, which have roughly 5,000 labeled examples per class. On extremely small datasets, such as the alternative splicing dataset, Bayesian methods outperform methods based on unsupervised pretraining (Srivastava, 2013). For these reasons, the popularity of unsupervised pretraining has declined. Nevertheless, unsupervised pretraining remains an important milestone in the history of deep learning research

and continues to influence contemporary approaches. The idea of pretraining has been generalized to **supervised pretraining** discussed in section 8.7.4, as a very common approach for transfer learning. Supervised pretraining for transfer learning is popular (Oquab *et al.*, 2014; Yosinski *et al.*, 2014) for use with convolutional networks pretrained on the ImageNet dataset. Practitioners publish the parameters of these trained networks for this purpose, just like pretrained word vectors are published for natural language tasks (Collobert *et al.*, 2011a; Mikolov *et al.*, 2013a).

15.2 Transfer Learning and Domain Adaptation

Transfer learning and domain adaptation refer to the situation where what has been learned in one setting (i.e., distribution P_1) is exploited to improve generalization in another setting (say distribution P_2). This generalizes the idea presented in the previous section, where we transferred representations between an unsupervised learning task and a supervised learning task.

In **transfer learning**, the learner must perform two or more different tasks, but we assume that many of the factors that explain the variations in P_1 are relevant to the variations that need to be captured for learning P_2. This is typically understood in a supervised learning context, where the input is the same but the target may be of a different nature. For example, we may learn about one set of visual categories, such as cats and dogs, in the first setting, then learn about a different set of visual categories, such as ants and wasps, in the second setting. If there is significantly more data in the first setting (sampled from P_1), then that may help to learn representations that are useful to quickly generalize from only very few examples drawn from P_2. Many visual categories *share* low-level notions of edges and visual shapes, the effects of geometric changes, changes in lighting, etc. In general, transfer learning, multi-task learning (section 7.7), and domain adaptation can be achieved via representation learning when there exist features that are useful for the different settings or tasks, corresponding to underlying factors that appear in more than one setting. This is illustrated in figure 7.2, with shared lower layers and task-dependent upper layers.

However, sometimes, what is shared among the different tasks is not the semantics of the input but the semantics of the output. For example, a speech recognition system needs to produce valid sentences at the output layer, but the earlier layers near the input may need to recognize very different versions of the same phonemes or sub-phonemic vocalizations depending on which person is speaking. In cases like these, it makes more sense to share the upper layers (near the output) of the neural network, and have a task-specific preprocessing, as

illustrated in figure 15.2.

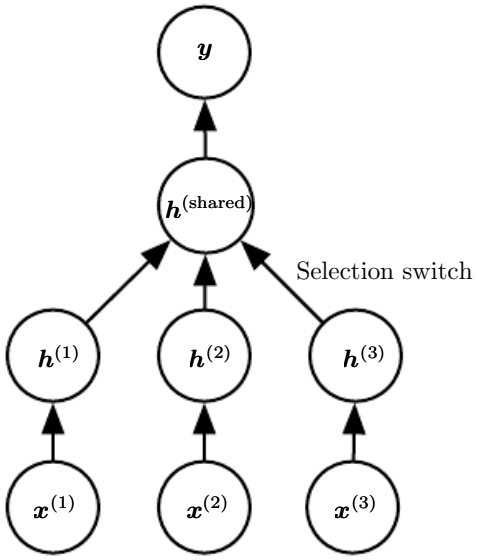

Figure 15.2: Example architecture for multi-task or transfer learning when the output variable $\mathbf{y}$ has the same semantics for all tasks while the input variable $\mathbf{x}$ has a different meaning (and possibly even a different dimension) for each task (or, for example, each user), called $\mathbf{x}^{(1)}$, $\mathbf{x}^{(2)}$ and $\mathbf{x}^{(3)}$ for three tasks. The lower levels (up to the selection switch) are task-specific, while the upper levels are shared. The lower levels learn to translate their task-specific input into a generic set of features.

In the related case of **domain adaptation**, the task (and the optimal input-to-output mapping) remains the same between each setting, but the input distribution is slightly different. For example, consider the task of sentiment analysis, which consists of determining whether a comment expresses positive or negative sentiment. Comments posted on the web come from many categories. A domain adaptation scenario can arise when a sentiment predictor trained on customer reviews of media content such as books, videos and music is later used to analyze comments about consumer electronics such as televisions or smartphones. One can imagine that there is an underlying function that tells whether any statement is positive, neutral or negative, but of course the vocabulary and style may vary from one domain to another, making it more difficult to generalize across domains. Simple unsupervised pretraining (with denoising autoencoders) has been found to be very successful for sentiment analysis with domain adaptation (Glorot *et al.*, 2011b).

A related problem is that of **concept drift**, which we can view as a form of transfer learning due to gradual changes in the data distribution over time. Both concept drift and transfer learning can be viewed as particular forms of

multi-task learning. While the phrase "multi-task learning" typically refers to supervised learning tasks, the more general notion of transfer learning is applicable to unsupervised learning and reinforcement learning as well.

In all of these cases, the objective is to take advantage of data from the first setting to extract information that may be useful when learning or even when directly making predictions in the second setting. The core idea of representation learning is that the same representation may be useful in both settings. Using the same representation in both settings allows the representation to benefit from the training data that is available for both tasks.

As mentioned before, unsupervised deep learning for transfer learning has found success in some machine learning competitions (Mesnil *et al.*, 2011; Goodfellow *et al.*, 2011). In the first of these competitions, the experimental setup is the following. Each participant is first given a dataset from the first setting (from distribution P_1), illustrating examples of some set of categories. The participants must use this to learn a good feature space (mapping the raw input to some representation), such that when we apply this learned transformation to inputs from the transfer setting (distribution P_2), a linear classifier can be trained and generalize well from very few labeled examples. One of the most striking results found in this competition is that as an architecture makes use of deeper and deeper representations (learned in a purely unsupervised way from data collected in the first setting, P_1), the learning curve on the new categories of the second (transfer) setting P_2 becomes much better. For deep representations, fewer labeled examples of the transfer tasks are necessary to achieve the apparently asymptotic generalization performance.

Two extreme forms of transfer learning are **one-shot learning** and **zero-shot learning**, sometimes also called **zero-data learning**. Only one labeled example of the transfer task is given for one-shot learning, while no labeled examples are given at all for the zero-shot learning task.

One-shot learning (Fei-Fei *et al.*, 2006) is possible because the representation learns to cleanly separate the underlying classes during the first stage. During the transfer learning stage, only one labeled example is needed to infer the label of many possible test examples that all cluster around the same point in representation space. This works to the extent that the factors of variation corresponding to these invariances have been cleanly separated from the other factors, in the learned representation space, and we have somehow learned which factors do and do not matter when discriminating objects of certain categories.

As an example of a zero-shot learning setting, consider the problem of having a learner read a large collection of text and then solve object recognition problems.

It may be possible to recognize a specific object class even without having seen an image of that object, if the text describes the object well enough. For example, having read that a cat has four legs and pointy ears, the learner might be able to guess that an image is a cat, without having seen a cat before.

Zero-data learning (Larochelle *et al.*, 2008) and zero-shot learning (Palatucci *et al.*, 2009; Socher *et al.*, 2013b) are only possible because additional information has been exploited during training. We can think of the zero-data learning scenario as including three random variables: the traditional inputs $\boldsymbol{x}$, the traditional outputs or targets $\boldsymbol{y}$, and an additional random variable describing the task, T. The model is trained to estimate the conditional distribution $p(\boldsymbol{y} \mid \boldsymbol{x}, T)$ where T is a description of the task we wish the model to perform. In our example of recognizing cats after having read about cats, the output is a binary variable y with $y = 1$ indicating "yes" and $y = 0$ indicating "no." The task variable T then represents questions to be answered such as "Is there a cat in this image?" If we have a training set containing unsupervised examples of objects that live in the same space as T, we may be able to infer the meaning of unseen instances of T. In our example of recognizing cats without having seen an image of the cat, it is important that we have had unlabeled text data containing sentences such as "cats have four legs" or "cats have pointy ears."

Zero-shot learning requires T to be represented in a way that allows some sort of generalization. For example, T cannot be just a one-hot code indicating an object category. Socher *et al.* (2013b) provide instead a distributed representation of object categories by using a learned word embedding for the word associated with each category.

A similar phenomenon happens in machine translation (Klementiev *et al.*, 2012; Mikolov *et al.*, 2013b; Gouws *et al.*, 2014): we have words in one language, and the relationships between words can be learned from unilingual corpora; on the other hand, we have translated sentences which relate words in one language with words in the other. Even though we may not have labeled examples translating word A in language X to word B in language Y, we can generalize and guess a translation for word A because we have learned a distributed representation for words in language X, a distributed representation for words in language Y, and created a link (possibly two-way) relating the two spaces, via training examples consisting of matched pairs of sentences in both languages. This transfer will be most successful if all three ingredients (the two representations and the relations between them) are learned jointly.

Zero-shot learning is a particular form of transfer learning. The same principle explains how one can perform **multi-modal learning**, capturing a representation

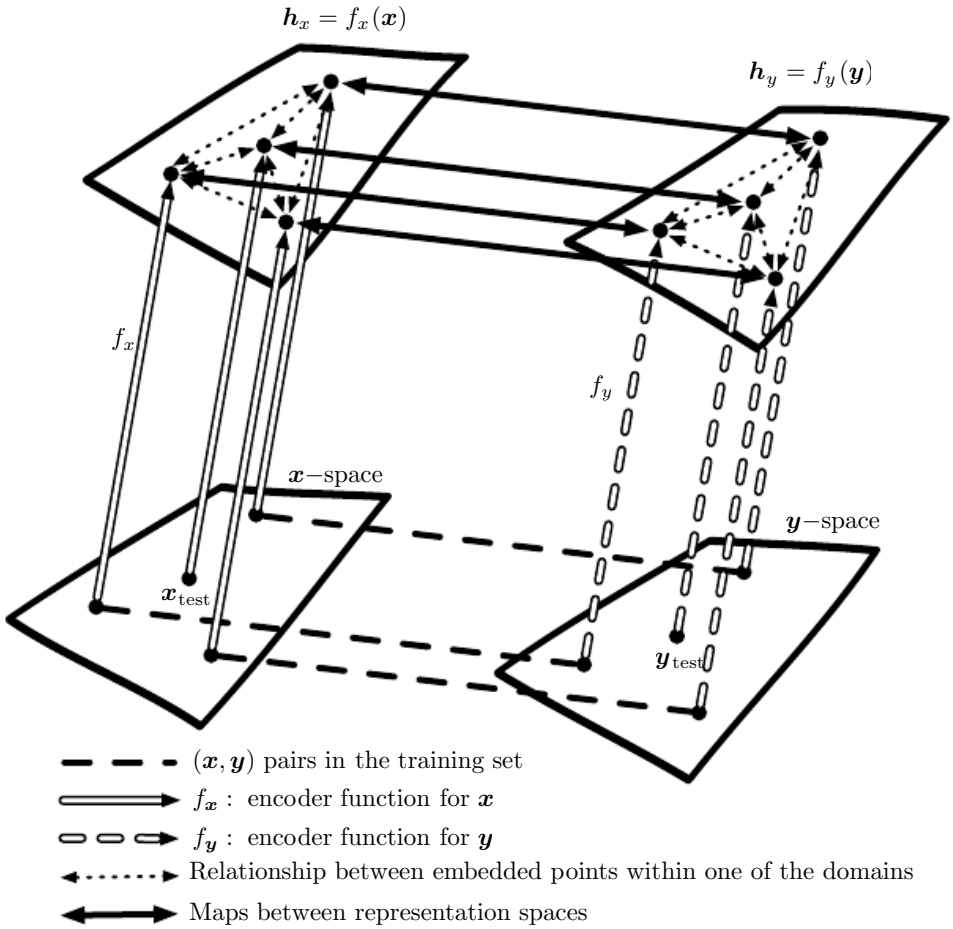

Figure 15.3: Transfer learning between two domains $\boldsymbol{x}$ and $\boldsymbol{y}$ enables zero-shot learning. Labeled or unlabeled examples of $\boldsymbol{x}$ allow one to learn a representation function f_x and similarly with examples of $\boldsymbol{y}$ to learn f_y. Each application of the f_x and f_y functions appears as an upward arrow, with the style of the arrows indicating which function is applied. Distance in $\boldsymbol{h}_x$ space provides a similarity metric between any pair of points in $\boldsymbol{x}$ space that may be more meaningful than distance in $\boldsymbol{x}$ space. Likewise, distance in $\boldsymbol{h}_y$ space provides a similarity metric between any pair of points in $\boldsymbol{y}$ space. Both of these similarity functions are indicated with dotted bidirectional arrows. Labeled examples (dashed horizontal lines) are pairs $(\boldsymbol{x}, \boldsymbol{y})$ which allow one to learn a one-way or two-way map (solid bidirectional arrow) between the representations $f_x(\boldsymbol{x})$ and the representations $f_y(\boldsymbol{y})$ and anchor these representations to each other. Zero-data learning is then enabled as follows. One can associate an image $\boldsymbol{x}_{\text{test}}$ to a word $\boldsymbol{y}_{\text{test}}$, even if no image of that word was ever presented, simply because word-representations $f_y(\boldsymbol{y}_{\text{test}})$ and image-representations $f_x(\boldsymbol{x}_{\text{test}})$ can be related to each other via the maps between representation spaces. It works because, although that image and that word were never paired, their respective feature vectors $f_x(\boldsymbol{x}_{\text{test}})$ and $f_y(\boldsymbol{y}_{\text{test}})$ have been related to each other. Figure inspired from suggestion by Hrant Khachatrian.

in one modality, a representation in the other, and the relationship (in general a joint distribution) between pairs $(\boldsymbol{x}, \boldsymbol{y})$ consisting of one observation $\boldsymbol{x}$ in one modality and another observation $\boldsymbol{y}$ in the other modality (Srivastava and Salakhutdinov, 2012). By learning all three sets of parameters (from $\boldsymbol{x}$ to its representation, from $\boldsymbol{y}$ to its representation, and the relationship between the two representations), concepts in one representation are anchored in the other, and vice-versa, allowing one to meaningfully generalize to new pairs. The procedure is illustrated in figure 15.3.

15.3 Semi-Supervised Disentangling of Causal Factors

An important question about representation learning is "what makes one representation better than another?" One hypothesis is that an ideal representation is one in which the features within the representation correspond to the underlying causes of the observed data, with separate features or directions in feature space corresponding to different causes, so that the representation disentangles the causes from one another. This hypothesis motivates approaches in which we first seek a good representation for $p(\boldsymbol{x})$. Such a representation may also be a good representation for computing $p(\boldsymbol{y} \mid \boldsymbol{x})$ if $\boldsymbol{y}$ is among the most salient causes of $\boldsymbol{x}$. This idea has guided a large amount of deep learning research since at least the 1990s (Becker and Hinton, 1992; Hinton and Sejnowski, 1999), in more detail. For other arguments about when semi-supervised learning can outperform pure supervised learning, we refer the reader to section 1.2 of Chapelle *et al.* (2006).

In other approaches to representation learning, we have often been concerned with a representation that is easy to model—for example, one whose entries are sparse, or independent from each other. A representation that cleanly separates the underlying causal factors may not necessarily be one that is easy to model. However, a further part of the hypothesis motivating semi-supervised learning via unsupervised representation learning is that for many AI tasks, these two properties coincide: once we are able to obtain the underlying explanations for what we observe, it generally becomes easy to isolate individual attributes from the others. Specifically, if a representation $\boldsymbol{h}$ represents many of the underlying causes of the observed $\boldsymbol{x}$, and the outputs $\boldsymbol{y}$ are among the most salient causes, then it is easy to predict $\boldsymbol{y}$ from $\boldsymbol{h}$.

First, let us see how semi-supervised learning can fail because unsupervised learning of $p(\mathbf{x})$ is of no help to learn $p(\mathbf{y} \mid \mathbf{x})$. Consider for example the case where $p(\mathbf{x})$ is uniformly distributed and we want to learn $f(\boldsymbol{x}) = \mathbb{E}[\mathbf{y} \mid \boldsymbol{x}]$. Clearly, observing a training set of $\boldsymbol{x}$ values alone gives us no information about $p(\mathbf{y} \mid \mathbf{x})$.

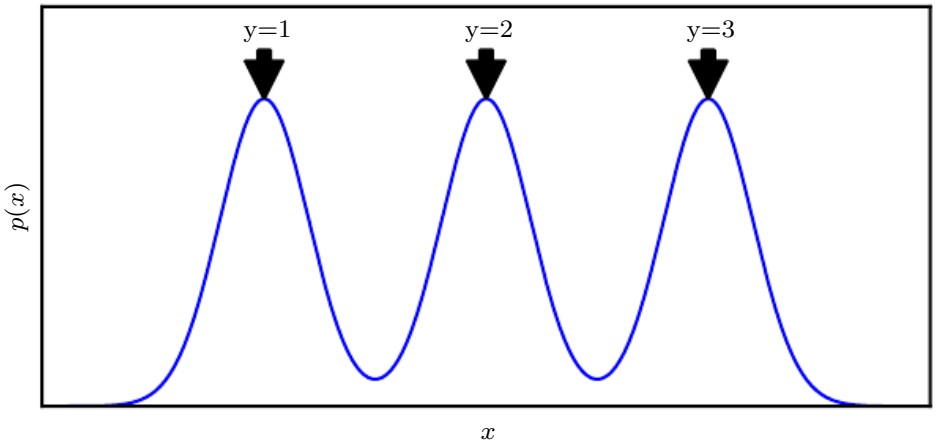

Figure 15.4: Example of a density over x that is a mixture over three components. The component identity is an underlying explanatory factor, y. Because the mixture components (e.g., natural object classes in image data) are statistically salient, just modeling $p(x)$ in an unsupervised way with no labeled example already reveals the factor y.

Next, let us see a simple example of how semi-supervised learning can succeed. Consider the situation where $\mathbf{x}$ arises from a mixture, with one mixture component per value of $\mathbf{y}$, as illustrated in figure 15.4. If the mixture components are well-separated, then modeling $p(\mathbf{x})$ reveals precisely where each component is, and a single labeled example of each class will then be enough to perfectly learn $p(\mathbf{y} \mid \mathbf{x})$. But more generally, what could make $p(\mathbf{y} \mid \mathbf{x})$ and $p(\mathbf{x})$ be tied together?

If $\mathbf{y}$ is closely associated with one of the causal factors of $\mathbf{x}$, then $p(\mathbf{x})$ and $p(\mathbf{y} \mid \mathbf{x})$ will be strongly tied, and unsupervised representation learning that tries to disentangle the underlying factors of variation is likely to be useful as a semi-supervised learning strategy.

Consider the assumption that $\mathbf{y}$ is one of the causal factors of $\mathbf{x}$, and let $\mathbf{h}$ represent all those factors. The true generative process can be conceived as structured according to this directed graphical model, with $\mathbf{h}$ as the parent of $\mathbf{x}$:

$$p(\mathbf{h}, \mathbf{x}) = p(\mathbf{x} \mid \mathbf{h})p(\mathbf{h}). \tag{15.1}$$

As a consequence, the data has marginal probability

$$p(\boldsymbol{x}) = \mathbb{E}_{\mathbf{h}} p(\boldsymbol{x} \mid \boldsymbol{h}). \tag{15.2}$$

From this straightforward observation, we conclude that the best possible model of $\mathbf{x}$ (from a generalization point of view) is the one that uncovers the above "true"

structure, with $\boldsymbol{h}$ as a latent variable that explains the observed variations in $\boldsymbol{x}$. The "ideal" representation learning discussed above should thus recover these latent factors. If $\mathbf{y}$ is one of these (or closely related to one of them), then it will be very easy to learn to predict $\mathbf{y}$ from such a representation. We also see that the conditional distribution of $\mathbf{y}$ given $\mathbf{x}$ is tied by Bayes' rule to the components in the above equation:

$$p(\mathbf{y} \mid \mathbf{x}) = \frac{p(\mathbf{x} \mid \mathbf{y})p(\mathbf{y})}{p(\mathbf{x})}. \tag{15.3}$$

Thus the marginal $p(\mathbf{x})$ is intimately tied to the conditional $p(\mathbf{y} \mid \mathbf{x})$ and knowledge of the structure of the former should be helpful to learn the latter. Therefore, in situations respecting these assumptions, semi-supervised learning should improve performance.

An important research problem regards the fact that most observations are formed by an extremely large number of underlying causes. Suppose $\mathbf{y} = \mathrm{h}_i$, but the unsupervised learner does not know which h_i. The brute force solution is for an unsupervised learner to learn a representation that captures *all* the reasonably salient generative factors h_j and disentangles them from each other, thus making it easy to predict $\mathbf{y}$ from $\mathbf{h}$, regardless of which h_i is associated with $\mathbf{y}$.

In practice, the brute force solution is not feasible because it is not possible to capture all or most of the factors of variation that influence an observation. For example, in a visual scene, should the representation always encode all of the smallest objects in the background? It is a well-documented psychological phenomenon that human beings fail to perceive changes in their environment that are not immediately relevant to the task they are performing—see, e.g., Simons and Levin (1998). An important research frontier in semi-supervised learning is determining *what* to encode in each situation. Currently, two of the main strategies for dealing with a large number of underlying causes are to use a supervised learning signal at the same time as the unsupervised learning signal so that the model will choose to capture the most relevant factors of variation, or to use much larger representations if using purely unsupervised learning.

An emerging strategy for unsupervised learning is to modify the definition of which underlying causes are most salient. Historically, autoencoders and generative models have been trained to optimize a fixed criterion, often similar to mean squared error. These fixed criteria determine which causes are considered salient. For example, mean squared error applied to the pixels of an image implicitly specifies that an underlying cause is only salient if it significantly changes the brightness of a large number of pixels. This can be problematic if the task we wish to solve involves interacting with small objects. See figure 15.5 for an example

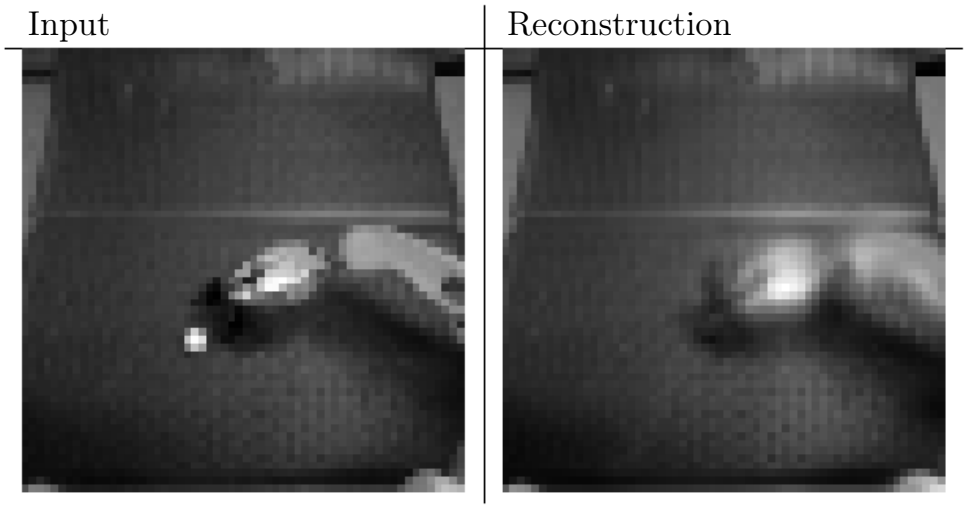

Figure 15.5: An autoencoder trained with mean squared error for a robotics task has failed to reconstruct a ping pong ball. The existence of the ping pong ball and all of its spatial coordinates are important underlying causal factors that generate the image and are relevant to the robotics task. Unfortunately, the autoencoder has limited capacity, and the training with mean squared error did not identify the ping pong ball as being salient enough to encode. Images graciously provided by Chelsea Finn.

of a robotics task in which an autoencoder has failed to learn to encode a small ping pong ball. This same robot is capable of successfully interacting with larger objects, such as baseballs, which are more salient according to mean squared error.

Other definitions of salience are possible. For example, if a group of pixels follow a highly recognizable pattern, even if that pattern does not involve extreme brightness or darkness, then that pattern could be considered extremely salient. One way to implement such a definition of salience is to use a recently developed approach called **generative adversarial networks** (Goodfellow *et al.*, 2014c). In this approach, a generative model is trained to fool a feedforward classifier. The feedforward classifier attempts to recognize all samples from the generative model as being fake, and all samples from the training set as being real. In this framework, any structured pattern that the feedforward network can recognize is highly salient. The generative adversarial network will be described in more detail in section 20.10.4. For the purposes of the present discussion, it is sufficient to understand that they *learn* how to determine what is salient. Lotter *et al.* (2015) showed that models trained to generate images of human heads will often neglect to generate the ears when trained with mean squared error, but will successfully generate the ears when trained with the adversarial framework. Because the ears are not extremely bright or dark compared to the surrounding skin, they are not especially salient according to mean squared error loss, but their highly

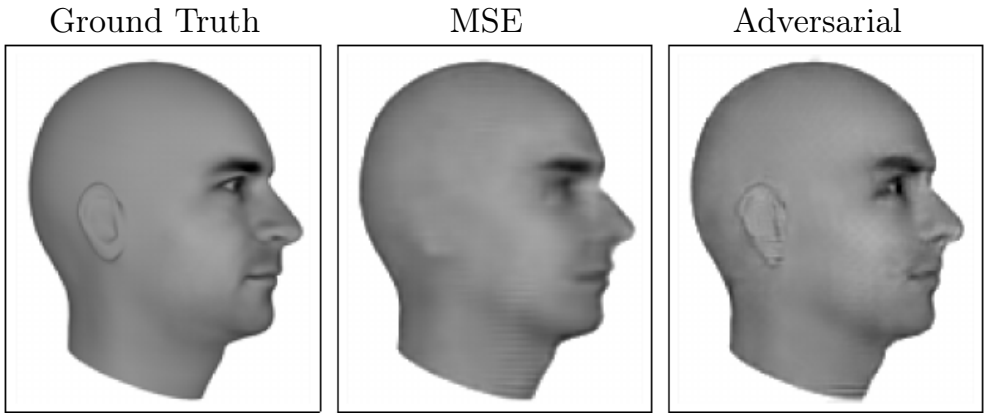

Figure 15.6: Predictive generative networks provide an example of the importance of learning which features are salient. In this example, the predictive generative network has been trained to predict the appearance of a 3-D model of a human head at a specific viewing angle. *(Left)*Ground truth. This is the correct image, that the network should emit. *(Center)*Image produced by a predictive generative network trained with mean squared error alone. Because the ears do not cause an extreme difference in brightness compared to the neighboring skin, they were not sufficiently salient for the model to learn to represent them. *(Right)*Image produced by a model trained with a combination of mean squared error and adversarial loss. Using this learned cost function, the ears are salient because they follow a predictable pattern. Learning which underlying causes are important and relevant enough to model is an important active area of research. Figures graciously provided by Lotter *et al.* (2015).

recognizable shape and consistent position means that a feedforward network can easily learn to detect them, making them highly salient under the generative adversarial framework. See figure 15.6 for example images. Generative adversarial networks are only one step toward determining which factors should be represented. We expect that future research will discover better ways of determining which factors to represent, and develop mechanisms for representing different factors depending on the task.

A benefit of learning the underlying causal factors, as pointed out by Schölkopf *et al.* (2012), is that if the true generative process has $\mathbf{x}$ as an effect and $\mathbf{y}$ as a cause, then modeling $p(\mathbf{x} \mid \mathbf{y})$ is robust to changes in $p(\mathbf{y})$. If the cause-effect relationship was reversed, this would not be true, since by Bayes' rule, $p(\mathbf{x} \mid \mathbf{y})$ would be sensitive to changes in $p(\mathbf{y})$. Very often, when we consider changes in distribution due to different domains, temporal non-stationarity, or changes in the nature of the task, *the causal mechanisms remain invariant* (the laws of the universe are constant) while the marginal distribution over the underlying causes can change. Hence, better generalization and robustness to all kinds of changes can

be expected via learning a generative model that attempts to recover the causal factors $\mathbf{h}$ and $p(\mathbf{x} \mid \mathbf{h})$.

15.4 Distributed Representation

Distributed representations of concepts—representations composed of many elements that can be set separately from each other—are one of the most important tools for representation learning. Distributed representations are powerful because they can use n features with k values to describe k^n different concepts. As we have seen throughout this book, both neural networks with multiple hidden units and probabilistic models with multiple latent variables make use of the strategy of distributed representation. We now introduce an additional observation. Many deep learning algorithms are motivated by the assumption that the hidden units can learn to represent the underlying causal factors that explain the data, as discussed in section 15.3. Distributed representations are natural for this approach, because each direction in representation space can correspond to the value of a different underlying configuration variable.

An example of a distributed representation is a vector of n binary features, which can take 2^n configurations, each potentially corresponding to a different region in input space, as illustrated in figure 15.7. This can be compared with a *symbolic representation*, where the input is associated with a single symbol or category. If there are n symbols in the dictionary, one can imagine n feature detectors, each corresponding to the detection of the presence of the associated category. In that case only n different configurations of the representation space are possible, carving n different regions in input space, as illustrated in figure 15.8. Such a symbolic representation is also called a one-hot representation, since it can be captured by a binary vector with n bits that are mutually exclusive (only one of them can be active). A symbolic representation is a specific example of the broader class of non-distributed representations, which are representations that may contain many entries but without significant meaningful separate control over each entry.

Examples of learning algorithms based on non-distributed representations include:

- Clustering methods, including the k-means algorithm: each input point is assigned to exactly one cluster.
- k-nearest neighbors algorithms: one or a few templates or prototype examples are associated with a given input. In the case of $k > 1$, there are multiple

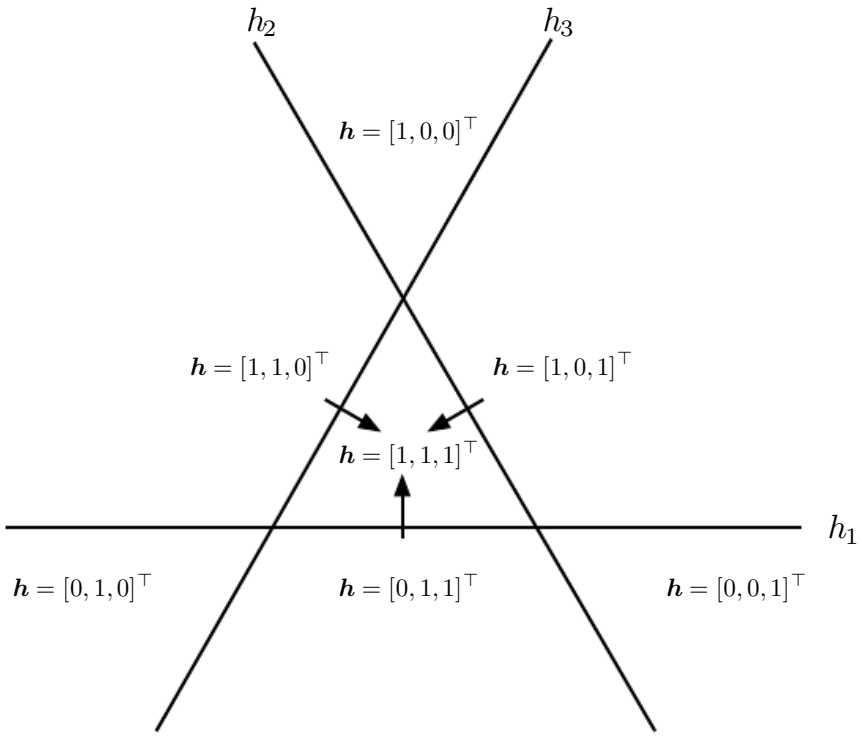

Figure 15.7: Illustration of how a learning algorithm based on a distributed representation breaks up the input space into regions. In this example, there are three binary features h_1, h_2, and h_3. Each feature is defined by thresholding the output of a learned, linear transformation. Each feature divides $\mathbb{R}^2$ into two half-planes. Let h_i^+ be the set of input points for which $h_i = 1$ and h_i^- be the set of input points for which $h_i = 0$. In this illustration, each line represents the decision boundary for one h_i, with the corresponding arrow pointing to the h_i^+ side of the boundary. The representation as a whole takes on a unique value at each possible intersection of these half-planes. For example, the representation value $[1, 1, 1]^\top$ corresponds to the region $h_1^+ \cap h_2^+ \cap h_3^+$. Compare this to the non-distributed representations in figure 15.8. In the general case of d input dimensions, a distributed representation divides $\mathbb{R}^d$ by intersecting half-spaces rather than half-planes. The distributed representation with n features assigns unique codes to $O(n^d)$ different regions, while the nearest neighbor algorithm with n examples assigns unique codes to only n regions. The distributed representation is thus able to distinguish exponentially many more regions than the non-distributed one. Keep in mind that not all $\boldsymbol{h}$ values are feasible (there is no $\boldsymbol{h} = \mathbf{0}$ in this example) and that a linear classifier on top of the distributed representation is not able to assign different class identities to every neighboring region; even a deep linear-threshold network has a VC dimension of only $O(w \log w)$ where w is the number of weights (Sontag, 1998). The combination of a powerful representation layer and a weak classifier layer can be a strong regularizer; a classifier trying to learn the concept of "person" versus "not a person" does not need to assign a different class to an input represented as "woman with glasses" than it assigns to an input represented as "man without glasses." This capacity constraint encourages each classifier to focus on few h_i and encourages $\boldsymbol{h}$ to learn to represent the classes in a linearly separable way.

values describing each input, but they can not be controlled separately from each other, so this does not qualify as a true distributed representation.

- Decision trees: only one leaf (and the nodes on the path from root to leaf) is activated when an input is given.
- Gaussian mixtures and mixtures of experts: the templates (cluster centers) or experts are now associated with a *degree* of activation. As with the k-nearest neighbors algorithm, each input is represented with multiple values, but those values cannot readily be controlled separately from each other.
- Kernel machines with a Gaussian kernel (or other similarly local kernel): although the degree of activation of each "support vector" or template example is now continuous-valued, the same issue arises as with Gaussian mixtures.
- Language or translation models based on n-grams. The set of contexts (sequences of symbols) is partitioned according to a tree structure of suffixes. A leaf may correspond to the last two words being w_1 and w_2, for example. Separate parameters are estimated for each leaf of the tree (with some sharing being possible).

For some of these non-distributed algorithms, the output is not constant by parts but instead interpolates between neighboring regions. The relationship between the number of parameters (or examples) and the number of regions they can define remains linear.

An important related concept that distinguishes a distributed representation from a symbolic one is that *generalization arises due to shared attributes* between different concepts. As pure symbols, "`cat`" and "`dog`" are as far from each other as any other two symbols. However, if one associates them with a meaningful distributed representation, then many of the things that can be said about cats can generalize to dogs and vice-versa. For example, our distributed representation may contain entries such as "`has_fur`" or "`number_of_legs`" that have the same value for the embedding of both "`cat`" and "`dog`." Neural language models that operate on distributed representations of words generalize much better than other models that operate directly on one-hot representations of words, as discussed in section 12.4. Distributed representations induce a rich *similarity space*, in which semantically close concepts (or inputs) are close in distance, a property that is absent from purely symbolic representations.

When and why can there be a statistical advantage from using a distributed representation as part of a learning algorithm? Distributed representations can

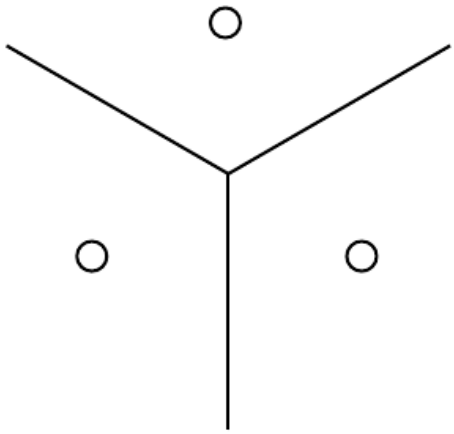

Figure 15.8: Illustration of how the nearest neighbor algorithm breaks up the input space into different regions. The nearest neighbor algorithm provides an example of a learning algorithm based on a non-distributed representation. Different non-distributed algorithms may have different geometry, but they typically break the input space into regions, *with a separate set of parameters for each region*. The advantage of a non-distributed approach is that, given enough parameters, it can fit the training set without solving a difficult optimization algorithm, because it is straightforward to choose a different output *independently* for each region. The disadvantage is that such non-distributed models generalize only locally via the smoothness prior, making it difficult to learn a complicated function with more peaks and troughs than the available number of examples. Contrast this with a distributed representation, figure 15.7.

have a statistical advantage when an apparently complicated structure can be compactly represented using a small number of parameters. Some traditional non-distributed learning algorithms generalize only due to the smoothness assumption, which states that if $u \approx v$, then the target function f to be learned has the property that $f(u) \approx f(v)$, in general. There are many ways of formalizing such an assumption, but the end result is that if we have an example (x, y) for which we know that $f(x) \approx y$, then we choose an estimator $\hat{f}$ that approximately satisfies these constraints while changing as little as possible when we move to a nearby input $x + \epsilon$. This assumption is clearly very useful, but it suffers from the curse of dimensionality: in order to learn a target function that increases and decreases many times in many different regions,[1] we may need a number of examples that is at least as large as the number of distinguishable regions. One can think of each of these regions as a category or symbol: by having a separate degree of freedom for each symbol (or region), we can learn an arbitrary decoder mapping from symbol to value. However, this does not allow us to generalize to new symbols for new regions.

If we are lucky, there may be some regularity in the target function, besides being smooth. For example, a convolutional network with max-pooling can recognize an object regardless of its location in the image, even though spatial translation of the object may not correspond to smooth transformations in the input space.

Let us examine a special case of a distributed representation learning algorithm, that extracts binary features by thresholding linear functions of the input. Each binary feature in this representation divides $\mathbb{R}^d$ into a pair of half-spaces, as illustrated in figure 15.7. The exponentially large number of intersections of n of the corresponding half-spaces determines how many regions this distributed representation learner can distinguish. How many regions are generated by an arrangement of n hyperplanes in $\mathbb{R}^d$? By applying a general result concerning the intersection of hyperplanes (Zaslavsky, 1975), one can show (Pascanu *et al.*, 2014b) that the number of regions this binary feature representation can distinguish is

$$\sum_{j=0}^{d} \binom{n}{j} = O(n^d). \tag{15.4}$$

Therefore, we see a growth that is exponential in the input size and polynomial in the number of hidden units.

[1] Potentially, we may want to learn a function whose behavior is distinct in exponentially many regions: in a d-dimensional space with at least 2 different values to distinguish per dimension, we might want f to differ in 2^d different regions, requiring $O(2^d)$ training examples.

This provides a geometric argument to explain the generalization power of distributed representation: with $O(nd)$ parameters (for n linear-threshold features in $\mathbb{R}^d$) we can distinctly represent $O(n^d)$ regions in input space. If instead we made no assumption at all about the data, and used a representation with one unique symbol for each region, and separate parameters for each symbol to recognize its corresponding portion of $\mathbb{R}^d$, then specifying $O(n^d)$ regions would require $O(n^d)$ examples. More generally, the argument in favor of the distributed representation could be extended to the case where instead of using linear threshold units we use nonlinear, possibly continuous, feature extractors for each of the attributes in the distributed representation. The argument in this case is that if a parametric transformation with k parameters can learn about r regions in input space, with $k \ll r$, and if obtaining such a representation was useful to the task of interest, then we could potentially generalize much better in this way than in a non-distributed setting where we would need $O(r)$ examples to obtain the same features and associated partitioning of the input space into r regions. Using fewer parameters to represent the model means that we have fewer parameters to fit, and thus require far fewer training examples to generalize well.

A further part of the argument for why models based on distributed representations generalize well is that their capacity remains limited despite being able to distinctly encode so many different regions. For example, the VC dimension of a neural network of linear threshold units is only $O(w \log w)$, where w is the number of weights (Sontag, 1998). This limitation arises because, while we can assign very many unique codes to representation space, we cannot use absolutely all of the code space, nor can we learn arbitrary functions mapping from the representation space $\boldsymbol{h}$ to the output $\boldsymbol{y}$ using a linear classifier. The use of a distributed representation combined with a linear classifier thus expresses a prior belief that the classes to be recognized are linearly separable as a function of the underlying causal factors captured by $\boldsymbol{h}$. We will typically want to learn categories such as the set of all images of all green objects or the set of all images of cars, but not categories that require nonlinear, XOR logic. For example, we typically do not want to partition the data into the set of all red cars and green trucks as one class and the set of all green cars and red trucks as another class.

The ideas discussed so far have been abstract, but they may be experimentally validated. Zhou *et al.* (2015) find that hidden units in a deep convolutional network trained on the ImageNet and Places benchmark datasets learn features that are very often interpretable, corresponding to a label that humans would naturally assign. In practice it is certainly not always the case that hidden units learn something that has a simple linguistic name, but it is interesting to see this emerge near the top levels of the best computer vision deep networks. What such features have in

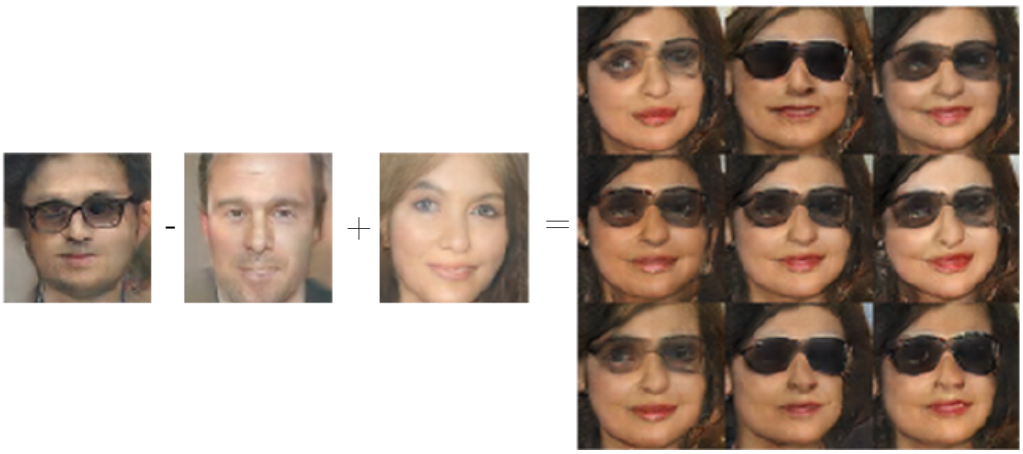

Figure 15.9: A generative model has learned a distributed representation that disentangles the concept of gender from the concept of wearing glasses. If we begin with the representation of the concept of a man with glasses, then subtract the vector representing the concept of a man without glasses, and finally add the vector representing the concept of a woman without glasses, we obtain the vector representing the concept of a woman with glasses. The generative model correctly decodes all of these representation vectors to images that may be recognized as belonging to the correct class. Images reproduced with permission from Radford *et al.* (2015).

common is that one could imagine *learning about each of them without having to see all the configurations of all the others*. Radford *et al.* (2015) demonstrated that a generative model can learn a representation of images of faces, with separate directions in representation space capturing different underlying factors of variation. Figure 15.9 demonstrates that one direction in representation space corresponds to whether the person is male or female, while another corresponds to whether the person is wearing glasses. These features were discovered automatically, not fixed a priori. There is no need to have labels for the hidden unit classifiers: gradient descent on an objective function of interest naturally learns semantically interesting features, so long as the task requires such features. We can learn about the distinction between male and female, or about the presence or absence of glasses, without having to characterize all of the configurations of the $n - 1$ other features by examples covering all of these combinations of values. This form of statistical separability is what allows one to generalize to new configurations of a person's features that have never been seen during training.

15.5 Exponential Gains from Depth

We have seen in section 6.4.1 that multilayer perceptrons are universal approximators, and that some functions can be represented by exponentially smaller deep networks compared to shallow networks. This decrease in model size leads to improved statistical efficiency. In this section, we describe how similar results apply more generally to other kinds of models with distributed hidden representations.

In section 15.4, we saw an example of a generative model that learned about the explanatory factors underlying images of faces, including the person's gender and whether they are wearing glasses. The generative model that accomplished this task was based on a deep neural network. It would not be reasonable to expect a shallow network, such as a linear network, to learn the complicated relationship between these abstract explanatory factors and the pixels in the image. In this and other AI tasks, the factors that can be chosen almost independently from each other yet still correspond to meaningful inputs are more likely to be very high-level and related in highly nonlinear ways to the input. We argue that this demands *deep* distributed representations, where the higher level features (seen as functions of the input) or factors (seen as generative causes) are obtained through the composition of many nonlinearities.

It has been proven in many different settings that organizing computation through the composition of many nonlinearities and a hierarchy of reused features can give an exponential boost to statistical efficiency, on top of the exponential boost given by using a distributed representation. Many kinds of networks (e.g., with saturating nonlinearities, Boolean gates, sum/products, or RBF units) with a single hidden layer can be shown to be universal approximators. A model family that is a universal approximator can approximate a large class of functions (including all continuous functions) up to any non-zero tolerance level, given enough hidden units. However, the required number of hidden units may be very large. Theoretical results concerning the expressive power of deep architectures state that there are families of functions that can be represented efficiently by an architecture of depth k, but would require an exponential number of hidden units (with respect to the input size) with insufficient depth (depth 2 or depth $k-1$).

In section 6.4.1, we saw that deterministic feedforward networks are universal approximators of functions. Many structured probabilistic models with a single hidden layer of latent variables, including restricted Boltzmann machines and deep belief networks, are universal approximators of probability distributions (Le Roux and Bengio, 2008, 2010; Montúfar and Ay, 2011; Montúfar, 2014; Krause *et al.*, 2013).

In section 6.4.1, we saw that a sufficiently deep feedforward network can have an exponential advantage over a network that is too shallow. Such results can also be obtained for other models such as probabilistic models. One such probabilistic model is the **sum-product network** or SPN (Poon and Domingos, 2011). These models use polynomial circuits to compute the probability distribution over a set of random variables. Delalleau and Bengio (2011) showed that there exist probability distributions for which a minimum depth of SPN is required to avoid needing an exponentially large model. Later, Martens and Medabalimi (2014) showed that there are significant differences between every two finite depths of SPN, and that some of the constraints used to make SPNs tractable may limit their representational power.

Another interesting development is a set of theoretical results for the expressive power of families of deep circuits related to convolutional nets, highlighting an exponential advantage for the deep circuit even when the shallow circuit is allowed to only approximate the function computed by the deep circuit (Cohen *et al.*, 2015). By comparison, previous theoretical work made claims regarding only the case where the shallow circuit must exactly replicate particular functions.

15.6 Providing Clues to Discover Underlying Causes

To close this chapter, we come back to one of our original questions: what makes one representation better than another? One answer, first introduced in section 15.3, is that an ideal representation is one that disentangles the underlying causal factors of variation that generated the data, especially those factors that are relevant to our applications. Most strategies for representation learning are based on introducing clues that help the learning to find these underlying factors of variations. The clues can help the learner separate these observed factors from the others. Supervised learning provides a very strong clue: a label $\boldsymbol{y}$, presented with each $\boldsymbol{x}$, that usually specifies the value of at least one of the factors of variation directly. More generally, to make use of abundant unlabeled data, representation learning makes use of other, less direct, hints about the underlying factors. These hints take the form of implicit prior beliefs that we, the designers of the learning algorithm, impose in order to guide the learner. Results such as the no free lunch theorem show that regularization strategies are necessary to obtain good generalization. While it is impossible to find a universally superior regularization strategy, one goal of deep learning is to find a set of fairly generic regularization strategies that are applicable to a wide variety of AI tasks, similar to the tasks that people and animals are able to solve.

We provide here a list of these generic regularization strategies. The list is clearly not exhaustive, but gives some concrete examples of ways that learning algorithms can be encouraged to discover features that correspond to underlying factors. This list was introduced in section 3.1 of Bengio *et al.* (2013d) and has been partially expanded here.

- *Smoothness*: This is the assumption that $f(\boldsymbol{x} + \epsilon \boldsymbol{d}) \approx f(\boldsymbol{x})$ for unit $\boldsymbol{d}$ and small ϵ. This assumption allows the learner to generalize from training examples to nearby points in input space. Many machine learning algorithms leverage this idea, but it is insufficient to overcome the curse of dimensionality.

- *Linearity*: Many learning algorithms assume that relationships between some variables are linear. This allows the algorithm to make predictions even very far from the observed data, but can sometimes lead to overly extreme predictions. Most simple machine learning algorithms that do not make the smoothness assumption instead make the linearity assumption. These are in fact different assumptions—linear functions with large weights applied to high-dimensional spaces may not be very smooth. See Goodfellow *et al.* (2014b) for a further discussion of the limitations of the linearity assumption.

- *Multiple explanatory factors*: Many representation learning algorithms are motivated by the assumption that the data is generated by multiple underlying explanatory factors, and that most tasks can be solved easily given the state of each of these factors. Section 15.3 describes how this view motivates semi-supervised learning via representation learning. Learning the structure of $p(\boldsymbol{x})$ requires learning some of the same features that are useful for modeling $p(\boldsymbol{y} \mid \boldsymbol{x})$ because both refer to the same underlying explanatory factors. Section 15.4 describes how this view motivates the use of distributed representations, with separate directions in representation space corresponding to separate factors of variation.

- *Causal factors*: the model is constructed in such a way that it treats the factors of variation described by the learned representation $\boldsymbol{h}$ as the causes of the observed data $\boldsymbol{x}$, and not vice-versa. As discussed in section 15.3, this is advantageous for semi-supervised learning and makes the learned model more robust when the distribution over the underlying causes changes or when we use the model for a new task.

- *Depth*, or *a hierarchical organization of explanatory factors*: High-level, abstract concepts can be defined in terms of simple concepts, forming a hierarchy. From another point of view, the use of a deep architecture

expresses our belief that the task should be accomplished via a multi-step program, with each step referring back to the output of the processing accomplished via previous steps.

- *Shared factors across tasks*: In the context where we have many tasks, corresponding to different y_i variables sharing the same input $\mathbf{x}$ or where each task is associated with a subset or a function $f^{(i)}(\mathbf{x})$ of a global input $\mathbf{x}$, the assumption is that each y_i is associated with a different subset from a common pool of relevant factors $\mathbf{h}$. Because these subsets overlap, learning all the $P(y_i \mid \mathbf{x})$ via a shared intermediate representation $P(\mathbf{h} \mid \mathbf{x})$ allows sharing of statistical strength between the tasks.

- *Manifolds*: Probability mass concentrates, and the regions in which it concentrates are locally connected and occupy a tiny volume. In the continuous case, these regions can be approximated by low-dimensional manifolds with a much smaller dimensionality than the original space where the data lives. Many machine learning algorithms behave sensibly only on this manifold (Goodfellow *et al.*, 2014b). Some machine learning algorithms, especially autoencoders, attempt to explicitly learn the structure of the manifold.

- *Natural clustering*: Many machine learning algorithms assume that each connected manifold in the input space may be assigned to a single class. The data may lie on many disconnected manifolds, but the class remains constant within each one of these. This assumption motivates a variety of learning algorithms, including tangent propagation, double backprop, the manifold tangent classifier and adversarial training.

- *Temporal and spatial coherence*: Slow feature analysis and related algorithms make the assumption that the most important explanatory factors change slowly over time, or at least that it is easier to predict the true underlying explanatory factors than to predict raw observations such as pixel values. See section 13.3 for further description of this approach.

- *Sparsity*: Most features should presumably not be relevant to describing most inputs—there is no need to use a feature that detects elephant trunks when representing an image of a cat. It is therefore reasonable to impose a prior that any feature that can be interpreted as "present" or "absent" should be absent most of the time.

- *Simplicity of Factor Dependencies*: In good high-level representations, the factors are related to each other through simple dependencies. The simplest

possible is marginal independence, $P(\mathbf{h}) = \prod_i P(\mathbf{h}_i)$, but linear dependencies or those captured by a shallow autoencoder are also reasonable assumptions. This can be seen in many laws of physics, and is assumed when plugging a linear predictor or a factorized prior on top of a learned representation.

The concept of representation learning ties together all of the many forms of deep learning. Feedforward and recurrent networks, autoencoders and deep probabilistic models all learn and exploit representations. Learning the best possible representation remains an exciting avenue of research.

Chapter 16

Structured Probabilistic Models for Deep Learning

Deep learning draws upon many modeling formalisms that researchers can use to guide their design efforts and describe their algorithms. One of these formalisms is the idea of **structured probabilistic models**. We have already discussed structured probabilistic models briefly in section 3.14. That brief presentation was sufficient to understand how to use structured probabilistic models as a language to describe some of the algorithms in part II. Now, in part III, structured probabilistic models are a key ingredient of many of the most important research topics in deep learning. In order to prepare to discuss these research ideas, this chapter describes structured probabilistic models in much greater detail. This chapter is intended to be self-contained; the reader does not need to review the earlier introduction before continuing with this chapter.

A structured probabilistic model is a way of describing a probability distribution, using a graph to describe which random variables in the probability distribution interact with each other directly. Here we use "graph" in the graph theory sense—a set of vertices connected to one another by a set of edges. Because the structure of the model is defined by a graph, these models are often also referred to as **graphical models**.

The graphical models research community is large and has developed many different models, training algorithms, and inference algorithms. In this chapter, we provide basic background on some of the most central ideas of graphical models, with an emphasis on the concepts that have proven most useful to the deep learning research community. If you already have a strong background in graphical models, you may wish to skip most of this chapter. However, even a graphical model expert

may benefit from reading the final section of this chapter, section 16.7, in which we highlight some of the unique ways that graphical models are used for deep learning algorithms. Deep learning practitioners tend to use very different model structures, learning algorithms and inference procedures than are commonly used by the rest of the graphical models research community. In this chapter, we identify these differences in preferences and explain the reasons for them.

In this chapter we first describe the challenges of building large-scale probabilistic models. Next, we describe how to use a graph to describe the structure of a probability distribution. While this approach allows us to overcome many challenges, it is not without its own complications. One of the major difficulties in graphical modeling is understanding which variables need to be able to interact directly, i.e., which graph structures are most suitable for a given problem. We outline two approaches to resolving this difficulty by learning about the dependencies in section 16.5. Finally, we close with a discussion of the unique emphasis that deep learning practitioners place on specific approaches to graphical modeling in section 16.7.

16.1 The Challenge of Unstructured Modeling

The goal of deep learning is to scale machine learning to the kinds of challenges needed to solve artificial intelligence. This means being able to understand high-dimensional data with rich structure. For example, we would like AI algorithms to be able to understand natural images,[1] audio waveforms representing speech, and documents containing multiple words and punctuation characters.

Classification algorithms can take an input from such a rich high-dimensional distribution and summarize it with a categorical label—what object is in a photo, what word is spoken in a recording, what topic a document is about. The process of classification discards most of the information in the input and produces a single output (or a probability distribution over values of that single output). The classifier is also often able to ignore many parts of the input. For example, when recognizing an object in a photo, it is usually possible to ignore the background of the photo.

It is possible to ask probabilistic models to do many other tasks. These tasks are often more expensive than classification. Some of them require producing multiple output values. Most require a complete understanding of the entire structure of

[1] A **natural image** is an image that might be captured by a camera in a reasonably ordinary environment, as opposed to a synthetically rendered image, a screenshot of a web page, etc.

the input, with no option to ignore sections of it. These tasks include the following:

- **Density estimation**: given an input $\boldsymbol{x}$, the machine learning system returns an estimate of the true density $p(\boldsymbol{x})$ under the data generating distribution. This requires only a single output, but it does require a complete understanding of the entire input. If even one element of the vector is unusual, the system must assign it a low probability.

- **Denoising**: given a damaged or incorrectly observed input $\tilde{\boldsymbol{x}}$, the machine learning system returns an estimate of the original or correct $\boldsymbol{x}$. For example, the machine learning system might be asked to remove dust or scratches from an old photograph. This requires multiple outputs (every element of the estimated clean example $\boldsymbol{x}$) and an understanding of the entire input (since even one damaged area will still reveal the final estimate as being damaged).

- **Missing value imputation**: given the observations of some elements of $\boldsymbol{x}$, the model is asked to return estimates of or a probability distribution over some or all of the unobserved elements of $\boldsymbol{x}$. This requires multiple outputs. Because the model could be asked to restore any of the elements of $\boldsymbol{x}$, it must understand the entire input.

- **Sampling**: the model generates new samples from the distribution $p(\boldsymbol{x})$. Applications include speech synthesis, i.e. producing new waveforms that sound like natural human speech. This requires multiple output values and a good model of the entire input. If the samples have even one element drawn from the wrong distribution, then the sampling process is wrong.

For an example of a sampling task using small natural images, see figure 16.1.

Modeling a rich distribution over thousands or millions of random variables is a challenging task, both computationally and statistically. Suppose we only wanted to model binary variables. This is the simplest possible case, and yet already it seems overwhelming. For a small, 32×32 pixel color (RGB) image, there are 2^{3072} possible binary images of this form. This number is over 10^{800} times larger than the estimated number of atoms in the universe.

In general, if we wish to model a distribution over a random vector $\mathbf{x}$ containing n discrete variables capable of taking on k values each, then the naive approach of representing $P(\mathbf{x})$ by storing a lookup table with one probability value per possible outcome requires k^n parameters!

This is not feasible for several reasons:

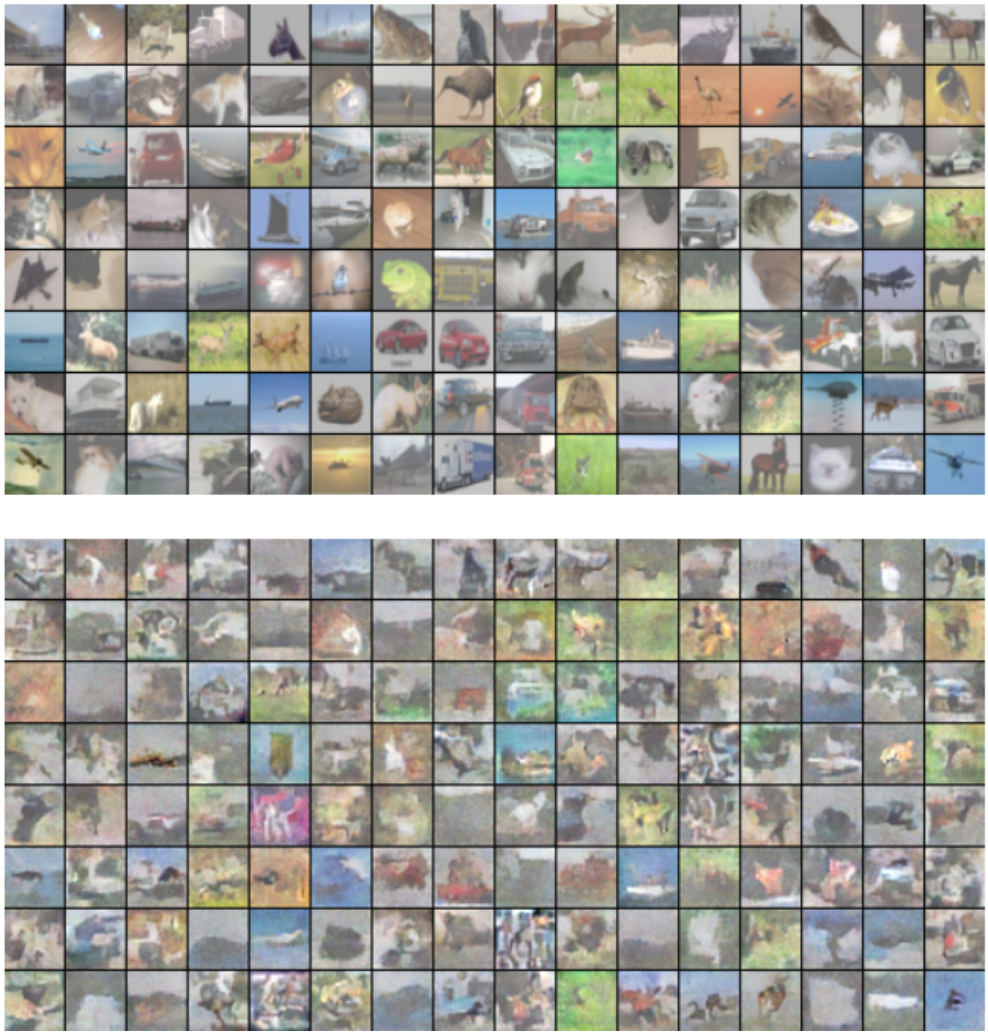

Figure 16.1: Probabilistic modeling of natural images. *(Top)*Example 32×32 pixel color images from the CIFAR-10 dataset (Krizhevsky and Hinton, 2009). *(Bottom)*Samples drawn from a structured probabilistic model trained on this dataset. Each sample appears at the same position in the grid as the training example that is closest to it in Euclidean space. This comparison allows us to see that the model is truly synthesizing new images, rather than memorizing the training data. Contrast of both sets of images has been adjusted for display. Figure reproduced with permission from Courville *et al.* (2011).

- *Memory: the cost of storing the representation*: For all but very small values of n and k, representing the distribution as a table will require too many values to store.

- *Statistical efficiency*: As the number of parameters in a model increases, so does the amount of training data needed to choose the values of those parameters using a statistical estimator. Because the table-based model has an astronomical number of parameters, it will require an astronomically large training set to fit accurately. Any such model will overfit the training set very badly unless additional assumptions are made linking the different entries in the table (for example, like in back-off or smoothed n-gram models, section 12.4.1).

- *Runtime: the cost of inference*: Suppose we want to perform an inference task where we use our model of the joint distribution $P(\mathbf{x})$ to compute some other distribution, such as the marginal distribution $P(\mathrm{x}_1)$ or the conditional distribution $P(\mathrm{x}_2 \mid \mathrm{x}_1)$. Computing these distributions will require summing across the entire table, so the runtime of these operations is as high as the intractable memory cost of storing the model.

- *Runtime: the cost of sampling*: Likewise, suppose we want to draw a sample from the model. The naive way to do this is to sample some value $\mathrm{u} \sim U(0, 1)$, then iterate through the table, adding up the probability values until they exceed u and return the outcome corresponding to that position in the table. This requires reading through the whole table in the worst case, so it has the same exponential cost as the other operations.

The problem with the table-based approach is that we are explicitly modeling every possible kind of interaction between every possible subset of variables. The probability distributions we encounter in real tasks are much simpler than this. Usually, most variables influence each other only indirectly.

For example, consider modeling the finishing times of a team in a relay race. Suppose the team consists of three runners: Alice, Bob and Carol. At the start of the race, Alice carries a baton and begins running around a track. After completing her lap around the track, she hands the baton to Bob. Bob then runs his own lap and hands the baton to Carol, who runs the final lap. We can model each of their finishing times as a continuous random variable. Alice's finishing time does not depend on anyone else's, since she goes first. Bob's finishing time depends on Alice's, because Bob does not have the opportunity to start his lap until Alice has completed hers. If Alice finishes faster, Bob will finish faster, all else being

equal. Finally, Carol's finishing time depends on both her teammates. If Alice is slow, Bob will probably finish late too. As a consequence, Carol will have quite a late starting time and thus is likely to have a late finishing time as well. However, Carol's finishing time depends only *indirectly* on Alice's finishing time via Bob's. If we already know Bob's finishing time, we will not be able to estimate Carol's finishing time better by finding out what Alice's finishing time was. This means we can model the relay race using only two interactions: Alice's effect on Bob and Bob's effect on Carol. We can omit the third, indirect interaction between Alice and Carol from our model.

Structured probabilistic models provide a formal framework for modeling only direct interactions between random variables. This allows the models to have significantly fewer parameters and therefore be estimated reliably from less data. These smaller models also have dramatically reduced computational cost in terms of storing the model, performing inference in the model, and drawing samples from the model.

16.2 Using Graphs to Describe Model Structure

Structured probabilistic models use graphs (in the graph theory sense of "nodes" or "vertices" connected by edges) to represent interactions between random variables. Each node represents a random variable. Each edge represents a direct interaction. These direct interactions imply other, indirect interactions, but only the direct interactions need to be explicitly modeled.

There is more than one way to describe the interactions in a probability distribution using a graph. In the following sections we describe some of the most popular and useful approaches. Graphical models can be largely divided into two categories: models based on directed acyclic graphs, and models based on undirected graphs.

16.2.1 Directed Models

One kind of structured probabilistic model is the **directed graphical model**, otherwise known as the **belief network** or **Bayesian network**[2] (Pearl, 1985).

Directed graphical models are called "directed" because their edges are directed,

[2] Judea Pearl suggested using the term "Bayesian network" when one wishes to "emphasize the judgmental" nature of the values computed by the network, i.e. to highlight that they usually represent degrees of belief rather than frequencies of events.

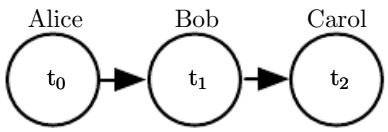

Figure 16.2: A directed graphical model depicting the relay race example. Alice's finishing time t_0 influences Bob's finishing time t_1, because Bob does not get to start running until Alice finishes. Likewise, Carol only gets to start running after Bob finishes, so Bob's finishing time t_1 directly influences Carol's finishing time t_2.

that is, they point from one vertex to another. This direction is represented in the drawing with an arrow. The direction of the arrow indicates which variable's probability distribution is defined in terms of the other's. Drawing an arrow from a to b means that we define the probability distribution over b via a conditional distribution, with a as one of the variables on the right side of the conditioning bar. In other words, the distribution over b depends on the value of a.

Continuing with the relay race example from section 16.1, suppose we name Alice's finishing time t_0, Bob's finishing time t_1, and Carol's finishing time t_2. As we saw earlier, our estimate of t_1 depends on t_0. Our estimate of t_2 depends directly on t_1 but only indirectly on t_0. We can draw this relationship in a directed graphical model, illustrated in figure 16.2.

Formally, a directed graphical model defined on variables $\mathbf{x}$ is defined by a directed acyclic graph $\mathcal{G}$ whose vertices are the random variables in the model, and a set of **local conditional probability distributions** $p(x_i \mid Pa_{\mathcal{G}}(x_i))$ where $Pa_{\mathcal{G}}(x_i)$ gives the parents of x_i in $\mathcal{G}$. The probability distribution over $\mathbf{x}$ is given by

$$p(\mathbf{x}) = \Pi_i p(x_i \mid Pa_{\mathcal{G}}(x_i)). \tag{16.1}$$

In our relay race example, this means that, using the graph drawn in figure 16.2,

$$p(t_0, t_1, t_2) = p(t_0)p(t_1 \mid t_0)p(t_2 \mid t_1). \tag{16.2}$$

This is our first time seeing a structured probabilistic model in action. We can examine the cost of using it, in order to observe how structured modeling has many advantages relative to unstructured modeling.

Suppose we represented time by discretizing time ranging from minute 0 to minute 10 into 6 second chunks. This would make t_0, t_1 and t_2 each be a discrete variable with 100 possible values. If we attempted to represent $p(t_0, t_1, t_2)$ with a table, it would need to store 999,999 values (100 values of t_0 $\times$ 100 values of t_1 $\times$ 100 values of t_2, minus 1, since the probability of one of the configurations is made

redundant by the constraint that the sum of the probabilities be 1). If instead, we only make a table for each of the conditional probability distributions, then the distribution over t_0 requires 99 values, the table defining t_1 given t_0 requires 9900 values, and so does the table defining t_2 given t_1. This comes to a total of 19,899 values. This means that using the directed graphical model reduced our number of parameters by a factor of more than 50!

In general, to model n discrete variables each having k values, the cost of the single table approach scales like $O(k^n)$, as we have observed before. Now suppose we build a directed graphical model over these variables. If m is the maximum number of variables appearing (on either side of the conditioning bar) in a single conditional probability distribution, then the cost of the tables for the directed model scales like $O(k^m)$. As long as we can design a model such that $m << n$, we get very dramatic savings.

In other words, so long as each variable has few parents in the graph, the distribution can be represented with very few parameters. Some restrictions on the graph structure, such as requiring it to be a tree, can also guarantee that operations like computing marginal or conditional distributions over subsets of variables are efficient.

It is important to realize what kinds of information can and cannot be encoded in the graph. The graph encodes only simplifying assumptions about which variables are conditionally independent from each other. It is also possible to make other kinds of simplifying assumptions. For example, suppose we assume Bob always runs the same regardless of how Alice performed. (In reality, Alice's performance probably influences Bob's performance—depending on Bob's personality, if Alice runs especially fast in a given race, this might encourage Bob to push hard and match her exceptional performance, or it might make him overconfident and lazy). Then the only effect Alice has on Bob's finishing time is that we must add Alice's finishing time to the total amount of time we think Bob needs to run. This observation allows us to define a model with $O(k)$ parameters instead of $O(k^2)$. However, note that t_0 and t_1 are still directly dependent with this assumption, because t_1 represents the absolute time at which Bob finishes, not the total time he himself spends running. This means our graph must still contain an arrow from t_0 to t_1. The assumption that Bob's personal running time is independent from all other factors cannot be encoded in a graph over t_0, t_1, and t_2. Instead, we encode this information in the definition of the conditional distribution itself. The conditional distribution is no longer a $k \times k - 1$ element table indexed by t_0 and t_1 but is now a slightly more complicated formula using only $k - 1$ parameters. The directed graphical model syntax does not place any constraint on how we define

our conditional distributions. It only defines which variables they are allowed to take in as arguments.

16.2.2 Undirected Models

Directed graphical models give us one language for describing structured probabilistic models. Another popular language is that of **undirected models**, otherwise known as **Markov random fields** (MRFs) or **Markov networks** (Kindermann, 1980). As their name implies, undirected models use graphs whose edges are undirected.

Directed models are most naturally applicable to situations where there is a clear reason to draw each arrow in one particular direction. Often these are situations where we understand the causality and the causality only flows in one direction. One such situation is the relay race example. Earlier runners affect the finishing times of later runners; later runners do not affect the finishing times of earlier runners.

Not all situations we might want to model have such a clear direction to their interactions. When the interactions seem to have no intrinsic direction, or to operate in both directions, it may be more appropriate to use an undirected model.

As an example of such a situation, suppose we want to model a distribution over three binary variables: whether or not you are sick, whether or not your coworker is sick, and whether or not your roommate is sick. As in the relay race example, we can make simplifying assumptions about the kinds of interactions that take place. Assuming that your coworker and your roommate do not know each other, it is very unlikely that one of them will give the other an infection such as a cold directly. This event can be seen as so rare that it is acceptable not to model it. However, it is reasonably likely that either of them could give you a cold, and that you could pass it on to the other. We can model the indirect transmission of a cold from your coworker to your roommate by modeling the transmission of the cold from your coworker to you and the transmission of the cold from you to your roommate.

In this case, it is just as easy for you to cause your roommate to get sick as it is for your roommate to make you sick, so there is not a clean, uni-directional narrative on which to base the model. This motivates using an undirected model. As with directed models, if two nodes in an undirected model are connected by an edge, then the random variables corresponding to those nodes interact with each other directly. Unlike directed models, the edge in an undirected model has no arrow, and is not associated with a conditional probability distribution.

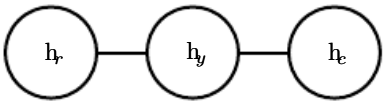

Figure 16.3: An undirected graph representing how your roommate's health h_r, your health h_y, and your work colleague's health h_c affect each other. You and your roommate might infect each other with a cold, and you and your work colleague might do the same, but assuming that your roommate and your colleague do not know each other, they can only infect each other indirectly via you.

We denote the random variable representing your health as h_y, the random variable representing your roommate's health as h_r, and the random variable representing your colleague's health as h_c. See figure 16.3 for a drawing of the graph representing this scenario.

Formally, an undirected graphical model is a structured probabilistic model defined on an undirected graph $\mathcal{G}$. For each clique $\mathcal{C}$ in the graph,[3] a **factor** $\phi(\mathcal{C})$ (also called a **clique potential**) measures the affinity of the variables in that clique for being in each of their possible joint states. The factors are constrained to be non-negative. Together they define an **unnormalized probability distribution**

$$\tilde{p}(\mathbf{x}) = \Pi_{\mathcal{C}\in\mathcal{G}}\,\phi(\mathcal{C}). \tag{16.3}$$

The unnormalized probability distribution is efficient to work with so long as all the cliques are small. It encodes the idea that states with higher affinity are more likely. However, unlike in a Bayesian network, there is little structure to the definition of the cliques, so there is nothing to guarantee that multiplying them together will yield a valid probability distribution. See figure 16.4 for an example of reading factorization information from an undirected graph.

Our example of the cold spreading between you, your roommate, and your colleague contains two cliques. One clique contains h_y and h_c. The factor for this clique can be defined by a table, and might have values resembling these:

	$\mathrm{h}_y = 0$	$\mathrm{h}_y = 1$
$\mathrm{h}_c = 0$	2	1
$\mathrm{h}_c = 1$	1	10

[3] A clique of the graph is a subset of nodes that are all connected to each other by an edge of the graph.

A state of 1 indicates good health, while a state of 0 indicates poor health (having been infected with a cold). Both of you are usually healthy, so the corresponding state has the highest affinity. The state where only one of you is sick has the lowest affinity, because this is a rare state. The state where both of you are sick (because one of you has infected the other) is a higher affinity state, though still not as common as the state where both are healthy.

To complete the model, we would need to also define a similar factor for the clique containing h_y and h_r.

16.2.3 The Partition Function

While the unnormalized probability distribution is guaranteed to be non-negative everywhere, it is not guaranteed to sum or integrate to 1. To obtain a valid probability distribution, we must use the corresponding normalized probability distribution:[4]

$$p(\mathbf{x}) = \frac{1}{Z}\tilde{p}(\mathbf{x}) \tag{16.4}$$

where Z is the value that results in the probability distribution summing or integrating to 1:

$$Z = \int \tilde{p}(\mathbf{x}) d\mathbf{x}. \tag{16.5}$$

You can think of Z as a constant when the ϕ functions are held constant. Note that if the ϕ functions have parameters, then Z is a function of those parameters. It is common in the literature to write Z with its arguments omitted to save space. The normalizing constant Z is known as the **partition function**, a term borrowed from statistical physics.

Since Z is an integral or sum over all possible joint assignments of the state $\mathbf{x}$ it is often intractable to compute. In order to be able to obtain the normalized probability distribution of an undirected model, the model structure and the definitions of the ϕ functions must be conducive to computing Z efficiently. In the context of deep learning, Z is usually intractable. Due to the intractability of computing Z exactly, we must resort to approximations. Such approximate algorithms are the topic of chapter 18.

One important consideration to keep in mind when designing undirected models is that it is possible to specify the factors in such a way that Z does not exist. This happens if some of the variables in the model are continuous and the integral

[4] A distribution defined by normalizing a product of clique potentials is also called a **Gibbs distribution**.

of $\tilde{p}$ over their domain diverges. For example, suppose we want to model a single scalar variable $\mathrm{x} \in \mathbb{R}$ with a single clique potential $\phi(x) = x^2$. In this case,

$$Z = \int x^2 dx. \tag{16.6}$$

Since this integral diverges, there is no probability distribution corresponding to this choice of $\phi(x)$. Sometimes the choice of some parameter of the ϕ functions determines whether the probability distribution is defined. For example, for $\phi(x; \beta) = \exp\left(-\beta x^2\right)$, the β parameter determines whether Z exists. Positive β results in a Gaussian distribution over x but all other values of β make ϕ impossible to normalize.

One key difference between directed modeling and undirected modeling is that directed models are defined directly in terms of probability distributions from the start, while undirected models are defined more loosely by ϕ functions that are then converted into probability distributions. This changes the intuitions one must develop in order to work with these models. One key idea to keep in mind while working with undirected models is that the domain of each of the variables has dramatic effect on the kind of probability distribution that a given set of ϕ functions corresponds to. For example, consider an n-dimensional vector-valued random variable $\mathbf{x}$ and an undirected model parametrized by a vector of biases $\boldsymbol{b}$. Suppose we have one clique for each element of $\mathbf{x}$, $\phi^{(i)}(\mathrm{x}_i) = \exp(b_i \mathrm{x}_i)$. What kind of probability distribution does this result in? The answer is that we do not have enough information, because we have not yet specified the domain of $\mathbf{x}$. If $\mathbf{x} \in \mathbb{R}^n$, then the integral defining Z diverges and no probability distribution exists. If $\mathbf{x} \in \{0, 1\}^n$, then $p(\mathbf{x})$ factorizes into n independent distributions, with $p(\mathrm{x}_i = 1) = \mathrm{sigmoid}(b_i)$. If the domain of $\mathbf{x}$ is the set of elementary basis vectors $(\{[1, 0, \ldots, 0], [0, 1, \ldots, 0], \ldots, [0, 0, \ldots, 1]\})$ then $p(\mathbf{x}) = \mathrm{softmax}(\boldsymbol{b})$, so a large value of b_i actually reduces $p(\mathrm{x}_j = 1)$ for $j \neq i$. Often, it is possible to leverage the effect of a carefully chosen domain of a variable in order to obtain complicated behavior from a relatively simple set of ϕ functions. We will explore a practical application of this idea later, in section 20.6.

16.2.4 Energy-Based Models

Many interesting theoretical results about undirected models depend on the assumption that $\forall \mathbf{x}, \tilde{p}(\mathbf{x}) > 0$. A convenient way to enforce this condition is to use an **energy-based model** (EBM) where

$$\tilde{p}(\mathbf{x}) = \exp(-E(\mathbf{x})) \tag{16.7}$$

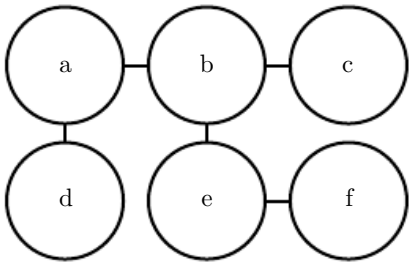

Figure 16.4: This graph implies that $p(\mathrm{a}, \mathrm{b}, \mathrm{c}, \mathrm{d}, \mathrm{e}, \mathrm{f})$ can be written as $\frac{1}{Z}\phi_{\mathrm{a,b}}(\mathrm{a}, \mathrm{b})\phi_{\mathrm{b,c}}(\mathrm{b}, \mathrm{c})\phi_{\mathrm{a,d}}(\mathrm{a}, \mathrm{d})\phi_{\mathrm{b,e}}(\mathrm{b}, \mathrm{e})\phi_{\mathrm{e,f}}(\mathrm{e}, \mathrm{f})$ for an appropriate choice of the ϕ functions.

and $E(\mathbf{x})$ is known as the **energy function**. Because $\exp(z)$ is positive for all z, this guarantees that no energy function will result in a probability of zero for any state $\mathbf{x}$. Being completely free to choose the energy function makes learning simpler. If we learned the clique potentials directly, we would need to use constrained optimization to arbitrarily impose some specific minimal probability value. By learning the energy function, we can use unconstrained optimization.[5] The probabilities in an energy-based model can approach arbitrarily close to zero but never reach it.

Any distribution of the form given by equation 16.7 is an example of a **Boltzmann distribution**. For this reason, many energy-based models are called **Boltzmann machines** (Fahlman *et al.*, 1983; Ackley *et al.*, 1985; Hinton *et al.*, 1984; Hinton and Sejnowski, 1986). There is no accepted guideline for when to call a model an energy-based model and when to call it a Boltzmann machine. The term Boltzmann machine was first introduced to describe a model with exclusively binary variables, but today many models such as the mean-covariance restricted Boltzmann machine incorporate real-valued variables as well. While Boltzmann machines were originally defined to encompass both models with and without latent variables, the term Boltzmann machine is today most often used to designate models with latent variables, while Boltzmann machines without latent variables are more often called Markov random fields or log-linear models.

Cliques in an undirected graph correspond to factors of the unnormalized probability function. Because $\exp(a)\exp(b) = \exp(a+b)$, this means that different cliques in the undirected graph correspond to the different terms of the energy function. In other words, an energy-based model is just a special kind of Markov network: the exponentiation makes each term in the energy function correspond to a factor for a different clique. See figure 16.5 for an example of how to read the

[5] For some models, we may still need to use constrained optimization to make sure Z exists.

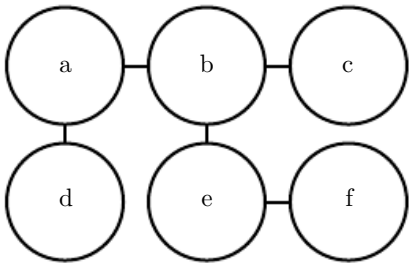

Figure 16.5: This graph implies that $E(\mathrm{a}, \mathrm{b}, \mathrm{c}, \mathrm{d}, \mathrm{e}, \mathrm{f})$ can be written as $E_{\mathrm{a,b}}(\mathrm{a}, \mathrm{b}) + E_{\mathrm{b,c}}(\mathrm{b}, \mathrm{c}) + E_{\mathrm{a,d}}(\mathrm{a}, \mathrm{d}) + E_{\mathrm{b,e}}(\mathrm{b}, \mathrm{e}) + E_{\mathrm{e,f}}(\mathrm{e}, \mathrm{f})$ for an appropriate choice of the per-clique energy functions. Note that we can obtain the ϕ functions in figure 16.4 by setting each ϕ to the exponential of the corresponding negative energy, e.g., $\phi_{\mathrm{a,b}}(\mathrm{a}, \mathrm{b}) = \exp(-E(\mathrm{a}, \mathrm{b}))$.

form of the energy function from an undirected graph structure. One can view an energy-based model with multiple terms in its energy function as being a **product of experts** (Hinton, 1999). Each term in the energy function corresponds to another factor in the probability distribution. Each term of the energy function can be thought of as an "expert" that determines whether a particular soft constraint is satisfied. Each expert may enforce only one constraint that concerns only a low-dimensional projection of the random variables, but when combined by multiplication of probabilities, the experts together enforce a complicated high-dimensional constraint.

One part of the definition of an energy-based model serves no functional purpose from a machine learning point of view: the $-$ sign in equation 16.7. This $-$ sign could be incorporated into the definition of E. For many choices of the function E, the learning algorithm is free to determine the sign of the energy anyway. The $-$ sign is present primarily to preserve compatibility between the machine learning literature and the physics literature. Many advances in probabilistic modeling were originally developed by statistical physicists, for whom E refers to actual, physical energy and does not have arbitrary sign. Terminology such as "energy" and "partition function" remains associated with these techniques, even though their mathematical applicability is broader than the physics context in which they were developed. Some machine learning researchers (e.g., Smolensky (1986), who referred to negative energy as **harmony**) have chosen to emit the negation, but this is not the standard convention.

Many algorithms that operate on probabilistic models do not need to compute $p_{\mathrm{model}}(\boldsymbol{x})$ but only $\log \tilde{p}_{\mathrm{model}}(\boldsymbol{x})$. For energy-based models with latent variables $\boldsymbol{h}$, these algorithms are sometimes phrased in terms of the negative of this quantity,

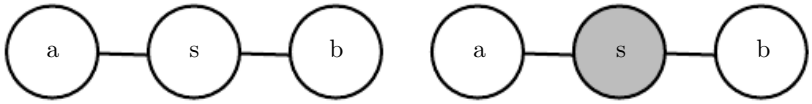

(a) (b)

Figure 16.6: (a) The path between random variable a and random variable b through s is active, because s is not observed. This means that a and b are not separated. (b) Here s is shaded in, to indicate that it is observed. Because the only path between a and b is through s, and that path is inactive, we can conclude that a and b are separated given s.

called the **free energy**:

$$\mathcal{F}(\boldsymbol{x}) = -\log \sum_{\boldsymbol{h}} \exp\left(-E(\boldsymbol{x}, \boldsymbol{h})\right). \tag{16.8}$$

In this book, we usually prefer the more general $\log \tilde{p}_{\text{model}}(\boldsymbol{x})$ formulation.

16.2.5 Separation and D-Separation

The edges in a graphical model tell us which variables directly interact. We often need to know which variables *indirectly* interact. Some of these indirect interactions can be enabled or disabled by observing other variables. More formally, we would like to know which subsets of variables are conditionally independent from each other, given the values of other subsets of variables.

Identifying the conditional independences in a graph is very simple in the case of undirected models. In this case, conditional independence implied by the graph is called **separation**. We say that a set of variables $\mathbb{A}$ is **separated** from another set of variables $\mathbb{B}$ given a third set of variables $\mathbb{S}$ if the graph structure implies that $\mathbb{A}$ is independent from $\mathbb{B}$ given $\mathbb{S}$. If two variables a and b are connected by a path involving only unobserved variables, then those variables are not separated. If no path exists between them, or all paths contain an observed variable, then they are separated. We refer to paths involving only unobserved variables as "active" and paths including an observed variable as "inactive."

When we draw a graph, we can indicate observed variables by shading them in. See figure 16.6 for a depiction of how active and inactive paths in an undirected model look when drawn in this way. See figure 16.7 for an example of reading separation from an undirected graph.

Similar concepts apply to directed models, except that in the context of directed models, these concepts are referred to as **d-separation**. The "d" stands for "dependence." D-separation for directed graphs is defined the same as separation

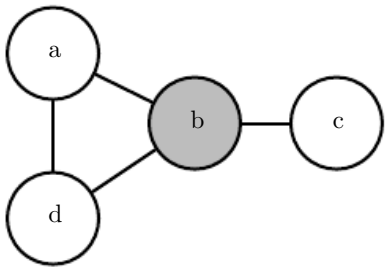

Figure 16.7: An example of reading separation properties from an undirected graph. Here b is shaded to indicate that it is observed. Because observing b blocks the only path from a to c, we say that a and c are separated from each other given b. The observation of b also blocks one path between a and d, but there is a second, active path between them. Therefore, a and d are not separated given b.

for undirected graphs: We say that a set of variables $\mathbb{A}$ is d-separated from another set of variables $\mathbb{B}$ given a third set of variables $\mathbb{S}$ if the graph structure implies that $\mathbb{A}$ is independent from $\mathbb{B}$ given $\mathbb{S}$.

As with undirected models, we can examine the independences implied by the graph by looking at what active paths exist in the graph. As before, two variables are dependent if there is an active path between them, and d-separated if no such path exists. In directed nets, determining whether a path is active is somewhat more complicated. See figure 16.8 for a guide to identifying active paths in a directed model. See figure 16.9 for an example of reading some properties from a graph.

It is important to remember that separation and d-separation tell us only about those conditional independences *that are implied by the graph.* There is no requirement that the graph imply all independences that are present. In particular, it is always legitimate to use the complete graph (the graph with all possible edges) to represent any distribution. In fact, some distributions contain independences that are not possible to represent with existing graphical notation. **Context-specific independences** are independences that are present dependent on the value of some variables in the network. For example, consider a model of three binary variables: a, b and c. Suppose that when a is 0, b and c are independent, but when a is 1, b is deterministically equal to c. Encoding the behavior when $a = 1$ requires an edge connecting b and c. The graph then fails to indicate that b and c are independent when $a = 0$.

In general, a graph will never imply that an independence exists when it does not. However, a graph may fail to encode an independence.

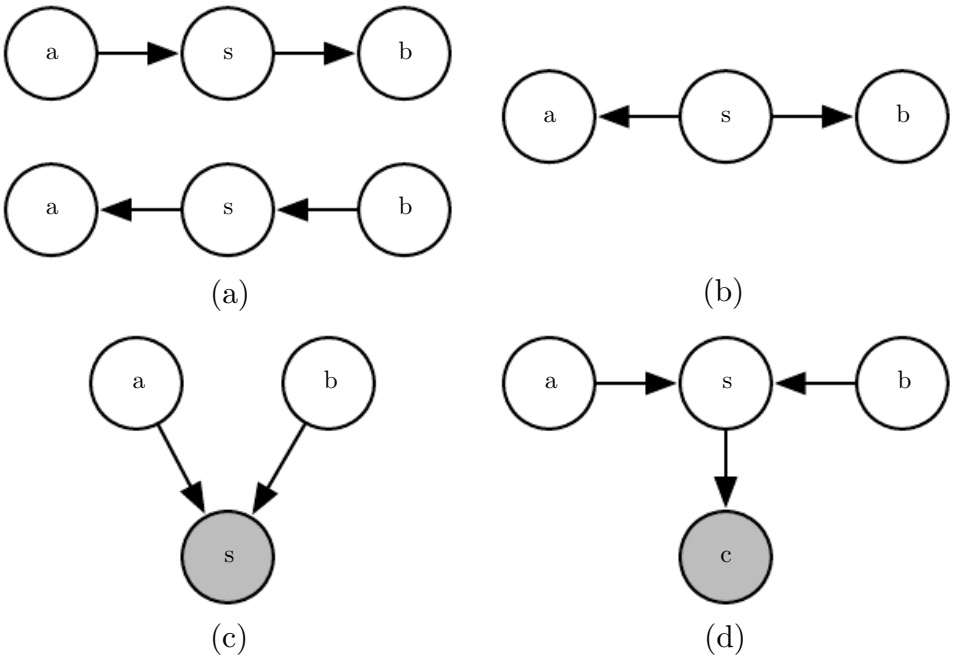

Figure 16.8: All of the kinds of active paths of length two that can exist between random variables a and b. *(a)*Any path with arrows proceeding directly from a to b or vice versa. This kind of path becomes blocked if s is observed. We have already seen this kind of path in the relay race example. *(b)*a and b are connected by a *common cause* s. For example, suppose s is a variable indicating whether or not there is a hurricane and a and b measure the wind speed at two different nearby weather monitoring outposts. If we observe very high winds at station a, we might expect to also see high winds at b. This kind of path can be blocked by observing s. If we already know there is a hurricane, we expect to see high winds at b, regardless of what is observed at a. A lower than expected wind at a (for a hurricane) would not change our expectation of winds at b (knowing there is a hurricane). However, if s is not observed, then a and b are dependent, i.e., the path is active. *(c)*a and b are both parents of s. This is called a **V-structure** or **the collider case**. The V-structure causes a and b to be related by the **explaining away effect**. In this case, the path is actually active when s is observed. For example, suppose s is a variable indicating that your colleague is not at work. The variable a represents her being sick, while b represents her being on vacation. If you observe that she is not at work, you can presume she is probably sick or on vacation, but it is not especially likely that both have happened at the same time. If you find out that she is on vacation, this fact is sufficient to *explain* her absence. You can infer that she is probably not also sick. *(d)*The explaining away effect happens even if any descendant of s is observed! For example, suppose that c is a variable representing whether you have received a report from your colleague. If you notice that you have not received the report, this increases your estimate of the probability that she is not at work today, which in turn makes it more likely that she is either sick or on vacation. The only way to block a path through a V-structure is to observe none of the descendants of the shared child.

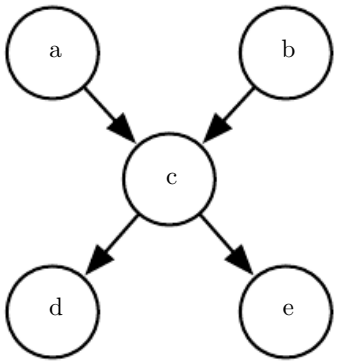

Figure 16.9: From this graph, we can read out several d-separation properties. Examples include:

- a and b are d-separated given the empty set.
- a and e are d-separated given c.
- d and e are d-separated given c.

We can also see that some variables are no longer d-separated when we observe some variables:

- a and b are not d-separated given c.
- a and b are not d-separated given d.

16.2.6 Converting between Undirected and Directed Graphs

We often refer to a specific machine learning model as being undirected or directed. For example, we typically refer to RBMs as undirected and sparse coding as directed. This choice of wording can be somewhat misleading, because no probabilistic model is inherently directed or undirected. Instead, some models are most easily *described* using a directed graph, or most easily described using an undirected graph.

Directed models and undirected models both have their advantages and disadvantages. Neither approach is clearly superior and universally preferred. Instead, we should choose which language to use for each task. This choice will partially depend on which probability distribution we wish to describe. We may choose to use either directed modeling or undirected modeling based on which approach can capture the most independences in the probability distribution or which approach uses the fewest edges to describe the distribution. There are other factors that can affect the decision of which language to use. Even while working with a single probability distribution, we may sometimes switch between different modeling languages. Sometimes a different language becomes more appropriate if we observe a certain subset of variables, or if we wish to perform a different computational task. For example, the directed model description often provides a straightforward approach to efficiently draw samples from the model (described in section 16.3) while the undirected model formulation is often useful for deriving approximate inference procedures (as we will see in chapter 19, where the role of undirected models is highlighted in equation 19.56).

Every probability distribution can be represented by either a directed model or by an undirected model. In the worst case, one can always represent any distribution by using a "complete graph." In the case of a directed model, the complete graph is any directed acyclic graph where we impose some ordering on the random variables, and each variable has all other variables that precede it in the ordering as its ancestors in the graph. For an undirected model, the complete graph is simply a graph containing a single clique encompassing all of the variables. See figure 16.10 for an example.

Of course, the utility of a graphical model is that the graph implies that some variables do not interact directly. The complete graph is not very useful because it does not imply any independences.

When we represent a probability distribution with a graph, we want to choose a graph that implies as many independences as possible, without implying any independences that do not actually exist.

From this point of view, some distributions can be represented more efficiently

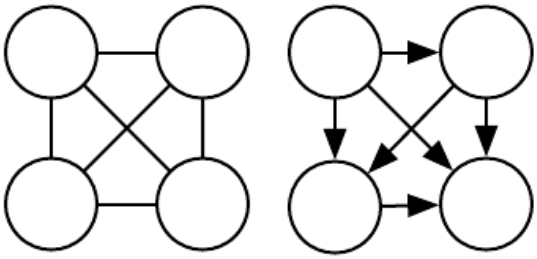

Figure 16.10: Examples of complete graphs, which can describe any probability distribution. Here we show examples with four random variables. *(Left)*The complete undirected graph. In the undirected case, the complete graph is unique. *(Right)*A complete directed graph. In the directed case, there is not a unique complete graph. We choose an ordering of the variables and draw an arc from each variable to every variable that comes after it in the ordering. There are thus a factorial number of complete graphs for every set of random variables. In this example we order the variables from left to right, top to bottom.

using directed models, while other distributions can be represented more efficiently using undirected models. In other words, directed models can encode some independences that undirected models cannot encode, and vice versa.

Directed models are able to use one specific kind of substructure that undirected models cannot represent perfectly. This substructure is called an **immorality**. The structure occurs when two random variables a and b are both parents of a third random variable c, and there is no edge directly connecting a and b in either direction. (The name "immorality" may seem strange; it was coined in the graphical models literature as a joke about unmarried parents.) To convert a directed model with graph $\mathcal{D}$ into an undirected model, we need to create a new graph $\mathcal{U}$. For every pair of variables x and y, we add an undirected edge connecting x and y to $\mathcal{U}$ if there is a directed edge (in either direction) connecting x and y in $\mathcal{D}$ or if x and y are both parents in $\mathcal{D}$ of a third variable z. The resulting $\mathcal{U}$ is known as a **moralized graph**. See figure 16.11 for examples of converting directed models to undirected models via moralization.

Likewise, undirected models can include substructures that no directed model can represent perfectly. Specifically, a directed graph $\mathcal{D}$ cannot capture all of the conditional independences implied by an undirected graph $\mathcal{U}$ if $\mathcal{U}$ contains a **loop** of length greater than three, unless that loop also contains a **chord**. A loop is a sequence of variables connected by undirected edges, with the last variable in the sequence connected back to the first variable in the sequence. A chord is a connection between any two non-consecutive variables in the sequence defining a loop. If $\mathcal{U}$ has loops of length four or greater and does not have chords for these loops, we must add the chords before we can convert it to a directed model. Adding

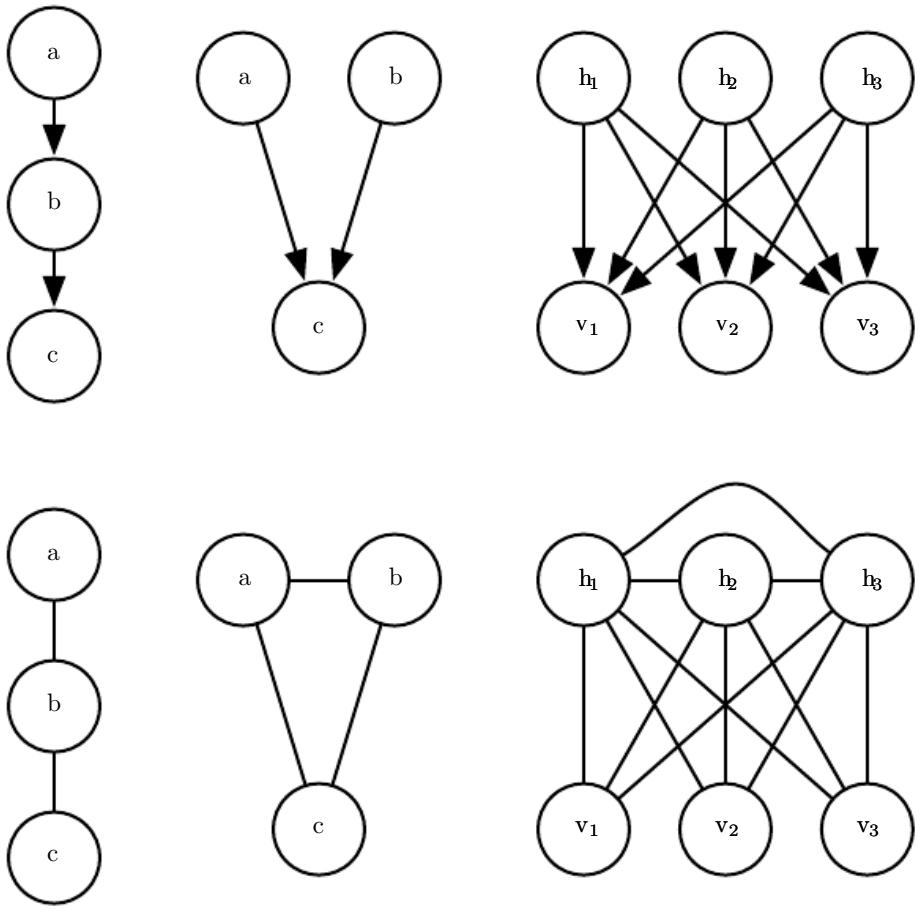

Figure 16.11: Examples of converting directed models (top row) to undirected models (bottom row) by constructing moralized graphs. *(Left)*This simple chain can be converted to a moralized graph merely by replacing its directed edges with undirected edges. The resulting undirected model implies exactly the same set of independences and conditional independences. *(Center)*This graph is the simplest directed model that cannot be converted to an undirected model without losing some independences. This graph consists entirely of a single immorality. Because a and b are parents of c, they are connected by an active path when c is observed. To capture this dependence, the undirected model must include a clique encompassing all three variables. This clique fails to encode the fact that $a \perp b$. *(Right)*In general, moralization may add many edges to the graph, thus losing many implied independences. For example, this sparse coding graph requires adding moralizing edges between every pair of hidden units, thus introducing a quadratic number of new direct dependences.

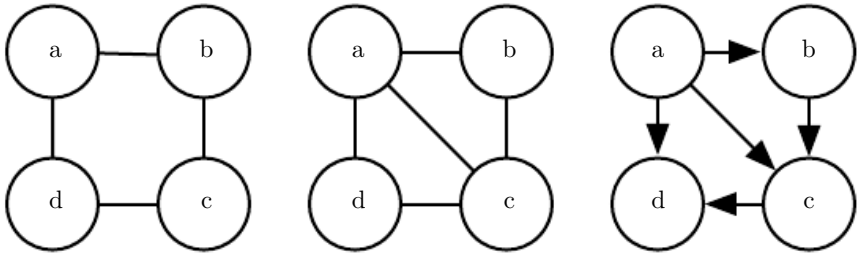

Figure 16.12: Converting an undirected model to a directed model. *(Left)*This undirected model cannot be converted directed to a directed model because it has a loop of length four with no chords. Specifically, the undirected model encodes two different independences that no directed model can capture simultaneously: $\mathrm{a} \perp \mathrm{c} \mid \{\mathrm{b}, \mathrm{d}\}$ and $\mathrm{b} \perp \mathrm{d} \mid \{\mathrm{a}, \mathrm{c}\}$. *(Center)*To convert the undirected model to a directed model, we must triangulate the graph, by ensuring that all loops of greater than length three have a chord. To do so, we can either add an edge connecting a and c or we can add an edge connecting b and d. In this example, we choose to add the edge connecting a and c. *(Right)*To finish the conversion process, we must assign a direction to each edge. When doing so, we must not create any directed cycles. One way to avoid directed cycles is to impose an ordering over the nodes, and always point each edge from the node that comes earlier in the ordering to the node that comes later in the ordering. In this example, we use the variable names to impose alphabetical order.

these chords discards some of the independence information that was encoded in $\mathcal{U}$. The graph formed by adding chords to $\mathcal{U}$ is known as a **chordal** or **triangulated** graph, because all the loops can now be described in terms of smaller, triangular loops. To build a directed graph $\mathcal{D}$ from the chordal graph, we need to also assign directions to the edges. When doing so, we must not create a directed cycle in $\mathcal{D}$, or the result does not define a valid directed probabilistic model. One way to assign directions to the edges in $\mathcal{D}$ is to impose an ordering on the random variables, then point each edge from the node that comes earlier in the ordering to the node that comes later in the ordering. See figure 16.12 for a demonstration.

16.2.7 Factor Graphs

Factor graphs are another way of drawing undirected models that resolve an ambiguity in the graphical representation of standard undirected model syntax. In an undirected model, the scope of every ϕ function must be a *subset* of some clique in the graph. Ambiguity arises because it is not clear if each clique actually has a corresponding factor whose scope encompasses the entire clique—for example, a clique containing three nodes may correspond to a factor over all three nodes, or may correspond to three factors that each contain only a pair of the nodes.

Factor graphs resolve this ambiguity by explicitly representing the scope of each ϕ function. Specifically, a factor graph is a graphical representation of an undirected model that consists of a bipartite undirected graph. Some of the nodes are drawn as circles. These nodes correspond to random variables as in a standard undirected model. The rest of the nodes are drawn as squares. These nodes correspond to the factors ϕ of the unnormalized probability distribution. Variables and factors may be connected with undirected edges. A variable and a factor are connected in the graph if and only if the variable is one of the arguments to the factor in the unnormalized probability distribution. No factor may be connected to another factor in the graph, nor can a variable be connected to a variable. See figure 16.13 for an example of how factor graphs can resolve ambiguity in the interpretation of undirected networks.

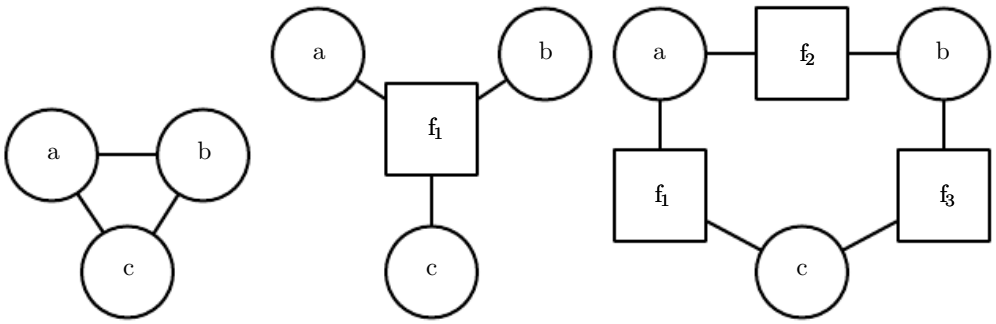

Figure 16.13: An example of how a factor graph can resolve ambiguity in the interpretation of undirected networks. *(Left)*An undirected network with a clique involving three variables: a, b and c. *(Center)*A factor graph corresponding to the same undirected model. This factor graph has one factor over all three variables. *(Right)*Another valid factor graph for the same undirected model. This factor graph has three factors, each over only two variables. Representation, inference, and learning are all asymptotically cheaper in this factor graph than in the factor graph depicted in the center, even though both require the same undirected graph to represent.

16.3 Sampling from Graphical Models

Graphical models also facilitate the task of drawing samples from a model.

One advantage of directed graphical models is that a simple and efficient procedure called **ancestral sampling** can produce a sample from the joint distribution represented by the model.

The basic idea is to sort the variables x_i in the graph into a topological ordering, so that for all i and j, j is greater than i if x_i is a parent of x_j. The variables

can then be sampled in this order. In other words, we first sample $\mathrm{x}_1 \sim P(\mathrm{x}_1)$, then sample $P(\mathrm{x}_2 \mid Pa_{\mathcal{G}}(\mathrm{x}_2))$, and so on, until finally we sample $P(\mathrm{x}_n \mid Pa_{\mathcal{G}}(\mathrm{x}_n))$. So long as each conditional distribution $p(\mathrm{x}_i \mid Pa_{\mathcal{G}}(\mathrm{x}_i))$ is easy to sample from, then the whole model is easy to sample from. The topological sorting operation guarantees that we can read the conditional distributions in equation 16.1 and sample from them in order. Without the topological sorting, we might attempt to sample a variable before its parents are available.

For some graphs, more than one topological ordering is possible. Ancestral sampling may be used with any of these topological orderings.

Ancestral sampling is generally very fast (assuming sampling from each conditional is easy) and convenient.

One drawback to ancestral sampling is that it only applies to directed graphical models. Another drawback is that it does not support every conditional sampling operation. When we wish to sample from a subset of the variables in a directed graphical model, given some other variables, we often require that all the conditioning variables come earlier than the variables to be sampled in the ordered graph. In this case, we can sample from the local conditional probability distributions specified by the model distribution. Otherwise, the conditional distributions we need to sample from are the posterior distributions given the observed variables. These posterior distributions are usually not explicitly specified and parametrized in the model. Inferring these posterior distributions can be costly. In models where this is the case, ancestral sampling is no longer efficient.

Unfortunately, ancestral sampling is applicable only to directed models. We can sample from undirected models by converting them to directed models, but this often requires solving intractable inference problems (to determine the marginal distribution over the root nodes of the new directed graph) or requires introducing so many edges that the resulting directed model becomes intractable. Sampling from an undirected model without first converting it to a directed model seems to require resolving cyclical dependencies. Every variable interacts with every other variable, so there is no clear beginning point for the sampling process. Unfortunately, drawing samples from an undirected graphical model is an expensive, multi-pass process. The conceptually simplest approach is **Gibbs sampling**. Suppose we have a graphical model over an n-dimensional vector of random variables $\mathbf{x}$. We iteratively visit each variable x_i and draw a sample conditioned on all of the other variables, from $p(\mathrm{x}_i \mid \mathrm{x}_{-i})$. Due to the separation properties of the graphical model, we can equivalently condition on only the neighbors of x_i. Unfortunately, after we have made one pass through the graphical model and sampled all n variables, we still do not have a fair sample from $p(\mathbf{x})$. Instead, we must repeat the

process and resample all n variables using the updated values of their neighbors. Asymptotically, after many repetitions, this process converges to sampling from the correct distribution. It can be difficult to determine when the samples have reached a sufficiently accurate approximation of the desired distribution. Sampling techniques for undirected models are an advanced topic, covered in more detail in chapter 17.

16.4 Advantages of Structured Modeling

The primary advantage of using structured probabilistic models is that they allow us to dramatically reduce the cost of representing probability distributions as well as learning and inference. Sampling is also accelerated in the case of directed models, while the situation can be complicated with undirected models. The primary mechanism that allows all of these operations to use less runtime and memory is choosing to not model certain interactions. Graphical models convey information by leaving edges out. Anywhere there is not an edge, the model specifies the assumption that we do not need to model a direct interaction.

A less quantifiable benefit of using structured probabilistic models is that they allow us to explicitly separate representation of knowledge from learning of knowledge or inference given existing knowledge. This makes our models easier to develop and debug. We can design, analyze, and evaluate learning algorithms and inference algorithms that are applicable to broad classes of graphs. Independently, we can design models that capture the relationships we believe are important in our data. We can then combine these different algorithms and structures and obtain a Cartesian product of different possibilities. It would be much more difficult to design end-to-end algorithms for every possible situation.

16.5 Learning about Dependencies

A good generative model needs to accurately capture the distribution over the observed or "visible" variables $\mathbf{v}$. Often the different elements of $\mathbf{v}$ are highly dependent on each other. In the context of deep learning, the approach most commonly used to model these dependencies is to introduce several latent or "hidden" variables, $\mathbf{h}$. The model can then capture dependencies between any pair of variables v_i and v_j indirectly, via direct dependencies between v_i and $\mathbf{h}$, and direct dependencies between $\mathbf{h}$ and v_j.

A good model of $\mathbf{v}$ which did not contain any latent variables would need to

have very large numbers of parents per node in a Bayesian network or very large cliques in a Markov network. Just representing these higher order interactions is costly—both in a computational sense, because the number of parameters that must be stored in memory scales exponentially with the number of members in a clique, but also in a statistical sense, because this exponential number of parameters requires a wealth of data to estimate accurately.

When the model is intended to capture dependencies between visible variables with direct connections, it is usually infeasible to connect all variables, so the graph must be designed to connect those variables that are tightly coupled and omit edges between other variables. An entire field of machine learning called **structure learning** is devoted to this problem For a good reference on structure learning, see (Koller and Friedman, 2009). Most structure learning techniques are a form of greedy search. A structure is proposed, a model with that structure is trained, then given a score. The score rewards high training set accuracy and penalizes model complexity. Candidate structures with a small number of edges added or removed are then proposed as the next step of the search. The search proceeds to a new structure that is expected to increase the score.

Using latent variables instead of adaptive structure avoids the need to perform discrete searches and multiple rounds of training. A fixed structure over visible and hidden variables can use direct interactions between visible and hidden units to impose indirect interactions between visible units. Using simple parameter learning techniques we can learn a model with a fixed structure that imputes the right structure on the marginal $p(\mathbf{v})$.

Latent variables have advantages beyond their role in efficiently capturing $p(\mathbf{v})$. The new variables $\mathbf{h}$ also provide an alternative representation for $\mathbf{v}$. For example, as discussed in section 3.9.6, the mixture of Gaussians model learns a latent variable that corresponds to which category of examples the input was drawn from. This means that the latent variable in a mixture of Gaussians model can be used to do classification. In chapter 14 we saw how simple probabilistic models like sparse coding learn latent variables that can be used as input features for a classifier, or as coordinates along a manifold. Other models can be used in this same way, but deeper models and models with different kinds of interactions can create even richer descriptions of the input. Many approaches accomplish feature learning by learning latent variables. Often, given some model of $\mathbf{v}$ and $\mathbf{h}$, experimental observations show that $\mathbb{E}[\mathbf{h} \mid \mathbf{v}]$ or $\text{argmax}_{\boldsymbol{h}} p(\boldsymbol{h}, \boldsymbol{v})$ is a good feature mapping for $\boldsymbol{v}$.

16.6 Inference and Approximate Inference

One of the main ways we can use a probabilistic model is to ask questions about how variables are related to each other. Given a set of medical tests, we can ask what disease a patient might have. In a latent variable model, we might want to extract features $\mathbb{E}[\mathbf{h} \mid \mathbf{v}]$ describing the observed variables $\mathbf{v}$. Sometimes we need to solve such problems in order to perform other tasks. We often train our models using the principle of maximum likelihood. Because

$$\log p(\boldsymbol{v}) = \mathbb{E}_{\mathbf{h} \sim p(\mathbf{h} \mid \boldsymbol{v})} \left[\log p(\boldsymbol{h}, \boldsymbol{v}) - \log p(\boldsymbol{h} \mid \boldsymbol{v}) \right], \tag{16.9}$$

we often want to compute $p(\mathbf{h} \mid \boldsymbol{v})$ in order to implement a learning rule. All of these are examples of **inference** problems in which we must predict the value of some variables given other variables, or predict the probability distribution over some variables given the value of other variables.

Unfortunately, for most interesting deep models, these inference problems are intractable, even when we use a structured graphical model to simplify them. The graph structure allows us to represent complicated, high-dimensional distributions with a reasonable number of parameters, but the graphs used for deep learning are usually not restrictive enough to also allow efficient inference.

It is straightforward to see that computing the marginal probability of a general graphical model is #P hard. The complexity class #P is a generalization of the complexity class NP. Problems in NP require determining only whether a problem has a solution and finding a solution if one exists. Problems in #P require counting the number of solutions. To construct a worst-case graphical model, imagine that we define a graphical model over the binary variables in a 3-SAT problem. We can impose a uniform distribution over these variables. We can then add one binary latent variable per clause that indicates whether each clause is satisfied. We can then add another latent variable indicating whether all of the clauses are satisfied. This can be done without making a large clique, by building a reduction tree of latent variables, with each node in the tree reporting whether two other variables are satisfied. The leaves of this tree are the variables for each clause. The root of the tree reports whether the entire problem is satisfied. Due to the uniform distribution over the literals, the marginal distribution over the root of the reduction tree specifies what fraction of assignments satisfy the problem. While this is a contrived worst-case example, NP hard graphs commonly arise in practical real-world scenarios.

This motivates the use of approximate inference. In the context of deep learning, this usually refers to variational inference, in which we approximate the

true distribution $p(\mathbf{h} \mid \boldsymbol{v})$ by seeking an approximate distribution $q(\mathbf{h}|\mathbf{v})$ that is as close to the true one as possible. This and other techniques are described in depth in chapter 19.

16.7 The Deep Learning Approach to Structured Probabilistic Models

Deep learning practitioners generally use the same basic computational tools as other machine learning practitioners who work with structured probabilistic models. However, in the context of deep learning, we usually make different design decisions about how to combine these tools, resulting in overall algorithms and models that have a very different flavor from more traditional graphical models.

Deep learning does not always involve especially deep graphical models. In the context of graphical models, we can define the depth of a model in terms of the graphical model graph rather than the computational graph. We can think of a latent variable h_i as being at depth j if the shortest path from h_i to an observed variable is j steps. We usually describe the depth of the model as being the greatest depth of any such h_i. This kind of depth is different from the depth induced by the computational graph. Many generative models used for deep learning have no latent variables or only one layer of latent variables, but use deep computational graphs to define the conditional distributions within a model.

Deep learning essentially always makes use of the idea of distributed representations. Even shallow models used for deep learning purposes (such as pretraining shallow models that will later be composed to form deep ones) nearly always have a single, large layer of latent variables. Deep learning models typically have more latent variables than observed variables. Complicated nonlinear interactions between variables are accomplished via indirect connections that flow through multiple latent variables.

By contrast, traditional graphical models usually contain mostly variables that are at least occasionally observed, even if many of the variables are missing at random from some training examples. Traditional models mostly use higher-order terms and structure learning to capture complicated nonlinear interactions between variables. If there are latent variables, they are usually few in number.

The way that latent variables are designed also differs in deep learning. The deep learning practitioner typically does not intend for the latent variables to take on any specific semantics ahead of time—the training algorithm is free to invent the concepts it needs to model a particular dataset. The latent variables are